89

AFCRL-64-127

AIR LAUNCHED ROCKETSOUNDING STUDY

C. P. Blackburn
D. B. George

The Bendix Corporation
Friez Instrument Division
1400 Taylor Avenue
Baltimore, Maryland 21204

Contract No. AF19(628)-3264

FINAL REPORT

Project 6020
Task 602001

April 1964

Prepared
for

AIR FORCE CAMBRIDGE RESEARCH LABORATORIES
OFFICE OF AEROSPACE RESEARCH
UNITED STATES AIR FORCE
BEDFORD, MASSACHUSETTS

DISCLAIMER NOTICE

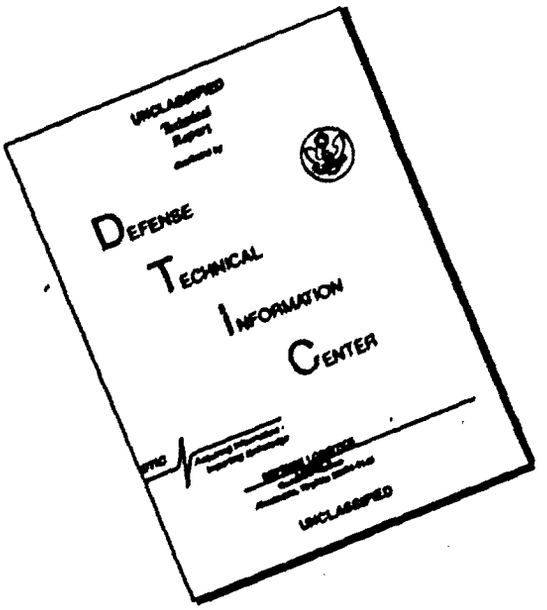

THIS DOCUMENT IS BEST QUALITY AVAILABLE. THE COPY FURNISHED TO DTIC CONTAINED A SIGNIFICANT NUMBER OF PAGES WHICH DO NOT REPRODUCE LEGIBLY.

Requests for additional copies by Agencies of the Department of Defense, their contractors, and other Government agencies should be directed to the:

Defense Documentation Center (DDC)
Cameron Station
Alexandria, Virginia 22314

All other persons and organizations should apply to the:

U. S. Department of Commerce
Office of Technical Services
Washington 25, D.C.

Bendix — Friez

AFCRL-64-127 EIR-549

AIR LAUNCHED ROCKETSOUNDING STUDY

C. P. Blackburn
D. B. George

The Bendix Corporation
Friez Instrument Division
1400 Taylor Avenue
Baltimore, Maryland 21204

Contract No. AF19(628)-3264

FINAL REPORT

Project 6020
Task 602001

April 1964

Prepared
for
AIR FORCE CAMBRIDGE RESEARCH LABORATORIES
OFFICE OF AEROSPACE RESEARCH
UNITED STATES AIR FORCE
BEDFORD, MASSACHUSETTS

Bendix - Friez

ABSTRACT

The results of a program to study, evaluate and recommend the most feasible techniques and equipment for an air launched rocket sounding system compatible with the AN/AMQ-19 Meteorological system are presented in this report. The purpose of the rocketsounding system is to extend the meteorological data envelope to an altitude of 120,000 feet and to provide a growth capability for future expansion to 250,000 and the area between 400,000 and 600,000 feet.

Several approaches to air launched meteorological soundings have been studied. These include various airframe installation configurations, rocket propelled flight vehicles, and a gun launched meteorological probe. The various factors involved in the program; Aircraft Flight Safety, installation, rocket vehicle configuration, meteorological instrument package, and system growth potential have resulted in the recommendation of one configuration as the optimum. These vehicles, carried in underwing external stores, are readily adaptable to either the W-47E or KC/C135B aircraft.

The sounding vehicle will be dropped from the aircraft, parachute stabilized and sequence fired to attain the desired 120,000 foot level. At apogee, the instrument package will separate from the vehicle and transmit pressure, temperature and humidity data. A control pressure capsule within the sonde will terminate the RF signal when it has descended to aircraft flight level. This cut-off permits optimization of instrument descent rate and precludes aircraft maneuvers to maintain data reception from the sonde. The vertical profile may be continued to ground level with an AN/AMT-13 Radiosonde which is an integral part of the AN/AMQ-19 system. Density of the air through which the sonde passes may be calculated by use of the temperature, pressure and altitude data obtained for the 120,000 and 250,000 foot systems as air may be considered as having a constant molecular weight at these altitudes. Functional descriptions of the AN/AMQ-19 and AN/GMH-4 systems have been included in this report, along with a description of the compatibility of the rocketsounding system. The incorporation of an available aircraft qualified rocket motor in the flight vehicle will contribute to reduction of cost during development and qualification of the system.

Bendix - Friez

TABLE OF CONTENTS

Bendix – Friez

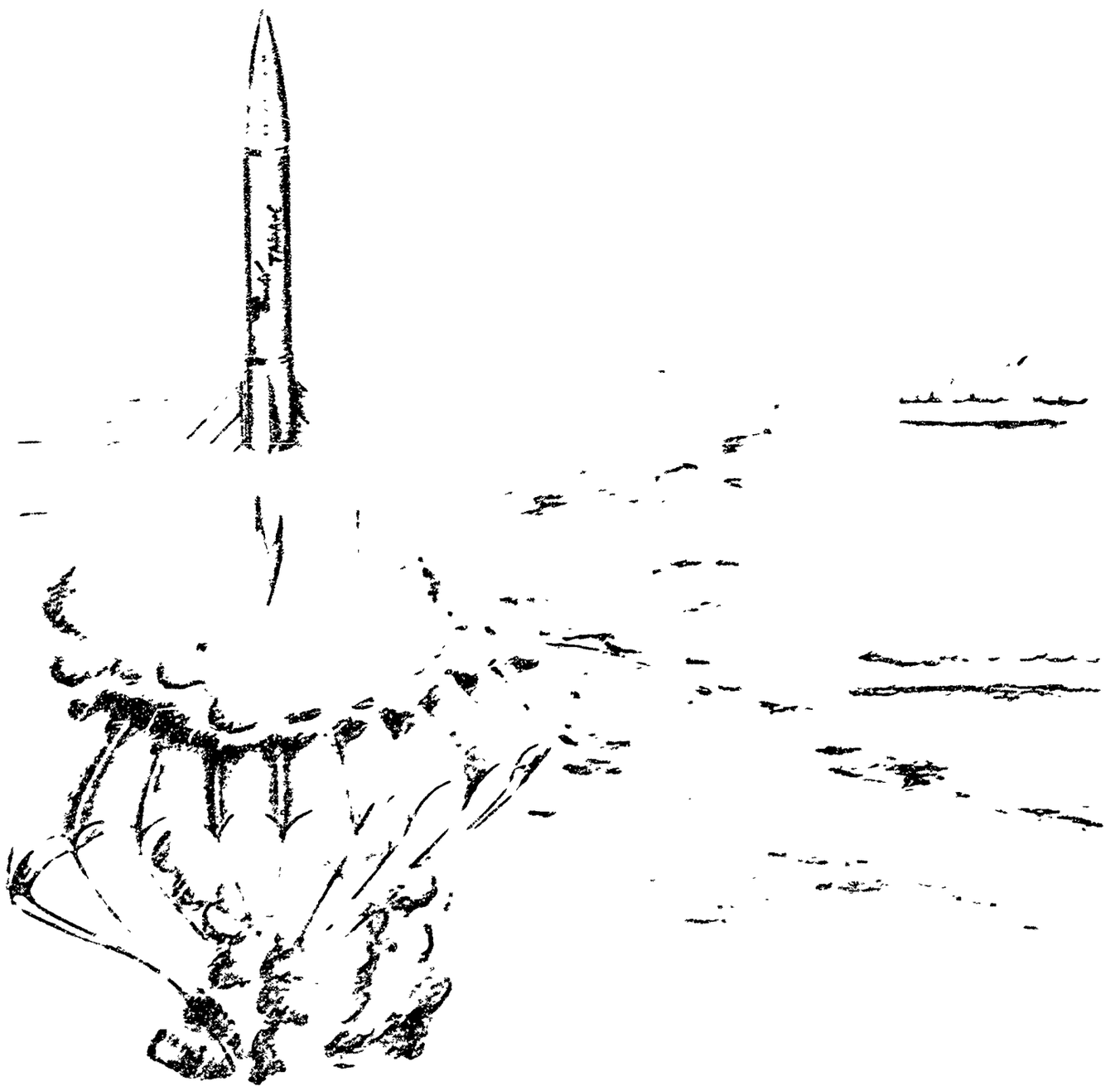

SECTION I

INTRODUCTION

The WC-47E Weather Reconnaissance Aircraft is equipped with the AN/AMQ-19 Meteorological System for the collection of weather and flight data at aircraft altitude (35,000 feet) and between flight level and the ground by dropsonde. The addition of an upper atmosphere rocket sounding capability, of the type investigated during this study program, will increase the vertical data envelope to an altitude of 120,000 feet. Meteorological Data obtained at these levels will greatly enhance the scope of data collection and will have application to the problems of optimizing the performance of ballistic missiles, boost glide vehicles, and airburst probes. It will also enable further study into the performance of tracking and search equipment and allow an expansion of existing studies on the high altitude atmospheric processes and their effects on stratospheric and tropospheric weather conditions. Since the sounding rocket is aircraft launched, instead of balloon or ground fired, vast areas of the atmosphere not covered by present systems can be sampled.

This report presents the results of the study program and recommendations for the system to be employed. It also includes investigations of several unusual approaches toward obtaining the desired goal. The sounding system, recommended as a result of this detailed study (PAULA I), consists of an instrument package, a proven rocket motor (Falcon M58A2), and a flight vehicle configuration. The complete sounding system includes externally installed stores each containing two sounding vehicles which are dropped individually from the aircraft, parachute stabilized, and sequence fired to a 135,000 foot apogee. At apogee, the ogive nose section containing the sounding instruments separates from the flight vehicle, is parachute-deployed, and proceeds to transmit humidity, pressure, temperature and reference data to the aircraft during descent. The external store concept was utilized, after careful consideration of the various methods studied, so that modification to the two aircraft concerned (WC-47E and KC/C-135B) would be held to a minimum, aircraft flight safety considerations would be maximized, and the pod containing the sounding rockets loaded aboard either aircraft without further handling. A detailed discussion of this and the other approaches studied is included in this report.

A rocket motor presently qualified for aircraft use was selected from those studied in an effort to reduce the total cost of the air launched rocket sounding program. Several other motors which could deliver the desired thrust were investigated during the program but were downgraded on this basis since the program to qualify a rocket motor for use aboard aircraft is extremely expensive. The flight vehicle and pod contain all components for the firing sequence. The pod, sounding vehicle, and aircraft umbilical

connections have been carefully planned for fail safe operation. A strip heater is utilized to maintain the solid state circuitry, batteries, and hypsometer fluid at acceptable temperatures prior to release from the aircraft. Since the "cost-per-shot" of the sounding vehicle will be higher than that of an AN/AMT-13 Radiosonde, careful study has been made of all components to assure a very high degree of reliability.

The system presented is completely compatible with the existing AN/AMQ-19 system currently in use by the Air Weather Service. Consideration has been given to the expansion of the vertical envelope to 250,000 feet and to the region between 400,000 and 600,000 feet when appropriate sensors are available. It is anticipated that these future investigations may be accomplished with only minor modifications to the flight vehicle and aircraft equipment.

In the following sections of this report the flight vehicle, instrument package and each meteorological sensor is discussed in detail and calculations supporting the operating parameters of the system, including rocket propelled flight vehicle characteristics, are presented.

SECTION II

PROGRAM OBJECTIVES

Certain features, characteristics, and performance must be incorporated into the design of an air launched high altitude meteorological sounding subsystem to assure compatibility with the AN/AMQ-19 System and the W-47E and KC/C-135B aircraft. These criteria also include flight safety considerations, reliable data collection and the anticipated operational environment. In initiating the study program, the first problem considered was the location of the sounding vehicle, its components, and its ultimate method of release from the aircraft. Operational safety precludes the possibility of firing the rocket motor while mounted within the aircraft. It is necessary to consider fuselage mounting with horizontal separation, and external stores with a downward separation. A careful study was made of each possible method with aircraft safety and consideration of cost per shot being paramount in selection of the final system.

The program objectives which were primary considerations during the study program can be summarized as follows:

1. Aircraft Flight Safety must be considered of paramount importance.

2. The system must be readily adaptable to both the W-47E and the KC/C-135B aircraft with a minimum of structural modification to the aircraft.

3. The telemetering equipment must be compatible with the AN/AMQ-19.

4. The rocket motor used for propulsion of the flight vehicle should be aircraft qualified and an Air Force stocked item.

5. The rocketsounding system should consist of state-of-the-art techniques for use at altitudes of 120,000 feet and be readily expandable to 250,000 feet with future development to the region between 400,000 feet and 600,000 feet as applicable sensors become available.

The objectives presented in the following paragraphs were carefully considered in evolving a final selection of sounding system components and aircraft installation.

FLIGHT SAFETY

The method selected for separation of the sounding vehicle from the W-47E and KC/C-135B must assure absolute safety of the aircraft. "Fail-safe" provisions must be incorporated in the subsystem to assure that the rocket motor and any jettison system will not function inadvertantly aboard the aircraft in flight or during any required ground handling.

COST PER SHOT

The air launched rocketsounding system recommended must offer a cost which is not prohibitive to operational use after acceptance. To fulfill this objective the study was directed toward investigation of not only the rocket motor, flight vehicle, and handling costs, but also the major areas of aircraft retrofit, system qualification and logistics support in operation, all of which must ultimately be amortized into the cost of each sounding taken. In an effort to assure that these problems were all considered, a variety of state-of-the-art hardware was investigated with careful consideration being given to existing AN/AMT-13 experience and to aircraft qualified rocket motors.

AIRCRAFT INSTALLATION

The aircraft position selected for the installation of sounding vehicles must be consistent with other systems aboard the aircraft, assuring that damage will not result during launch due to debris or malfunction. Further, the location selected must minimize the environmental conditioning (heating) required for the instrument package and assure that transmitter operation can be confirmed prior to launch. The location chosen should result in a minimum of modification to either of the specified aircraft. The panel provided for control of the sounding subsystem must be consistent with those presently used in the AN/AMQ-19 System in information display and electrical functioning. Interlocks must be provided so that during the launch sequence only the desired package may be armed and released. This will assure that a dropsonde cannot be released when a rocketsonde is desired and that the converse could not occur.

ALTITUDE PERFORMANCE

The rocket motor selected to propel the flight vehicle to altitude must be of a type available from Government stock or at least be a proven if not qualified motor, and of sufficient performance (thrust and burning time) to assure that the instrument package reaches the desired altitude.

IN-FLIGHT STABILITY

The rocketsounding vehicle configuration must be designed to assure smooth, stable flight from launch to apogee. Unstable, erratic, flight can result in damaging accelerations to the instrument package and in failure to reach the desired altitude and position relative to the launch aircraft.

INSTRUMENT PACKAGE

The instrument package must be designed to accommodate sensors for detecting pressure, temperature, humidity and to allow calculation of density to an altitude of 120,000 feet. The design concept of the package must allow for simple substitution of alternate sensors for higher altitudes and provide sufficient power for their operation. The electronics section of the package must be designed to transmit the weather data collected over a carrier frequency of 403 megacycles at a pulse repetition rate compatible with the Receiver in the AN/AMQ-19 System. The data transmission format must be similar with that used in the AN/AMT-13 Radiosonde although differences in data sequence are permissible.

GROWTH POTENTIAL

The system will be designed to permit expansion to 250,000 feet with a minimum of modification in the launching sequence of the flight vehicle. The primary concern for this phase, PAULA II, will be the use of a more powerful transmitter. Additional development in flight vehicle and sensors will provide a system, PAULA III, for data collection in the 400,000 to 600,000 foot level. Requirements for the type and quantity of data needed must also be generated prior to this phase in the logical development of an expanded system.

SECTION III

CONCLUSIONS AND RECOMMENDATIONS

As a result of the efforts expended in this study program, conducted under the provision of Contract AF19(628)-3264, the following conclusions and recommendations are presented:

1. The concept of an air launched meteorological sounding vehicle, compatible with the AN/AMQ-19 System, ascending to 120,000 foot apogee from either the W-47E or the KC/C-135B aircraft is feasible with state-of-the-art hardware.

2. The air launched sounding system should carry the sounding vehicles and their deployment mechanism as an external store of the aircraft.

3. An upward looking receiving antenna should be mounted in the aft fuselage of the aircraft and an additional control panel added to the AN/AMQ-19 System.

4. The sounding vehicle should be installed in a pod, deployed from the aircraft by a thruster, parachute stabilized and fired to apogee via timing mechanisms with inherent safety devices.

5. The radiosonde should be deployed at apogee for parachute descent. The data transmitted shall be completely compatible with the AN/AMQ-19 System.

6. The radiosonde shall transmit analog signals representative of the temperature, humidity and pressure environment through which it is passing. In addition, reference data will be supplied at regular intervals. The data obtained may also be used to calculate density.

7. The sensors shall be a ten mil diameter thermistor, a carbon or aluminum oxide type humidity element, and a hypsometer.

8. The rocket motor shall be a Falcon M-58A2 for the 120,000 foot altitude, an M-60 for the 250,000 foot altitude. It is possible that an M-60, plus a booster, may be used for the 600,000 foot altitude. These shall require only minor changes within the flight vehicle and require no changes to the dispensing system.

9. The gun launched probe should not be considered.

10. The aft mounted dispenser should not be considered.

SECTION IV

PAULA I

(Air Launched Upper Atmosphere Probe)

The result of the detailed investigations outlined in the preceding section was the concept of PAULA I presented in detail in this section. This final design was made possible through close cooperation between the Thiokol Chemical Corporation and The Bendix Corporation. The Thiokol Chemical Corporation's extensive background in rocket motors, flight vehicles, and rocket handling, coupled with the Bendix Corporation's background in upper atmospheric sounding techniques, instrumentation, and sensors, as well as the design and installation of the AN/AMQ-19 System, made this an ideal combination of talent to investigate the rocketsounding system.

The recommended system is completely compatible with the existing AN/AMQ-19 Meteorological System, and sounding equipment as presented in Section VI, and represents state-of-the-art techniques which can be applied with a minimum of aircraft modification and system qualification problems. This system is readily adaptable to both the W-47E and the KC/C-135B aircraft. Maximum use has been made of existing AN/AMT-13 Radiosonde components and operational techniques. This, together with further advances in sounding vehicles and instrument packages, requires a minimum of ground handling prior to operational deployment. This advance is possible since the sounding vehicle rocket motor is of a proven design, presently qualified for manned aircraft use. Meteorological sensors and probe components have been chosen so that baseline checks need consist only of setting the desired transmitter radio frequency and charging the battery power supply. The flight vehicle configuration utilized is a further result of the cooperative effort between the Friez Instrument Division of The Bendix Corporation, and the Astro-Met Division of Thiokol Chemical Corporation. The payload capability of this motor, the M58A2, permits the incorporation of many existing AN/AMT-13 components, and a proven Bendix rocket-borne hypsometer, into the meteorological probe, with optimum potential for future growth. This hypsometer is similar to the VST and AN/DMQ-9 types developed under Air Force Contracts: AF33(600)-41821, AF19(628)-1655 and AF19(604)-8433. Another major advantage of the Falcon M58A2 rocket motor is its qualification for use aboard aircraft in accordance with MIL-E-25534. Qualification and production of this motor were accomplished under the provisions of Contract DA-01-021506 Ord. Over 40,000 of these motors have been manufactured. In addition to providing 12.5 per cent overperformance for this 120,000 feet altitude sounding requirement (which permits changes in payload and configuration), the published performance data show an expected reliability (expressed as the ra .o of successes to total trials) of 99.99 per cent for flight testing. Consequently,

utilization of this reliable, qualified, rocket motor represents a substantial savings in the time and cost required to design, develop and qualify the system.

A detailed study has been made of both the flight vehicle utilizing this motor and the meteorological package. This sounding vehicle is described in detail in the following paragraphs. The meteorological package and sensors are covered in subsequent paragraphs.

DESCRIPTION OF THE SOUNDING SYSTEM

The sounding system recommended as a result of the study program utilizes the M58A2 Falcon rocket motor in a six inch diameter fixed fin flight vehicle, as illustrated in Figures 4-1 and 4-4. This rocket vehicle is capable of propelling a nine and one-half pound payload to an altitude of 135,000 feet when ignited at an altitude of 31,500 feet. The W-47E normal cruise altitude is 35,000 feet. The flight vehicle, PAULA I, is contained in a pod 24 inches in diameter and 78 inches long, as illustrated in Figures 4-2 and 4-5. This pod contains the necessary firing circuitry to launch the sounding vehicle, externally-powered strip heaters to maintain payload conditioning temperatures, a flight safety interlock system, and a two-stage paracnute system. The first parachute stage is a three-foot diameter drogue designed to maintain pod stability after jettison from the aircraft. The second stage is a 24 foot diameter parachute intended to maintain vertical altitude stability of the pod for launching of the M58A2 powered sounding vehicle.

External aerodynamic stores will be installed on pylons beneath the wing of the weather reconnaissance aircraft. The external stores will be used to house the sounding vehicle pods. Two vehicles will be carried in each store. The external store will be based upon the aerodynamic shape presently used with the B-47E aircraft as an auxiliary fuel cell. This unit is 47.25 inches in diameter and 299 inches in length as shown in Figure 4-6. Use of this proven unit is recommended since its flight characteristics and effect upon aircraft performance have been established. These effects are noted in a subsequent paragraph. Arrangement of the sounding vehicle pods within the external store is shown in Figure 4-3. On command, the external store ejection ports are opened and the drop pod is ready for jettison. The pod is jettisoned downward with a velocity relative to the aircraft of approximately 50 feet per second which will be obtained through the mechanism of a folded piston and cylinder operated by either a gas generator or a dry gas storage system. Break links will be used to constrain the pod until the jettison system pressure is at the proper operating level. After pod jettison, the ejection ports are closed upon command.

SOUNDING SYSTEM PERFORMANCE

Aircraft flight safety is of paramount importance during the aircraft flight, pod jettison, and sounding rocket launch phases of the mission. A safety

system recommended for the airborne pyrotechnics would include timer inactivation, firing current interrupt, and pyrotechnic short circuiting. These functions can be accomplished by relays activated by aircraft power, by contact switches between pod and aircraft, and by acceleration switches sensing pod jettison acceleration or parachute opening shocks.

The operational sequence of the sounding system is shown in Figures 4-7 through 4-17. Subsequent to pod jettison, a three-foot diameter ribless guide surface drogue parachute will be deployed from the sounding vehicle pod by means of a blast bag system. This system consists of a parachute packed in a heavy duck bag which is turned inside out by gas pressure cartridges, forceably deploying the parachute into the relative wind. After the drogue parachute inflates and stabilizes the pod, it decelerates the pod to a velocity of 275 feet per second at an altitude of 32,750 feet. At this time, the drogue parachute is used to pull a twenty-four foot diameter ring-slot parachute from the pod. The ring-slot parachute was selected for its extreme stability. This main parachute, constructed with a large central vent to facilitate launching of the sounding rocket through it, is attached to the pod with a geodetic suspension line system to further enhance stability and to minimize the pendulum effect. The pod is slowed to a vertical velocity of 55 feet per second by this parachute when the pod has reached the rocket launch altitude of 31,650 feet. The launch angle can be held to within $\pm 5^{\circ}$ of the vertical, with a figure of $\pm 2\ 1/2^{\circ}$ being within the limits of existing parachute technology.

The M5dA2 motor accelerates the sounding vehicle to a velocity of approximately 2,980 feet per second at an altitude of 37,100 feet, whereupon the rocket coasts to its apogee altitude of 135,500 feet. At apogee, a timer within the sounding rocket payload jettisons the nose cone and deploys the descent parachute attached to the meteorological measurement package. The instrument package then collects and transmits meteorological information to the launch aircraft while descending to an altitude of 35,000 feet, an internal barometric switch turns off the telemetry transmitter.

During the 111 seconds of elapsed time from pod jettison to apogee, as detailed in Appendix II, the aircraft will cover a horizontal distance of approximately 95,000 feet from the point of launch. The estimated three sigma dispersion radius of the rocket at apogee is 13,200 feet, produced by the following factors:

1.	5	Degree/second pitch rate at launch.
2.	10	Feet per second horizontal wind relative to the rocket.
3.	0.1	Degree thrust axis misalignment.
4.	0.1	Degree mass imbalance.
5.	2 1/2	Degree Launch angle error.

A combination of aircraft travel and this dispersion at apogee results in a minimum angle from the aircraft zenith to the sonde of approximately 39°. This dispersion is presented in graphical format in Figure 4-18. Performance

of the sounding vehicle is presented in Figures 4-19 through 4-23 and in Appendix III.

Since many M58A2 motors are currently in Air Force stock and available from the Ogden Air Materiel Area, it is anticipated that these motors would be available as GFM. Utilization of this reliable qualified motor will result in a substantial savings of time and cost required in system design and qualification. It is anticipated that B-47E external auxiliary fuel tanks would also be available as GFM for modification during the program.

Timers, switches, parachutes, and other components to be utilized in the air launched sounding rocket system are available as off-the-shelf items which will guarantee aircraft safety without degradation of reliability or performance, and at the same time maintain a low system cost. An additional advantage gained through the use of the standard wing fuel tanks is that in the event of aircraft malfunction the two tanks may be jettisoned. The wing tank separation parachute and associated hardware will be left intact. Consultation with the aircraft manufacturer confirms that this auxiliary tank can be mounted on the B-47E aircraft with no airframe modification. The modification required to mount stores on KC/C-135B aircraft involves installation of hard points in the wing for attachment. The wing is adequately stressed for the loads involved. Ground handling of the tanks may be accomplished with existing equipment as no change in external configuration is anticipated. The same external store will be useable aboard either the KC/C-135B or B-47E.

EFFECT ON AIRCRAFT PERFORMANCE

The external stores containing the four PAULA I Rocketsondes will weigh approximately 2500 pounds and are based on modification of the external underwing fuel stores presently used with the B-47E. The external configuration of the rocket stores will be exactly like the present unit but the internal structure will be somewhat different. The B-47E is equipped for the installation of the external stores pylon at present. The wing design of the KC/C-135B is compatible with the installation of pylons but such an installation has not as yet been made according to the Boeing Airplane Company.

The installation of external stores does not have a great effect, approximately 7 per cent loss, on the performance of either aircraft. Examples of the performance of the B-47E are presented in the Flight Handbook, T.O. 1B-47E-1. Assuming a take-off gross weight of 170,000 pounds, and a constant operational air speed of Mach 0.80, the range of the aircraft is stated as 4,000 miles with the wing tanks installed (T.O. Figure A4-24). During operation at 35,000 foot altitude, under the above flight conditions without wing tanks (T.O. Figure A4-1), the operational range would be 4300 miles, indicating a range loss of 300 miles representing about a seven per cent performance loss. The maximum air speed of the B-47E will be decreased approximately 10 knots (98 per cent RPM) with the rocket pods installed.

AIRCRAFT FLIGHT SAFETY

A factor of paramount importance during W-47E and EC/C-135B operations, particularly with regard to the air launched sounding rockets, is the flight safety of the aircraft. Safety of the aircraft will be assured during all phases of the sounding operation. The PAULA I System will incorporate features to assure that positive separation occurs between the aircraft and the rocket pod at launch, and interlocks to positively prevent functioning or rocket ignition until the proper operational sequencing requirements have been fulfilled. Evaluations have been made of the relative position of the aircraft, pod, and flight vehicle during the sounding operation. These evaluations show that positive clearance will exist between the vehicles throughout the launch and flight sequence. The additional advantage of a proven system for the jettison of the wing tanks further enhances the safety factors.

The following flight safety interlocks will be incorporated in the rocketsonde and its pod to preclude premature rocket firings or firings with the flight vehicle in an incorrect altitude:

a. Interlocks which prevent rocket ignition and timing sequence actuation in the event that the sounding vehicle pod should fail to separate from the external store.

b. Interlocks which prevent rocket ignition and timing sequence actuation in the event the pod drogue parachute or main stabilization parachute fail to deploy.

c. Time interlock to prevent rocket ignition until the pod has reached the point at which stabilized vertical descent begins.

d. Attitude interlock to prevent rocket ignition if the rocket is not stabilized within $\pm 10°$ of the vertical for a preset time period.

e. Provisions for jettison of the external stores in the event of an in-flight emergency or system malfunction.

METEOROLOGICAL INSTRUMENT PACKAGE

The Meteorological instrument package is similar in configuration to the AN/DMQ-6 and AN/DMQ-9 rocketsonde instrument packages which have been designed and built by Bendix for use with the ARCAS sounding rocket. The experience gained in these programs is directly applicable with regard to accelerations, "g" loading, and descent profile in the range we are considering. The pressure sensor used is the Bendix hypsometer, Part No. B-1143967. This hypsometer is insensitive to the attitude changes experienced during handling and ascent. No significant amount of liquid is lost during normal handling and flight attitudes. The liquid chosen

has a relatively low vapor pressure so that explosive boiling does not occur during ascent. Heat is constantly added to the liquid during both vehicle ascent and sonde descent to keep the liquid boiling. Relative humidity will be measured with either the carbon humidity element or an aluminum oxide sensor, while temperature will be determined by a ten mil rod thermistor. These sensors are presented in detail in subsequent paragraphs of this section.

Meteorological instrument packages, to date, have been designed so that a baseline check is required for proper reduction of flight data. This "normal" baseline procedure will be eliminated in the PAULA I instrument package. This will be accomplished by selecting electronic components such that the frequency versus resistance curve is held to close tolerances. The PAULA I nominal audio characteristics will be identical to those of the AN/AMT-13 Radiosonde. Pressure versus resistance and temperature versus resistance sensors that fall within narrow limits will also be used. The instrument package serial number can be coded so as to indicate the particular sensor response characteristics. The introduction of this "standard radiosonde" procedure will have the following advantages at a comparatively small increase in cost.

a. The ability to store exact sensor and radiosonde characteristics for computer data reduction.

b. Elimination of baseline check equipment.

c. Elimination of long preflight procedures.

d. Elimination of a procedural step and its associated probability for error.

e. Ease of use in tactical situations.

The humidity sensors presently available will not lend themselves to being categorized like pressure or temperature sensors. It is suggested that the humidity sensor be used as a relative indication of the moisture content of the air.

A. Meteorological Package Configuration

The basic configuration of the meteorological package is shown in Figure 4-24. The temperature sensor is located in the forward section of the instrument package protected by its own radiation shield and completely exposed to the air stream. The humidity sensor is located in the air path behind the temperature radiation shield. The next compartment aft houses the hypsometer. The actual location of the static pressure port of the hypsometer will be determined in wind tunnel tests. Previous work of this type was accomplished during the AN/AMQ-15 development program under Air Force Contract AF33(600)-37984 and is presented in Bendix technical memorandum FS-59-1 "Wind Tunnel

Investigation to Determine Favorable Static Pressure Orifice Location on AN/AMQ-15 Rocketsonde and Dropsonde Packages".

The commutator with its constant rate of rotation drive motor is located in the compartment aft of the hypsometer, followed by the battery pack and the 300 ± 1 millibar pressure cut-off switch. This cut-off pressure can be established at other pressures if desired. The compartment in the base of the instrument package houses the modulator package, transmitter, antenna coupler, descent parachute and parachute anchor.

Estimated weights of the rocketsonde instrument package are as follows:

TABLE I

Hypsometer (with liquid)	4.0 ozs.
Electronics Scanner and Sensors	58.0 ozs.
Batteries	34.0 ozs.
Relay and Mounting	3.0 ozs.
Aneroid	7.0 ozs.
Hardware	21.0 ozs.
	127.0 ozs. (7.93 lbs.)

During ascent this weight is increased by the ogive nose cone and separation sequencing components of the flight vehicle. The complete instrument package payload weight is approximately 9.5 pounds.

B. Electronic Circuitry

Every effort has been made to utilize components from, and functions similar to, the existing AN/AMT-13 radiosonde. Sonde differences, as recommended in this report, are attributable to one of three reasons and in each case are discussed in detail as they appear in this report.

a. System reliability as governed by aircraft environment and flight vehicle characteristics and the higher "cost-per-shot" in comparison to AN/AMT-13 Radiosonde drops.

b. Distance between instrument package and aircraft during sonde descent and the resulting transmitter power requirements.

c. Sequence of vertical data collection (amount of each sensor's intelligence collected based on the altitude envelope and rate of descent of the instrument package).

The basic schematic for the electronic packages is shown in Figure 4-25. The physical layout of the package is shown in Figure 4-24. Inspection of the schematic diagram shows that the frequency of the blocking oscillator, Q1, is dependent on the value of C1, C3, R1, and the resistance placed between R1 and ground. R2 and R3 determine the "between segment frequency". The motor driven scanner chooses the sensor intelligence or reference resistance to be transmitted. The oscillator operates at frequencies between 2450 and 6110 pulses per second, the same frequencies used in the AN/AMT-13. These pulses are then amplified by Q2, which drives the triggered blocking oscillator Q3. Q3 and its associated circuitry produce a nominal 16 microsecond pulse for each trigger pulse received. Q4 is a current switch with a pulse transformer T2 which has a large step-up ratio (1:28), providing approximately 475 volts at the secondary. This positive voltage pulse is applied to the plate circuits of the push-pull r.f. oscillator V1 and V2. The r.f. oscillator develops 16 usec. pulses of 403 mc energy which, in turn, are coupled to the one-half wave length end fed antenna through the RFI filter. This filter reduces the harmonic emanations to a level 60 db below the fundamental. The nominal peak radiated power is approximately 30 watts at apogee and will not be less than 18 watts at flight termination.

Relay K1 is a magnetically latched relay which may be reset to "off" position electrically. This relay circuitry allows access to the battery to provide for external charging. External power may also be applied for long term operation and checkout prior to flight.

The battery pack consists of three six-volt nickel cadmium batteries connected in series. The rated current capacity of this battery pack is 750 milliampere hours. In the case of this package the current drain will be:

TABLE II

Motor Scanner	30 MA
Tubes and Oscillators	200 MA
Pulser	650 MA
Hypsometer	250 MA
Total	1,150 MA

For the purpose of proving the safety factor applied to the batteries, a very conservative calculation is presented below taking into account our high rate of current drain, flight time, and the cold environment:

1. 750 MAH X 4 = 3,000 MA for 15 minutes of useful battery life.

2. 3,000 MA derated by 50 per cent = 1,500 MA for 15 minutes of useful battery life in cold environment.

3. Flight time will be:

TABLE III

Turn on and package drops	0.5 min.
Chute Stabilization	0.5 min.
Rocket Ascent	2.0 min.
Meteorological packaging descent	10.0 min.
Total	13.0 min.

Inspection of these figures, which are very conservative, indicates, that applying heavy safety corrections, we will have approximately 13 per cent of our battery life still available when the flight is terminated under the worst conditions. In practice this figure will more realistically approach 40 per cent.

The battery is assisted in the delivery of the required five ampere surges by the storage capacitor C8 and the battery supply to the Q1 circuitry is voltage regulated by the zener diode VR1. The choice of nickel cadmium over other possible types of batteries is based upon a compromise of reliability, size, cost, maintenance, and shelf life. More exotic batteries are available which are lighter in weight but their cost is significantly greater. The nickel cadmium cell recommended for use in this design offers a minimum shelf life of three years with no maintenance other than a charge cycle prior to intended use. The battery may be shipped and stored in the instrument itself and charged through an umbilical connection. Nickel cadmium batteries have excellent low temperature characteristics making the 50 per cent derating for cold environments an extremely conservative figure.

The Altitude Termination Switch consists of a snap-action aneroid which closes an electrical circuit on descending to a specific altitude. This device will actuate at 35,000 feet (250 millibars) and terminate the flight by turning off the transmitter. This circuit

operation is inhibited by the nose cone switch, S-1, which prevents the altitude termination switch from performing its function until nose cone separation has occurred. The termination of transmission will define the pressure altitude at 250 ± 1.0 millibars. This point may be used as a reference point for data reduction purposes. It is possible to adjust the Altitude Termination Switch to provide for cut-off altitudes other than 35,000 feet.

The motor-scanner system will be similar to that used in the present AN/AMT-13 Radiosonde in that the sensors will be scanned on a time sharing basis. However, since the initial descent velocity is approximately 500 feet per second and the termination velocity is 64 feet per second (which is a somewhat faster rate than the AN/AMT-13) some change in the scan rate is required. The scanner will provide one scan every three seconds. The AN/AMT-13 scan data at a rate of once each six seconds. The commutator pattern used in the instrument package will be changed from that of the AN/AMT-13, to provide the necessary switching time required to maintain compatibility with the AN/AMQ-19 system. The scan rate of the instrument package will consist of 200 milliseconds of "on" contact time and 50 milliseconds of "off" contact time. The scan sequence in the AN/AMT-13 consists of a high reference, a low reference, two pressures, four temperatures, and four humidities per scan. Since most interest centers on pressure and temperature in the upper atmosphere, the scan sequence will be changed to provide four pressures and two humidities per scan in the following manner: High Reference, Temperature, Pressure, Humidity, Temperature, Pressure, Low Reference, Temperature, Pressure, Humidity, Temperature, Pressure.

This system will allow accurate determination of density by the method outlined later in this report

C. Transmitter Design Considerations

The transmitter is designed to be effective under even the most adverse conditions. Power requirements have been carefully studied, both at Apogee and through flight termination. In the case of the transmitter located at apogee taking the basic radiated power equation and using the minimum transmitter radiated power of 1d watts:

1. Transmitter at Apogee

$$P_r = \frac{P_T \; G_r \; G_T \; \lambda^2}{(4 \pi \; R)^2}$$

P_r = Power at Receiving Antenna

P_T = Transmitter Power

G_r = Gain of Receiving Antenna over an Isotropic Radiator

G_T = Gain of Transmitting Antenna over an Isotropic Radiator

λ = Wavelength in Meters

R = Distance in Meters

Gain of half-wave dipole, G_T, is equal to 1.64 of isotropic radiator.

At apogee assuming worst conditions, greatest angle of Trajectory in direction of the aircraft gives an angle of 41° below the horizontal plane of the transmitter. A typical 403 mc pulsed transmitter antenna pattern shows this angle to be the half power points.

Assuming half-power for both transmitting antenna and receiving antenna, and distance from Figure 4-18 the resulting equation is:

$$P_r = \frac{(18)\left(\frac{1.64^2}{2}\right)(0.75)^2}{4\pi\,(4.0036 \times 10^4)^2}$$

$$P_r = \frac{(18)\,(.6724)\,(.5625)}{(12.5664)\,(4.0036 \times 10^4)^2}$$

$$P_r = \frac{6.808}{(5.0311)^2 \times 10^{10}}$$

$$P_r = \frac{6.808}{2.5312 \times 10^{11}}$$

$$P_r = 2.6896 \times 10^{-11} \text{ watts}$$

To calculate the power in terms of microvolts at the receiver, we use Ohms law:

$$P = \frac{E^2}{R}$$

where:

P = P_r = Power in watts at the receiver

E = Power in Microvolts at the receiver

R = 50 ohms Receiver input impedance

$$E = \sqrt{P_T R}$$

$$E = \sqrt{26.896 \times 10^{-12} \times 50}$$

$$E = 7.07 \sqrt{26.896 \times 10^{-12}}$$

$$E = 7.07 \times 5.19 \times 10^{-6}$$

$$E = 36.69 \text{ uv to receiving antenna at apogee}$$

2. Transmitter located at Termination point.

$$P_r = \frac{P_T G_r G_T \lambda^2}{(4\pi R)^2}$$

P_r = Power at receiving antenna

P_T = Transmitter power

G_r = Gain of receiving antenna over an isotropic radiator

G_T = Gain of transmitting antenna over an isotropic radiator

λ = Wavelength in meters

R = Distance in meters at flight termination

Assuming an aircraft speed of 430 knots T.A.S. and a nine minute descent time to flight level plus three minutes from drop to apogee.

R = 168,965.6 meters.

A corner reflector receiving antenna will be used. This antenna has a 3 db gain over a regular dipole.

$$G_r = 2(1.64) = 3.28.$$

$$P_r = \frac{(18)\ (3.28)\ (1.64)\ (.75)^2}{(4\pi)\ (1.6897 \times 10^5)^2}$$

$$P_r = \frac{54.464}{(21.2335 \times 105)^2}$$

$$P_r = \frac{54.464}{450.862 \times 10^{10}}$$

$$P_r = 12.08 \times 10^{-12} \text{ watts}$$

There signal level in microvolts at the receiver:

$$P = \frac{E^2}{R}$$

$$E = \sqrt{PR}$$

$$P = P_r$$

$$R = 50 \text{ ohms}$$

$$E = 7.07 \sqrt{12.08 \times 10^{-12}}$$

$$E = (7.07)(3.475 \times 10^{-6})$$

$$E = 24.8 \text{ uv at the receiving antenna at flight termination.}$$

3. Calculation for Maximum Range of Transmitter:

E = 14 uv at receiver, minimum sensitivity of Receiver R-1196/AMR-19

$E^2 = P_r R$ $\qquad R = 50$ ohms

$196 \times 10^{-12} = P_r (50)$

$3.92 \times 10^{-12} = P_r$

$$P_r = \frac{P_T G_r G_T \lambda^2}{(4\pi R)^2} \qquad R^2 = \frac{P_T G_r G_T \lambda^2}{16 \pi^2 P_r}$$

$$R = \sqrt{\frac{P_T G_r G_T \lambda^2}{16 \pi^2 P_r}}$$

$$R = \sqrt{\frac{54.464}{(157.9136)(3.92 \times 10^{-12})}}$$

$$R = \sqrt{\frac{54.464}{6.1902 \times 10^{-10}}}$$

$$R = \sqrt{8.798423 \times 10^{10}}$$

$$R = 296{,}600 \text{ meters}$$

$$R = 184.338 \text{ miles statute}$$

Antenna patterns from a typical 403 mc pulsed unit using a half-wave, end-fed, dipole antenna are shown in Figures 4-26, 4-27, and 4-28.

The three db points were selected from these typical patterns for use in the range calculations shown earlier in this section.

With the radiation angles that will be encountered by the rocketsonde package the half-wave dipole antenna is definitely the best suited for this application.

Careful study of these calculations indicate that the transmitter design allows ample power for this requirement. It is anticipated that the upward looking receiving dipole antenna and its reflective shield will be mounted as shown in Figure 4-29.

Another change from the AN/AMT-13 Radiosonde is the use of the push-pull carrier oscillator rather than the single-ended oscillator configuration. Two reasons for this change are:

a. Suppression of undesirable radio frequency interference in accordance with the requirements of MIL-I-6181, requires the use of filtering between the oscillator and the antenna. Such filters introduce losses, requiring a higher initial level of power.

b. Use of the push-pull oscillator of proper design results in a lower level of even harmonic radiation.

The radio frequency interference filter used in this design is constructed in the well known strip-line filter configuration. It will consist of a double layer of etched printed circuit board which produces a uniform design at an economical price.

D. Sensors

After a careful study of the environmental profile through which the rocketsonde must descend during transmission of data, a selection of

sensors was made. The Bendix aypsometer Part No. B-1143967, similar to that currently used in the AN/DMQ-9 rocketsonde, will be used for pressure measurement. This instrument is ideal for this application and will furnish more pressure data of greater accuracy in the range we are considering than a conventional radiosonde type baroswitch. It does not require temperature corrections to the data obtained or baseline check prior to the use of the instrument. Humidity sensing will be accomplished with either a miniature carbon humidity element, or the newer aluminum oxide element still under development. Temperature will be measured with a ten mil (diameter) ceramic rod thermistor. Each of these sensors is discussed in detail in following paragraphs of this report. Since the development and testing of new sensing techniques for the measurement of atmospheric parameters is a costly and time consuming project, state-of-the-art sensing techniques are recommended for use with PAULA I. Slight modifications have been made in some cases to better adapt these sensors to the specific problems associated with rocket sounding at the required altitudes.

1. Temperature

Various types of temperature sensors (thermistors, wire wound resistors, thermocouples) can be used to collect upper atmosphere data. The problem of measuring temperature during descent from high altitude is to mount the temperature sensing element in a manner which will permit proper sensing of ambient conditions and to minimize sensing errors due to solar radiation impinging on the sensor. Care must also be taken to eliminate the conduction of heat between the sensor and the sounding vehicle. In addition, errors may be introduced in the sensed temperature by stagnation heating of the sensor, by the measuring current passing through the sensing element, and by the time lag of the sensor.

Certain requirements suggest contradictory solutions. For example, an immersion type temperature sensor should be larger than the mean free path of a molecule in order to properly sense the environment, also the larger the sensor the less the self-heating caused by the measuring current. However, the larger the sensor the longer the time lag error that will be introduced into the system. Where such contradictory criteria affect the final sensor shape, a detailed study of the effects of each error source is needed in order to determine the final sensor configuration. Problems of this type were encountered and solved in the development of the AN/AMQ-15 and AN/DMQ-9 Rocketsondes. Bendix Friez has developed a sensor we believe to have the best combination of characteristics for upper atmospheric soundings. This sensor, an aluminum coated 0.010 inch

diameter rod thermistor, is suggested for use as the temperature sensor in this system.

The PAULA I instrument package will operate over the altitude range of 30,000 to 120,000 feet. Over this altitude range, the temperature variation to be expected will be approximately 0°C to -80°C. The temperature sensor in this vehicle can be designed to take advantage of this fairly small temperature range. The resistance versus temperature characteristics of the thermistor will be controlled so that the complete audio frequency spectrum of the sonde will be used to cover a temperature range of approximately +10°C to -90°C. This will result in greater temperature resolution and, therefore, greater ease and accuracy of data reduction. This range has been predicted through use of known atmospheric temperature ranges.

a. Mounting - The sensor mounting configuration has been evolved as the result of careful consideration of each of the sources of errors mentioned in the preceding paragraph. This configuration is shown in Figure 4-30.

In order to remove all doubt as to the undisturbed nature of the air sample, the temperature sensor was placed at the front, or descending end, of the instrument package. There is no possible way for the air sample to become contaminated by contact with massive portions of the package before impinging upon the thermistor.

In previous configurations (such as the AN/AMT-6 Radiosonde) the temperature sensor has been located in the proximity of the r.f. section, where considerable disturbance of the air sample was possible. Thermistor locations other than the forward end of the instrument package have been used, but they fail to meet all of the requirements for consistent temperature measurement. For instance, the possible heating effect of interrupted radio frequency radiation could have been significant (i.e., for 100 mw average power emanating isotropically from a point source 2 cm distant, a hypothetical 10 mil diameter spherical absorber would absorb four microwatts of power). This quantity, could introduce a sizeable error in the bead thermistor measurement and a more radical error in a rod thermistor placed in the same proximity. For this reason, as well as to obtain a better radiation pattern, the antenna on the instrument package has been placed at the rear of the unit.

Convective heat transfer has been maximized by giving the sensor exposure to air flow in the forward mounting location.

Solar radiation impinging upon the conical shielf contains approximately 50 per cent visible and ultraviolet and 50 per cent infrared radiation. The aluminum shield reflects some 90 per cent of the visible radiation and 95 per cent of the infrared radiation. With radiation normally impinging upon only a portion of the outer surface of the cone, and two complete conical surfaces being cooled convectively, the temperature rise of this shield is small. Reradiated energy is reflected from the aluminized thermistor (95 per cent reflective to this radiation), producing negligible heating of the thermistor.

Radiation from below (earth's surface, cloud tops, and air) is still another factor. This radiation is assumed to be effectively that from a blackbody at approximately 235°K. The up-welling radiation reaching the thermistor is reflected by the aluminum coating. That radiation reaching the conical shield is absorbed by the black internal surface and dissipated away by the convective heat removal.

The radiational heat contribution from the rocketsonde body is reduced to negligible proportions by the conical shield and the disc shield above it.

Heat conduction from the structure is kept to a minimum by using constantan support legs (constantan has a thermal conductivity of approximately one-tenth that of copper).

The thermistor is attached to constantan leads which are extended and curved in a manner to expose a large heat conduction path to the convective cooling of the air stream. The thermistor leads (platinum-iridium alloy) also have low thermal conductivity and very small cross sectional area.

Electrical heating is a function of the resistance being measured, and is never greater than twenty-five (25) microwatts.

Total aerodynamic heating at the highest expected descent velocity is approximately 5°C. If a recovery factor (R) of 0.9 ± 0.1 is used, it will cover the practical range of recovery factors and yet most of the error will be removed, using:

$$T\ (\text{aerodynamic heating}) = \frac{RV^2}{2Cp}$$

This reduces the uncertainty to approximately 1.5°C at the highest altitude at the descent velocity of this instrument package.

The time lag error will be a function of vertical temperature gradient, descent velocity, and the time constant of the sensor. The thermistor time constant is 1 1/2 seconds at 100,000 feet. The error due to lag will be the product of the thermistor time constant and the temperature gradient. For example, if the descent velocity is 500 feet per second and the temperature gradient is constant at 1 degree per 1,000 feet, the error due to lag would be:

$$1°C/1{,}000 \text{ ft.} \times 1.5 \text{ sec.} \times 500 \text{ ft./sec.} = 0.75°C$$

b. Error Analysis - Certain assumptions can be made to permit an estimate of the accuracy anticipated with this sensor. The factors in the heat balance will be considered first.

A broad estimate of the convective heat transfer will be used. Laboratory tests at 106,000 feet density altitude, and 37 feet per second air speed, yielded a convective heat removal of one millivatt per degree Centigrade temperature difference between the air and the thermistor. This test was performed with the thermistor mounted in a specially constructed housing, such that conductive and radiated heat transfer were reduced to a negligible magnitude. The inner wall of two inch diameter by two feet long, plastic tube was lined with aluminum foil. A fan was installed at one end of the tube to induce air flow. The thermistor under test was placed toward the opposite end of the tube (air intake end) within a concentric one inch diameter cardboard tube three inches long. The thermistor was supported across the air flow path by its leads which were approximately 3/8 inch long.

A thermistor one centimeter long by 0.030 cm in diameter has a projected area of 0.030 sq. cm. This intercepts 3.8 mw of direct solar radiation. This radiation consists of 55 per cent visible plus ultraviolet energy, and 45 per cent infrared energy. For simplicity, use 50-50 energy distribution, and compare white versus aluminum coated thermistors. Table IV presents a summary of the analysis:

TABLE IV

	Aluminum	White
Visible Absorption	10%	2%
Infrared	5%	100%
Visible Power Absorbed (uw)	190	38
Infrared	95	1900
Total Power Absorbed (uw)	285	1938

This result demonstrates the usefulness of the aluminum coating on the thermistor and the improvement over the normal white coating.

However, the direct solar rays never reach the sensor. They are received on a second reflecting surface (the cone) and later received at the thermistor as long wave radiation. Therefore, only a maximum ten per cent of the solar radiation will reach the thermistor, and this will be infrared. With 0.38 milliwatts reaching the thermistor and reflected at 95 per cent, the solar energy input is reduced to 0.02 mw (or 20 microwatts, maximum).

It is estimated that the projected area will receive radiation from below of approximately 1900 microwatts. However, with the reflectivity of aluminum equal to 95 per cent, only 95 microwatts of this energy are absorbed. The energy absorbed on the conical shield is lost to convection and reradiated at a temperature very near ambient temperature and is thus neglected.

The structure is isolated from the sensor by triple radiation shielding and contributes a negligible heat input.

The constantan supports to the thermistor are isolated from the shields by the epoxy glue used to affix them. Therefore, using a double conduction path (two supports), we find a possible heat conduction of one milliwatt per degree of temperature difference between the two ends of the constantan. This has eight centimeters of conduction path in which to dissipate itself by convective cooling.

The 0.003 inch diameter platinum leads are typically 0.5 inches long. They (both together) can conduct 50 microwatt per degree of temperature difference between their ends. This is greatly reduced by convection, which is of the order of 50 microwatts

per centimeter per degree above ambient in the high altitude case. These two factors will very nearly cancel each other, contributing only a negligible conduction input to the thermistor. If we use 50 microwatts, for conduction error we shall be conservative. In addition, an error will be caused by the dissipation of electrical power in the thermistor. The maximum electrical power input is 25 microwatts.

The summary of these errors may be seen in Table V.

TABLE V

Solar Radiation:	20 microwatts
Radiation from below:	95 microwatts
Conduction:	50 microwatts
Electrical:	25 microwatts
Radiation from structure:	Negligible
Total	190 microwatts

Convection will remove heat at the rate of approximately 1,000 microwatts per degree of temperature difference between the sensor and the air. The 190 microwatts inserted therefore implies a corresponding 190 microwatts to be removed by convection, requiring a sensor temperature elevation of 0.190°C (or 0.2°C) above the ambient air temperature. This figure represents the maximum predicted error due to heat balance.

The other errors, as discussed earlier are aerodynamic heating (0.5°C error after correction), time lag, and calibration.

The Bendix Friez calibrations can be shown to be accurate to ±0.1°C, and the stability maintained high by artificial aging before calibration. The time lag error is a factor which must be handled by computation. Generally, at eight seconds lag, or 2,000 feet in the high altitudes, this will not introduce more than 1°C of error. These errors are summarized in Table VI.

TABLE VI

Heat balance	±0.2°C
Aerodynamic heating	±0.5°C
Time lag	±1.0°C
Sensor calibration	±0.1°C
Total possible error	±1.8°C
Probable error (RMS)	1.4°C

This value represents the total probable error contributed by the sensor and its mounting.

2. Humidity

The humidity sensors presently used in synoptic sounding are not used to measure humidity at temperatures below -40°C. Originally this cut-off was not considered a serious handicap. However, meteorologists have learned with the advent of satellite and rocket meteorological data that small changes in the constituents of the upper atmosphere can have a profound effect on the surface weather patterns. For this reason, it was considered desirable to include the capability of measuring humidity in this instrument package. The humidity sensor is located in clips directly beneath the thermistor at the forward end of the instrument package, as shown in Figure 4-30.

In this location an unobstructed flow of air will pass over the sensor. The clips holding the sensor in place prevent slippage of the sensor during maximum acceleration conditions. The sensor will be smaller and lower in mass than the standard sensors presently in use to improve its low temperature operational characteristics.

a. Carbon Element - For this application, where cost and availability are major considerations, a modified carbon humidity element is suggested for use as the humidity sensor. The response of this sensor at low temperatures leaves much to be desired but it is the best proven humidity sensor available for use in an inexpensive expendable package.

b. Aluminum Oxide Element - Another possible element for use in this sounding application is the Aluminum Oxide Humidity

Element. Sensors of this type are under development at Bendix Friez and possess attributes that suit it for this particular application where the expected moisture concentration is low.

The aluminum oxide humidity element gives indications of relative humidity with changes in the electrical properties of an anodized aluminum oxide layer. The need for a simple, stable, hygrometer which is capable of indicating and recording relative humidity over a wide range of conditions has long been recognized. The feasibility of the sensing element has been demonstrated by test elements manufactured at Bendix Friez.

Many indirect measuring instruments suffer from disadvantages such as hysteresis, long time period drift, large temperature coefficients, or high sensitivity to contamination. Although absolute methods such as chemical or dewpoint determinations avoid these defects, they are not always suitable for continuous recording or instrumentation. It is, therefore, very desirable that the indication of humidity be presented directly in the form of an electrical parameter without the need for complex ancillary equipment. Two additional features required for successful instrumentation are that the speed of response be rapid, and that no temperature measurement be additionally required. The Aluminum Oxide element fulfills many of these necessary requirements. It behaves as an electrical transducer responding to changes in Relative Humidity by variation of its capacitance and resistance. The additional parameters of impedance can also be correlated to direct measurement instrumentation. The temperature range through which we have tested the capabilities of the sensor have been from -100°F to +125°F, and a pressure change from 1,000 mb to below 2 mb. During all of these changes, the element is capable of indicating from 0 to 100 per cent changes in relative humidity, even though it frequently could encounter rain or snow during flight.

A porous oxide layer (formed by anodizing with an acid electrolytic) provides by virtue of its structure, a large surface area for absorption. In general, the capacitance of a condenser formed between two conducting layers would vary with the absorption of water vapor into the dielectric. The humidity sensing element consists of a base of aluminum, an oxide made by anodizing the base material, and an evaporated conductive coating of aluminum metal. An increase in relative humidity causes a decrease in impedance, and the reverse being true when the relative humidity decreases. The resistance and

capacitance are recorded and calculated in terms of relative humidity and water vapor content.

It has been observed, and we have substantiated this phenomenon in the laboratory, that a hysteresis effect does occur with the aluminum oxide humidity element on exposure to humidities above 90 per cent relative humidity. We would like to suggest a possible reason for the existence of this condition. The sensor construction, either disc or rod type, is essentially dependent upon the anodizing process. This process of boiling the sensors in the oxidizing acid solution, tends to open the many hundreds of minute pores in the surface of the sensor. These pores are, quite logically, now extremely sensitive to any change in moisture content. Since the pores are so sensitive, they are extremely reluctant to give up any absorbed moisture. A method of forced migration of these minute water vapor particles to the surface will permit a complete range of relative humidity measurement. This has been verified such that once the moisture has been driven off, either by air or a heat source, the element will immediately return to its original resistance and capacitance value calibration.

The aluminum oxide humidity element can be constructed either in disc or rod type construction. Rods have been made in the Friez Engineering Laboratory as small as one-half inch in length and approximately one-sixteenth inch in diameter. The disc type construction has been prepared approximately one-quarter inch in diameter and one-sixteenth inches in thickness. Both types of construction can be fabricated such that the resistance and capacitance nominal values can vary in accordance with the ancillary electronic instrumentation. Resistance value elements have been prepared in the nominal range of seven thousand to thirty-five thousand ohms at [illegible], and 33 per cent relative humidity. The elements can also be accurately calibrated to measure super saturation or dew content quite easily.

The sensor will operate in a range of [illegible] to 100 per cent relative humidity. The sensitivity can be increased in the high or low portion of the relative humidity by proper design. The long term stability, life expectancy, and aging effects of the sensor are all not completely defined. The speed of response has been observed at Friez to be less than two seconds for a change in humidity from [illegible] to 90 per cent relative humidity at 25°C. Considerable data is being compiled on the effects on response of varying low temperatures. One additional advantage to the aluminum oxide sensor is that it

does not have to be baselined prior to rocket flight, since a nominal resistance capacitance value could be specified and maintained.

3. Pressure Altitude

The Bendix Corporation has recently perfected a small, lightweight, expendable hypsometric pressure sensor suitable for use where the rate of change of pressure with time is positive or varying in sign. It has been designed primarily for use in descending radiosondes in the pressure range of 0.2 mb to 300 mb but may be adapted for other applications and different pressure ranges. In operation, a thermistor is used to measure the boiling temperature of a pure liquid in phase equilibrium with its vapor. From this temperature measurement, and known physical properties of the liquid employed, the pressure environment in which the instrument is located may be accurately determined. This unit, under laboratory conditions, offers the accuracies shown in Table VII.

The hypsometer employs a percolator column - total reflux system of such configuration that virtually no working fluid is lost, even when tumbling. During its period of operation however, the hypsometer must be essentially upright. The "spill-proof' design is a key feature of the unit resulting in small physical size and low thermal mass which are necessary requirements for minimum power consumption. The instrument is always armed and ready to operate, requiring only the actuation of the heater circuit just prior to the time pressure observations are to be made.

This hypsometer has been made electrically compatible with most existing meteorological sounding systems and can be installed within the vehicle by any convenient means that will result in proper orientation during its operating period. The pressure sampling tube can be opened to the atmosphere wherever the aerodynamic features of the vehicle and the needs of the user permit.

TABLE VII

Range:	2.0 mb to 350 mb
Accuracy: (Laboratory conditions)	2 mb to 20 mb: ± 0.25 mb 20 mb to 300 mb: ± 0.5 mb
Heater Power:	Approximately 5 watts (any convenient voltage)
Measurement Power:	Up to 700 microwatts dissipation through the thermistor
Output Form:	Resistance analog of boiling liquid vapor equilibrium temperature
Envelope:	Cylindrical, 2" diameter by 4" high

a. Hypsometer - A hypsometer has been chosen for the pressure sensor in this rocket sounding vehicle because it offers a wide operating range, high accuracy, and low cost as an expendable pressure sensor. It is a fairly simple device and is readily adaptable to radiosonde circuitry.

The hypsometer vapor and the subject medium are allowed to contact each other so that pressure equilibrium is assured. Diffusion mixing is prevented at the temperature sensor by the flow of vapor from evaporating fluid. The vapor may be lost or it may be condensed and returned to the boiler. The design problem may best be illustrated by discussing the heat transfer in a hypsometer.

$$Q_{in} - C_b \frac{d\theta}{dt} - L_v \frac{dm}{dt} - c_f (\theta_c - \theta) \frac{dm}{dt}$$

$$- k_1 (\theta - \theta_c) - k_2 (\theta - \theta_0) = 0$$

where: Q_{in} is power output

C_b is to the total heat capacity of the boiler and fluid

θ is the boiling point

L_v is the latent heat of vaporization

$\frac{dm}{dt}$ is the mass evaporation rate

c_f is the specific heat of the fluid

θ_c is the condenser temperature

k_1 is the thermal conductance between the boiler and the condenser

C_c is the total heat capacity of the condenser

The last term expresses loss directly to the environment at temperature θ through conductance k_2 in parallel with k_1.

If condensation refluxing is not used, the fourth and fifth terms are zero. When a condenser is used, θ_c can be coarsely programmed by the proper choice of k_1.

$\frac{d\Theta}{dt}$ is determined by the fluid characteristics and the pressure-time profile. $L_v \frac{dm}{dt}$ is limited to values less than those at which liquid loss occurs through violent boiling. As a result, a particular hypsometer design, fluid, and boiler power must be used in a pressure-time regime having rather narrow limits. This last necessity is the source of the most difficulty in hypsometer design.

If the power is constant, variations in the remaining terms must balance. In an ascending hypsometer $\frac{d\Theta}{dt}$ is negative so that the the second term acts as a power source, and very little external power is necessary. In a constant pressure-altitude sounding, $\frac{d\Theta}{dt}$ is very small and, over long periods, averages near zero. Only enough power is necessary for following the expected fluctuations in pressure. In a descending sounding, all these terms have sizable values and it is of the essence to optimize for a maximum $\frac{dm}{dt}$ and a minimum C_b. Most of the boiler power is expended in raising the temperature of the thermal masses C_b and C_c.

In practice, the heat transfer equation serves as a design guide rather than as a precise criterion. The difficulties of achieving smooth boiling over large pressure ranges of simulating precise pressure-time profiles for testing and of acquiring precise reference data in design tests usually outweigh the problems directly implied in the heat transfer equation.

The scale law for the hypsometer may be developed by utilizing the Clapeyron-Clausius equation as follows:

$$\frac{dT}{dp} = \frac{T\,(V_g - V_L)}{L}$$

where: T is the absolute temperature

L is the molar heat of vaporization

V_g is the molar volume of the vapor

V_L is the molar volume of the liquid

p is absolute pressure

$\frac{dT}{dp}$ is a measure of the hypsometric sensitivity

Since $V_g \gg V_L$

$$\frac{dT}{dp} = \frac{T\,V_g}{L}$$

Under the conditions of interest, the vapor may be treated as an ideal gas so that,

$$v_g = \frac{RT}{p}$$

and:

$$\frac{dT}{dp} = \frac{RT^2}{pL}$$

It is seen then that operating temperature should be high and molar heat of vaporization should be small in order to achieve high hypsometric sensitivity.

The temperature will be measured in this hypsometer by means of a thermistor. The variation of the resistance of the thermistor with temperature is described to the first approximation by the following equation:

$$r = Ae^{-B/T}$$

where: r = resistance

A and B are constants

e is the base of natural logarithms

T is the absolute temperature

differentiating gives:

$$\frac{1}{r}\frac{dr}{dt} = -B/T^2$$

Combining the fourth and sixth equations above gives:

$$\frac{dr}{r} = \left(\frac{BR}{L}\right)\frac{dp}{p}$$

This equation shows that the fractional change in the resistance of the thermistor is proportional to the fractional change in the pressure measured. This type of scale law preserves the sensitivity of the measuring device throughout the large range of pressure.

The basic design of the hypsometer proposed for this rocketsonde was established under Contract No. AF33(600)-41821, by the Bendix

Research Laboratories Division. This design is shown in Figure 4-31. The container used is a small Dewar flask which is used to provide the maximum thermal isolation between a hypsometer and its environment. The pressure port is of a no-spill design and is very effective. With this design the hypsometer containing fluid may be tumbled quite violently without spilling any liquid. The hypsometer may be loaded with liquid prior to flight vehicle installation aboard the aircraft and no further seal is required. The tube used to supply connection to the pressure to be measured must be large enough so that the flow of boiling vapor does not create a back-pressure which is large in comparison with the pressure being measured. The cap on the hypsometer is a rather heavy metal piece which has a high heat capacity and which serves to condense some of the vapor and return the liquid to the boiling chamber. This feature is necessary to minimize the amount of liquid required to keep the hypsometer operating throughout the flight. The heater and percolator are designed to promote smooth, even boiling of the liquid and to supply a uniform flow of liquid to wet the thermistor. In actual practice the liquid will flow somewhat unevenly onto the thermistor and for this reason a small amount of felt is placed on the thermistor to prevent sharp fluctuations in the temperature measured by the thermistor.

The thermistor is a small bead thermistor and is chosen to have a resistance value suitable for the temperature range of the boiling liquid and the characteristics of the telemetry used. For the PAULA I rocketsonde we plan to use two thermistors connected in series and to select the two thermistors so that the resistance versus temperature characteristics of the combination will be exactly the same from one hypsometer to another. By this means, the need for baseline checks or for identification of the particular hypsometer used will not be required in order to reduce the data.

A hypsometer liquid will be selected such that its boiling temperature at the maximum altitude of the rocketsonde will be between 20 and 35°C. This is done so that the liquid will not have any tendency to flash vaporize when the rocketsonde is launched. This is one of the most important characteristics the liquid must have. Other important characteristics are its purity, its stability and storeability, its viscosity, surface tension and its ability to dissolve air. Air dissolved in the liquid will make it boil unevenly and bump violently and thus entertain a great deal of liquid in the vapor.

In operation, constant power will be supplied to the heater from the time the rocketsonde is launched. When the rocketsonde starts

its descent, the liquid will surround the heater and boiling will begin provided a high enough altitude has been reached. If the rocketsonde fails to reach its expected altitude, the liquid may be too cold to boil and the heater will have to supply heat for some period of time before the boiling temperature is reached. If the rocket reaches or exceeds its designated altitude, boiling will begin when the descent starts.

Hypsometers of this general design have been flown with the AN/DMQ-9 rocketsonde with good results. It is anticipated that even better results will be achieved by limiting operation of the hypsometer to a range of 120,000 feet to 30,000 feet.

4. Density

Since the vehicle will have the capability of measuring temperature and pressure the air density can be calculated using the Ideal Gas Law.

$$P = \frac{\rho RT}{M}$$

or

$$\rho = \frac{MP}{RT}$$

Where ρ is density, P pressure, T temperature, R the universal gas constant and M the mean molecular weight of the air.

The molecular weight of air is constant to an altitude of approximately 250,000 feet where oxygen molecules begin to dissociate. Therefore, for flight altitude expected using this vehicle the mean molecular weight of the air is constant and density can be calculated using the measured temperature and pressure values.

PAULA I AND THE AN/AMQ-19 METEOROLOGICAL SYSTEM

The PAULA I Rocketsonde is compatible with the AN/AMQ-19 Meteorological System and the AN/GMH-4 Data Analysis Central. With the addition of the PAULA I system, several additions will be made to the AN/AMQ-19 System. A block diagram of this system is presented in Figure 4-33. There are three major operational differences between the PAULA I and the AN/AMT-13 Radiosondes. These are scan rate, commutator contact time and data collection sequence. Each of these items has been discussed quantitatively elsewhere in this report. These three radiosonde output characteristics are completely compatible with the AN/AMQ-19 System data input requirements.

To achieve optimum data collection performance from the PAULA I Rocketsonde, several additions are required in the airborne launch platform. Since the rocketsonde ascends to altitudes far above the launching altitude, and transmits from these altitudes, improved reception of weather data is accomplished by utilizing an antenna located in the aft section of the aircraft. This antenna, as shown in Figure 4-29, is activated and the present AT896/A antenna (located beneath the aircraft) deactivated, by a switch located on the Rocket Control Panel as shown in Figure 4-32. The Rocket Control Panel is required to match the standard control panels associated with the AN/AMQ-19 System in order to select, arm and dispense the rocketsondes. Separate jettison controls are required since the rocketsondes are contained in external stores located beneath the wings and are a separate subsystem from the dropsonde operation.

The PAULA I Rocketsonde differs from the AN/AMT-13 Radiosonde in another important respect, namely, the sensors used for detecting weather conditions. The PAULA I Rocketsonde utilizes a hypsometer for sensing pressure, a thermistor for sensing temperature and a carbon-type electrical hygrometer for sensing relative humidity. The resistance curves for these sensors are different from the resistance curves for the sensors used in the AN/AMT-13 and the correct transfer function must be known in order to reduce the collected data accurately. In addition, the advanced design of PAULA I Rocketsonde has made possible the elimination of baseline correction for each sensor of every sonde. The electronics, transmitter, and sensors of each PAULA I rocketsonde will be assembled and adjusted to comply with the characteristics of one of several groups of calibration data. The particular group of calibration data which applies to a specific PAULA I instrument package will be indicated by a code number prominently displayed on the package, ogive nose cone, and pod. At the time the pod is loaded into the external store, this identification will be noted in the System Operations Log. Prior to jettison the operator will adjust switches 10, 11 and 12 as shown in Figure 6-5 on the AN/AMQ-19 Observer Input Panel so that the rocketsonde is identified in subsequent data handling operations. The identification will be processed during the two scans of horizontal data preceding the start of vertical data storage. Additional information on the data handling process in the AN/AMQ-19 System is presented in Section VI. Both manual reduction and computer programming techniques for the reduction of data will require the group of transfer functions and sensor baseline curves associated with the code identification of the PAULA I Rocketsonde.

The AN/GMH-4 Data Analysis Central is in every respect compatible with the PAULA I Rocketsonde data. The AN/GMH-4 System receives data directly from the airborne meteorological system and reproduces it in teletype printout form. The data it receives is that which is recorded by tape on the Recorder-Reproducer unit of the airborne AN/AMQ-19 System and it is necessary only that the Recorder-Reproducer be capable of recording the rocketsonde data in order for the ground data system to receive and reproduce it. The AN/AMQ-19 System is capable of recording the rocketsonde data and, therefore, the integration of the PAULA I Rocketsonde with the AN/AMQ-19 Meteorological System and the

AN/GMH-4 Ground Data Handling System can be accomplished without difficulty. The AN/AMQ-19 System is presented in Section VI of this report.

PAULA II AND PAULA III

The PAULA I instrument package and flight vehicle are almost directly applicable for the measurement of temperature and pressure to 250,000 feet (PAULA II). In this vehicle the M60 Falcon rocket motor is substituted for the M58. The .010 inch diameter rod thermistor and the hypsometer have been shown to provide accurate measurements to 200,000 feet in the AN/DMQ-9 tests performed in 1963 by AFCRL. The hypsometer may require a different fluid because of the extension to lower pressures. The measurement of moisture in the PAULA II vehicle, however, should not be attempted using the humidity strip sensors suggested for use in PAULA I.

More sophisticated techniques are required to measure the minute quantities of water vapor in the atmosphere at these high altitudes. The use of improved instrumentation along the lines of a mirror, or alpha absorption dewpoint hygrometer, or an infrared hygrometer is required. Until an adequate moisture measuring instrument for use in a rocketborne instrument package is developed, it is recommended that the measurement of moisture be eliminated in the PAULA II package. In place of a moisture measurement in PAULA II, a measurement of ozone concentration may be more appropriate over this altitude regime. Ozone sensors have been developed based on spectrometric methods (Paetzold Ozonesonde), chemical methods (Regener Ozonesonde), and by the detection of the effects of ozone reactions (Regener "dry" luminescent method). The amount of ozone concentration on a synoptic basis has been postulated for use as an indication of vertical transport in the stratosphere. Ozone data would also be useful in other atmospheric studies. To date, little effort has been applied to sensing ozone concentration from rocketsondes. However, there seems to be no reason why the ozone sensors could not be adapted to this type of deployment.

The PAULA III instrument package will of necessity be completely different than its two predecessors. The philosophy used in atmospheric sensing of meteorological parameters must be altered considerably when considering extension of the measurements to altitudes at 400,000 feet and above. The measurement of pressure in a region where the pressure is approximately 2×10^{-5} mb becomes a problem in counting molecules. Measuring temperature in an atmosphere where the mean free path is approximately 14 feet becomes a problem of defining temperature.

The most important meteorological measurement that can be made over this altitude regime is density. Density measurements in the pressure range below 2×10^{-5} mb can be made using ionization gages (Alphatron) or Radiation scatter techniques. Measurements of the composition of the atmosphere at these altitudes can be made using a mass spectrometer. In general, any measurements made at these high altitudes require very sophisticated measuring techniques. This

fact, in combination with the possible need for longer transmission distance (larger transmitter and larger power supply) will probably limit this vehicle to a maximum of two sensors. The purpose of the PAULA III vehicle should be to fill the void between present rocket measurements and satellite measurements. Therefore, in PAULA III measurement of parameters concerning the environment in the vicinity of the vehicle should be given preference rather than those such as solar and terrestrial radiation which can be more completely determined through the use of satellite data. The possibility of other parameters such as the determination of atmospheric composition, electron and ion density and local magnetic field are some of the measurements which could be considered.

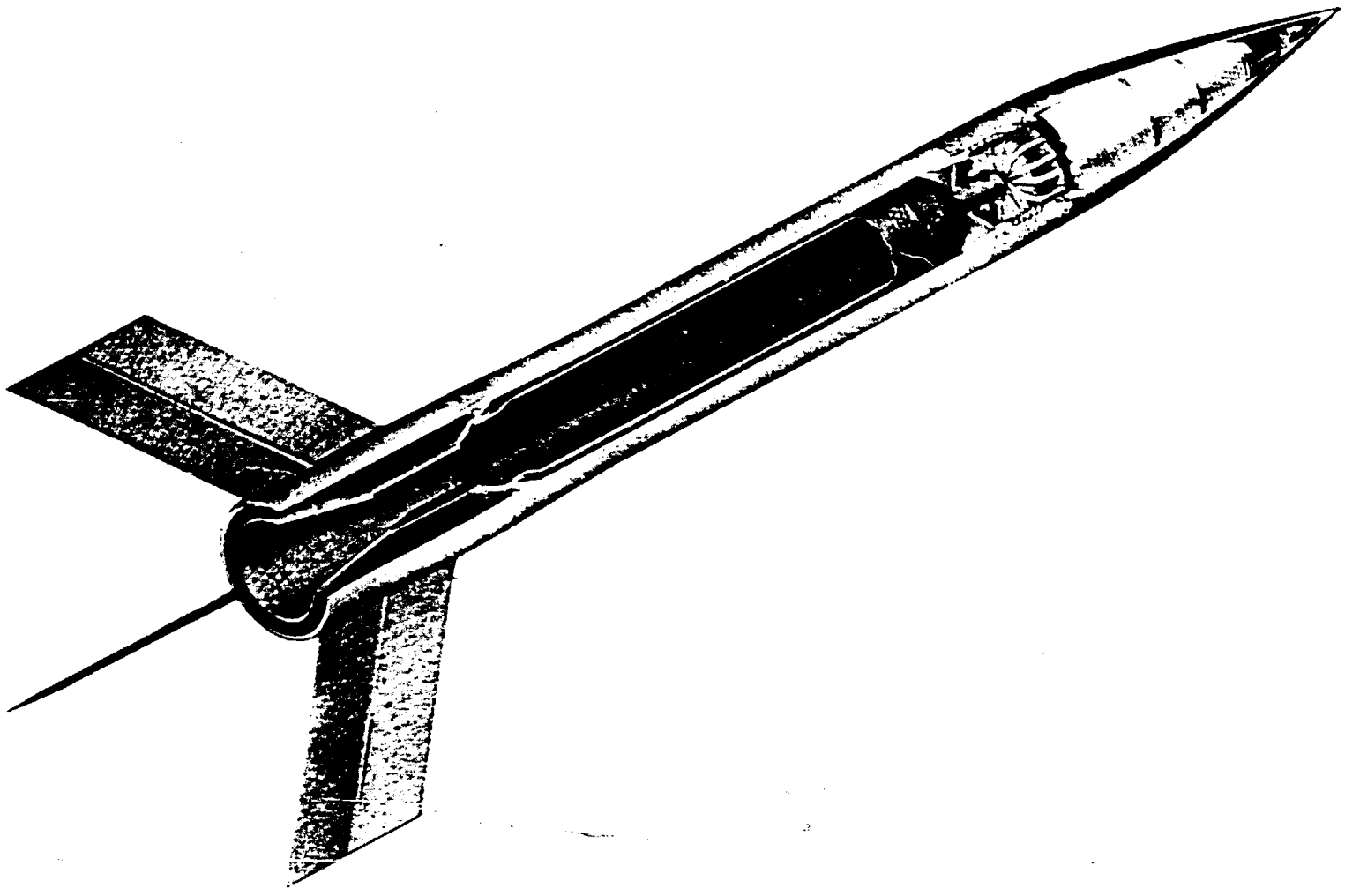

FIGURE 4-1

CUTAWAY VIEW OF PAULA I SOUNDING VEHICLE

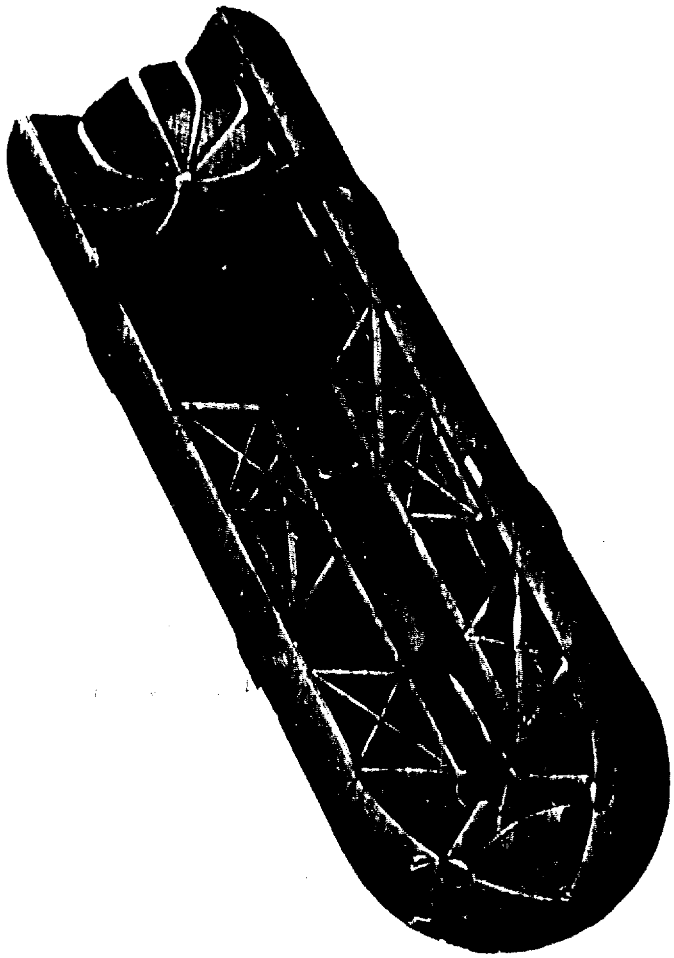

FIGURE 4-2

CUTAWAY VIEW OF PAULA I DROP POD

Bendix Prog

FIGURE 4-3

CUTAWAY VIEW OF EXTERNAL STORE

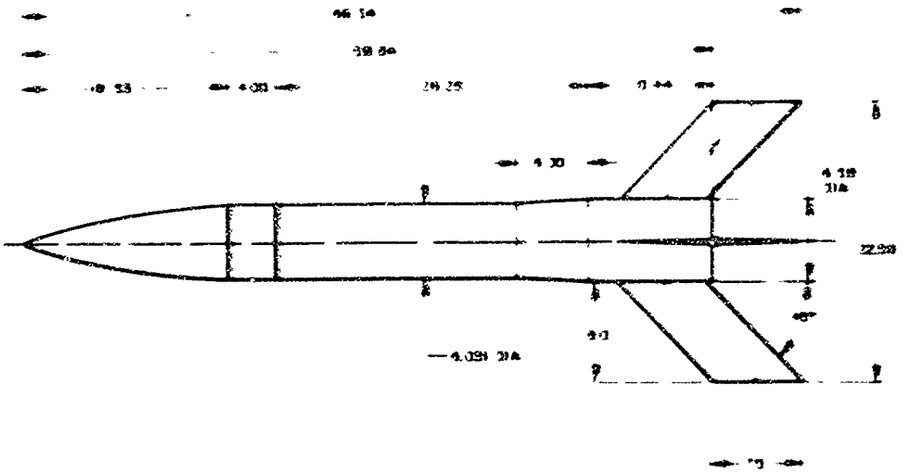

FIGURE 4-4

PAMLA I SOUNDING ROCKET

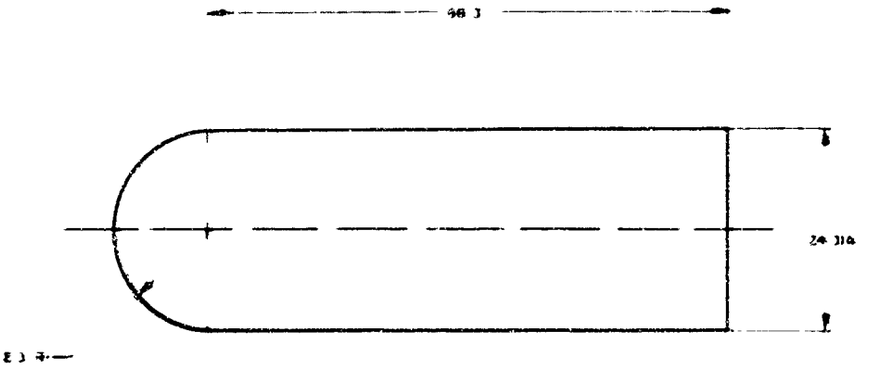

FIGURE 4-5

DROP POD

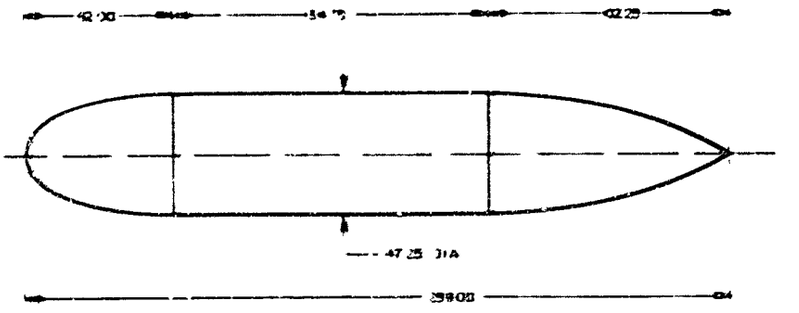

FIGURE 4-6

EXTERNAL STORE

Bendix - Friez

FIGURE 4-7

V-47 AIRCRAFT EQUIPPED WITH EXTERNAL STORES

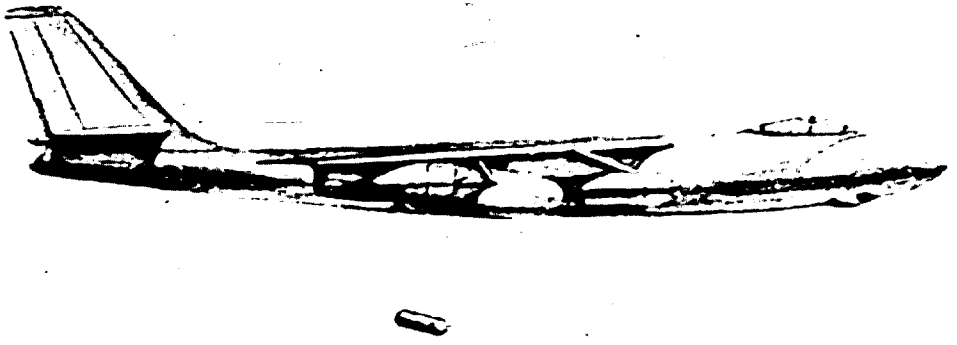

FIGURE 4-8

DROP POD JETTISON AT
FLIGHT ALTITUDE

Bendix - Fries

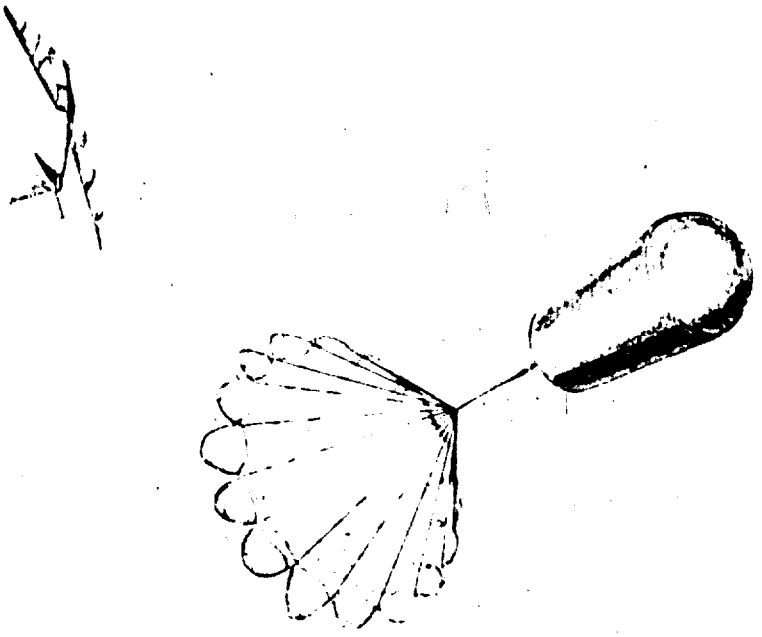

FIGURE 4-9

DROGUE PARACHUTE DEPLOYMENT

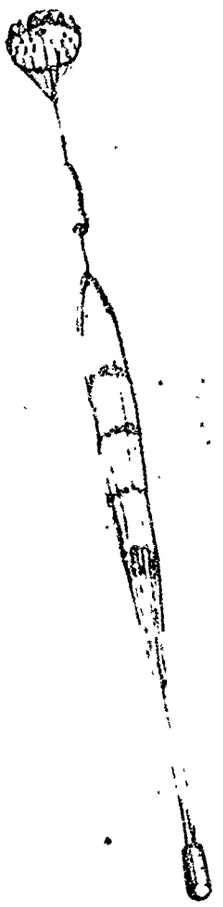

FIGURE 4-10

MAIN PARACHUTE DEPLOYMENT

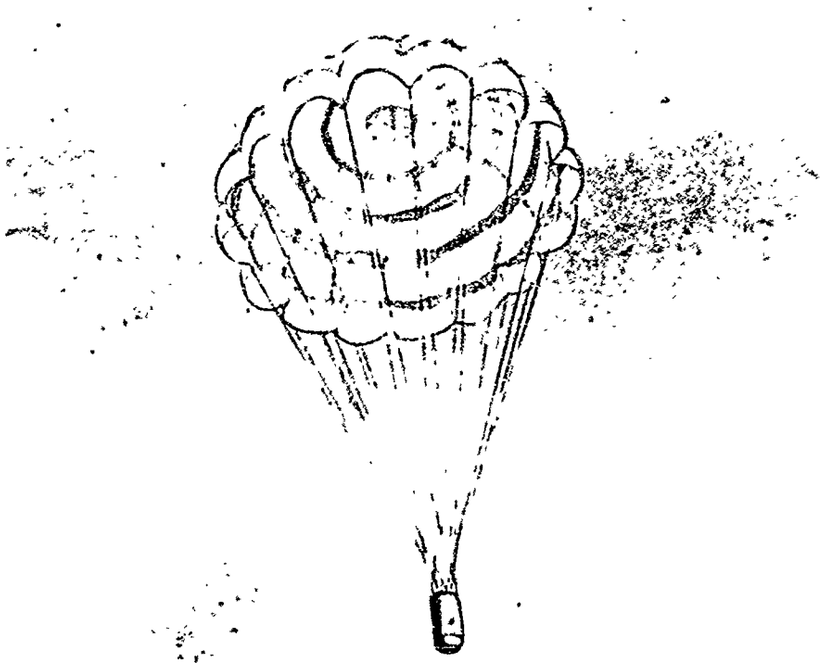

FIGURE 4-11

MAIN PARACHUTE INFLATION

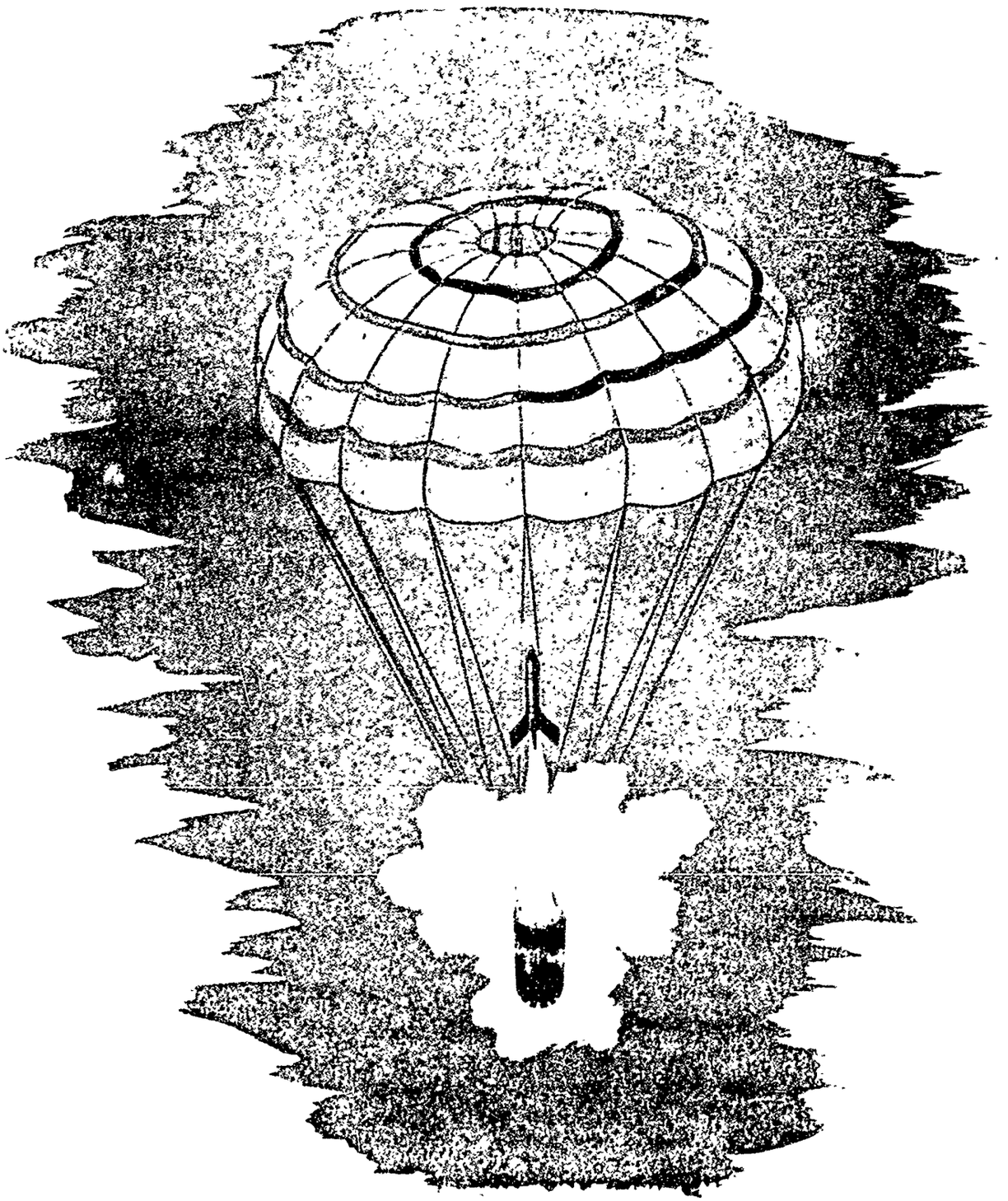

FIGURE 4-12

SOUNDING ROCKET IGNITION

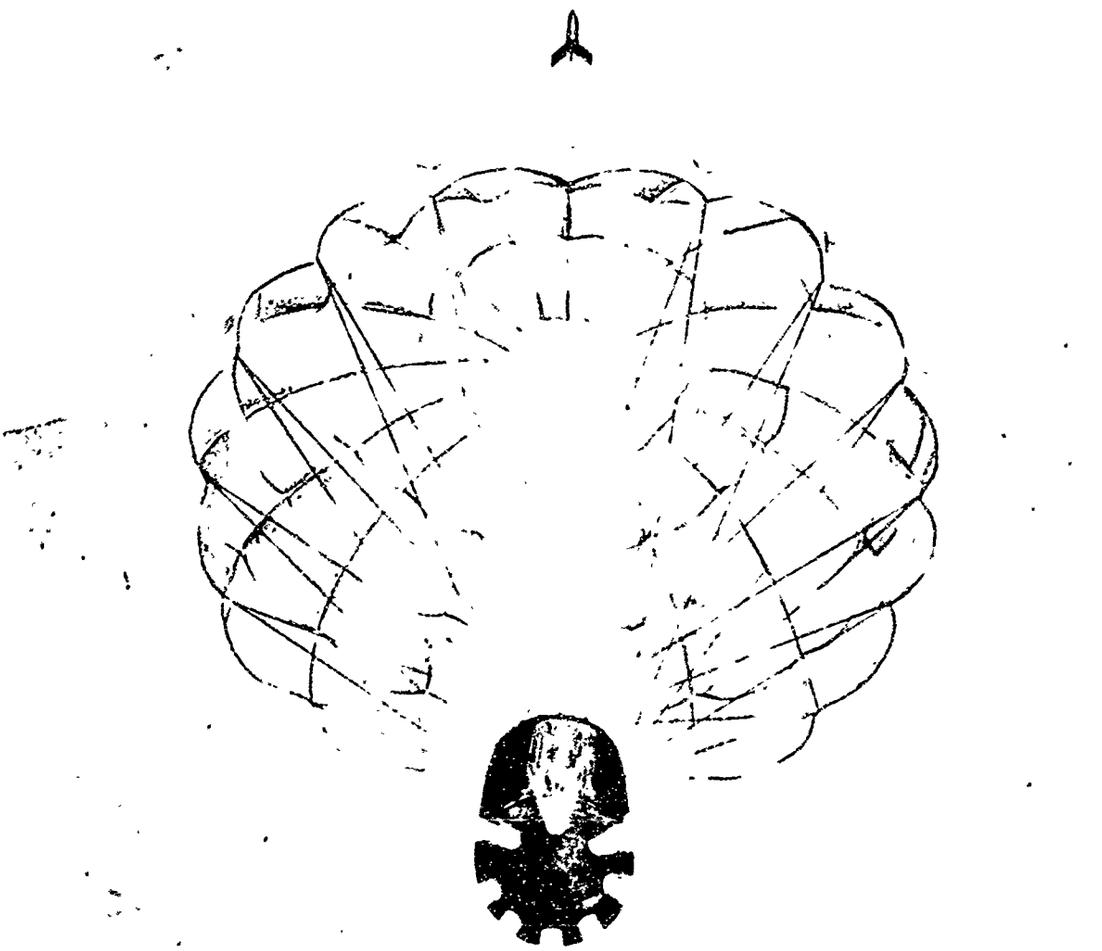

FIGURE 4-13

SOUNDING ROCKET ASCENT

Bendix – Friez

FIGURE 4-14

PAULA I SOUNDING ROCKET IMMEDIATELY PRIOR TO APOGEE

Bendix – Friez

FIGURE 4-15

NOSE CONE JETTISON SHOWING SONDE
AND PARACHUTE BEING EJECTED

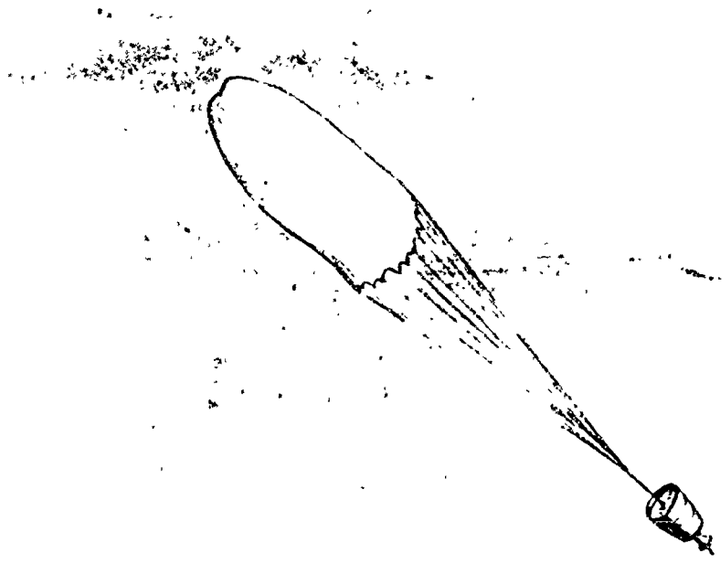

FIGURE 4-16

PAYLOAD PARACHUTE INFLATION AND STABILIZATION

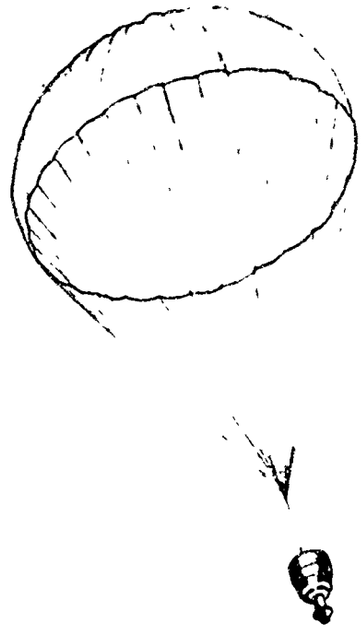

FIGURE 4-17

SONDE DESCENDING ON PAYLOAD PARACHUTE

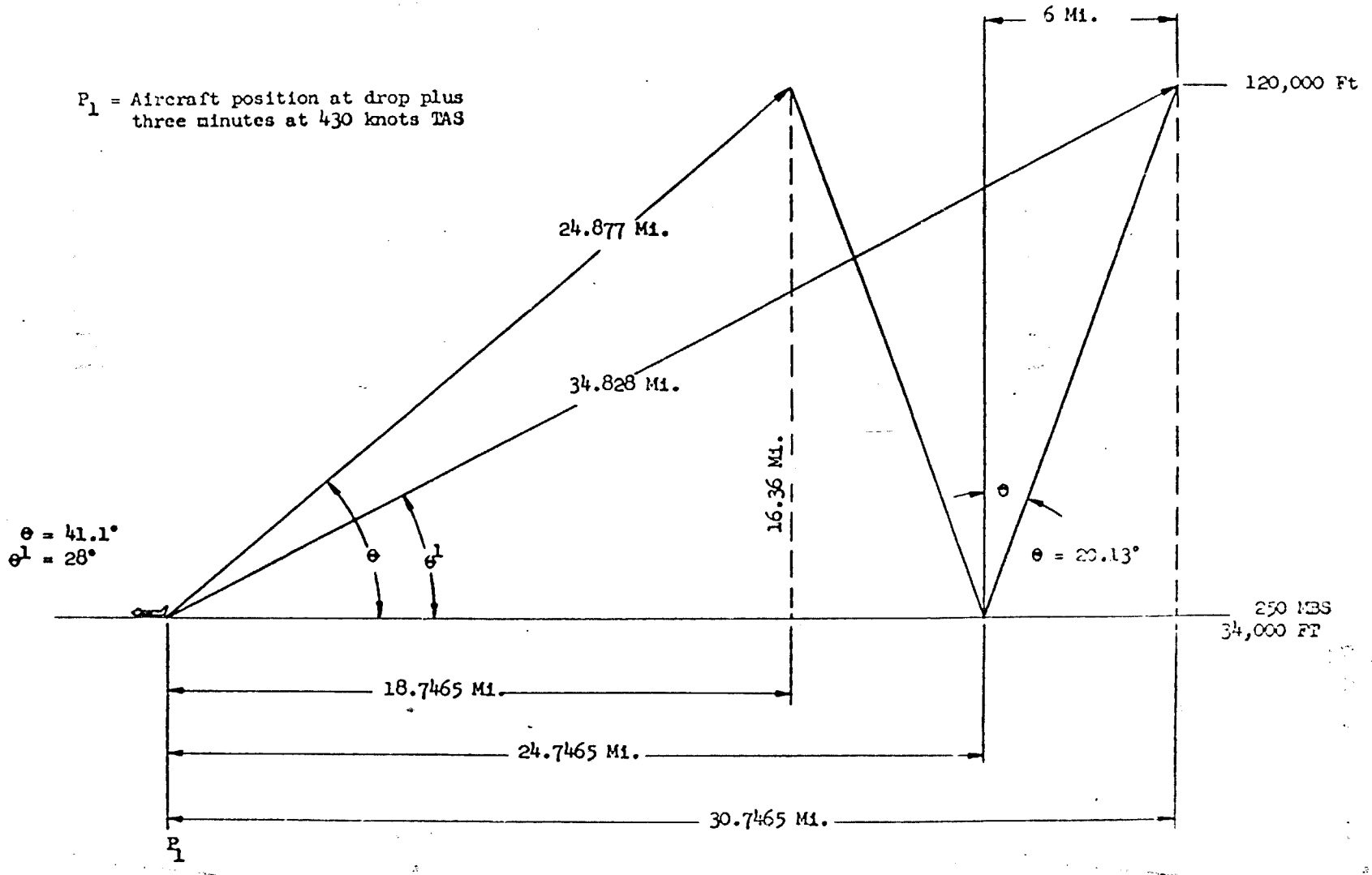

FIGURE 4-18

PAULA I
RELATIVE AIRCRAFT POSITION

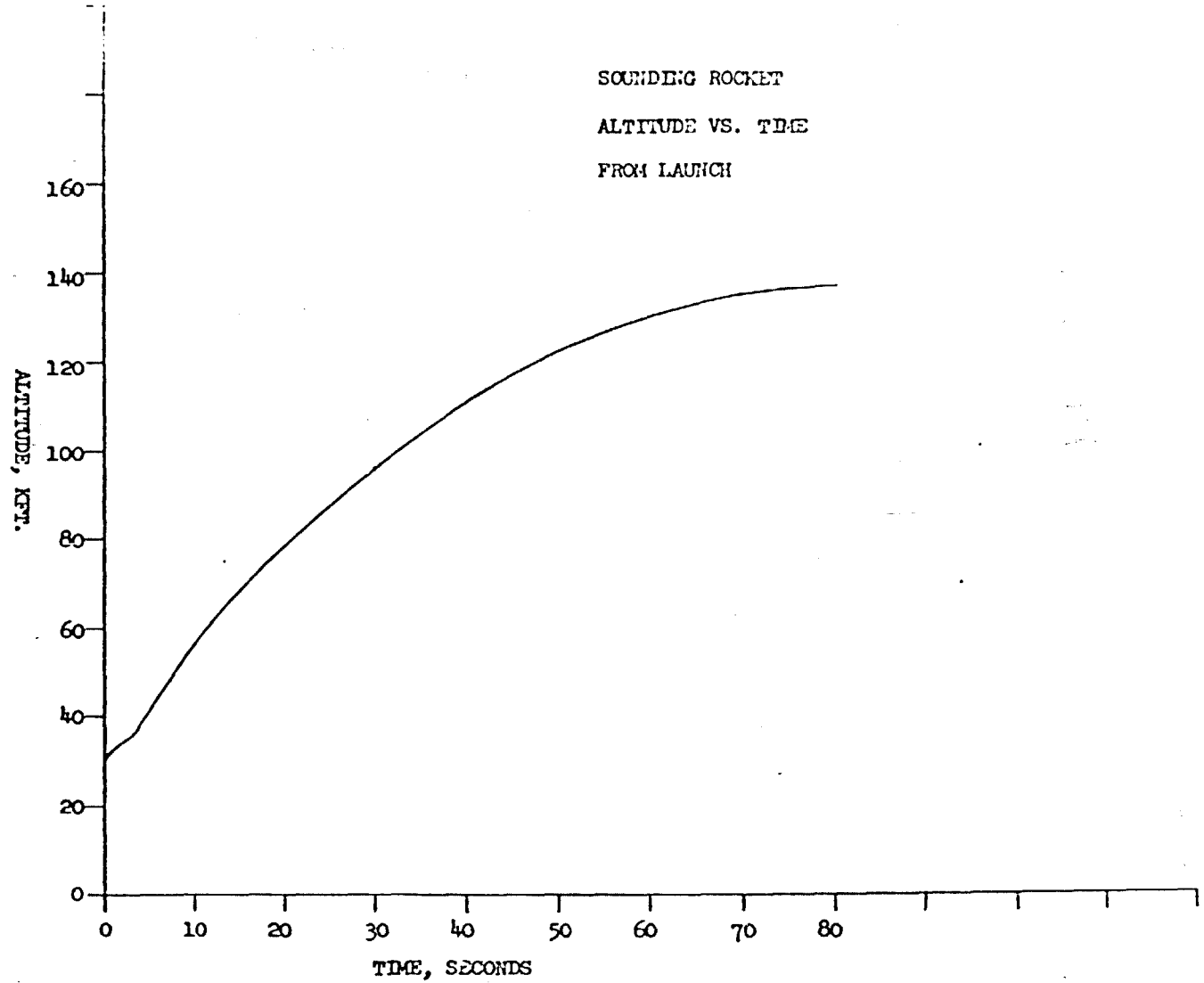

FIGURE 4-19

PAULA I SOUNDING VEHICLE
ALTITUDE VS. TIME FROM LAUNCH

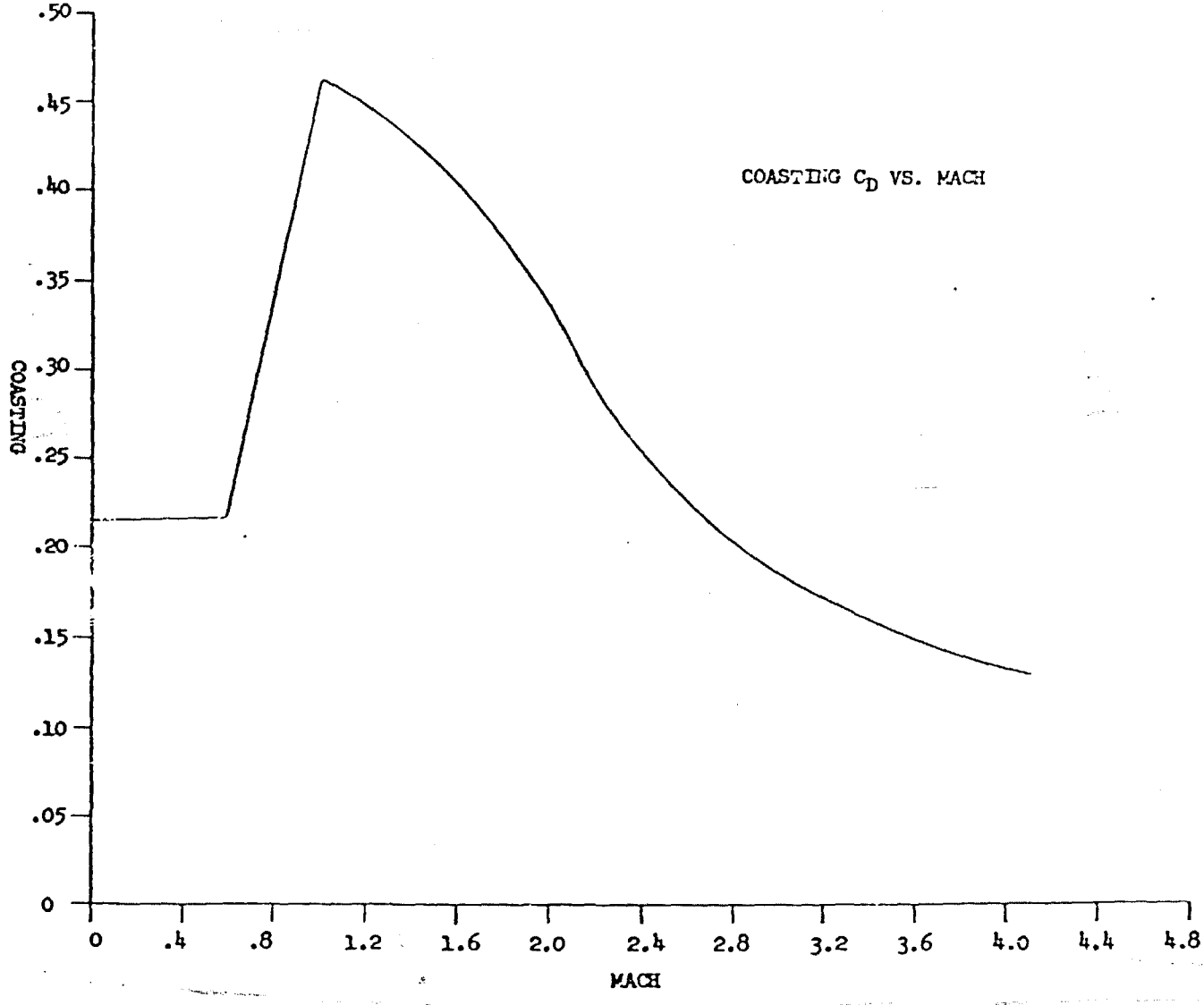

FIGURE 4-20

PAULA I SOUNDING VEHICLE
COASTING C_D VS. MACH

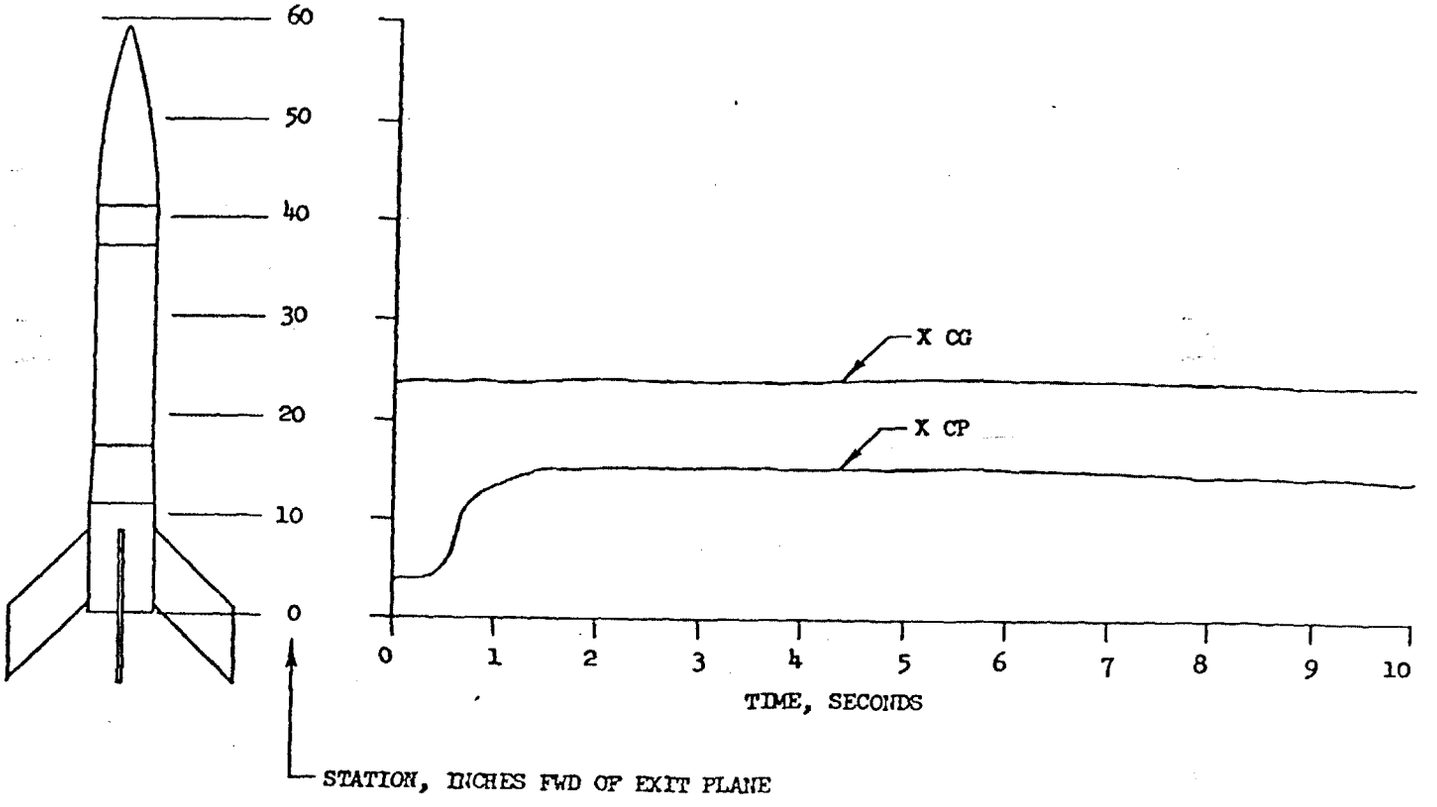

FIGURE 4-21

PAULA I SOUNDING VEHICLE STABILITY CHARACTERISTICS

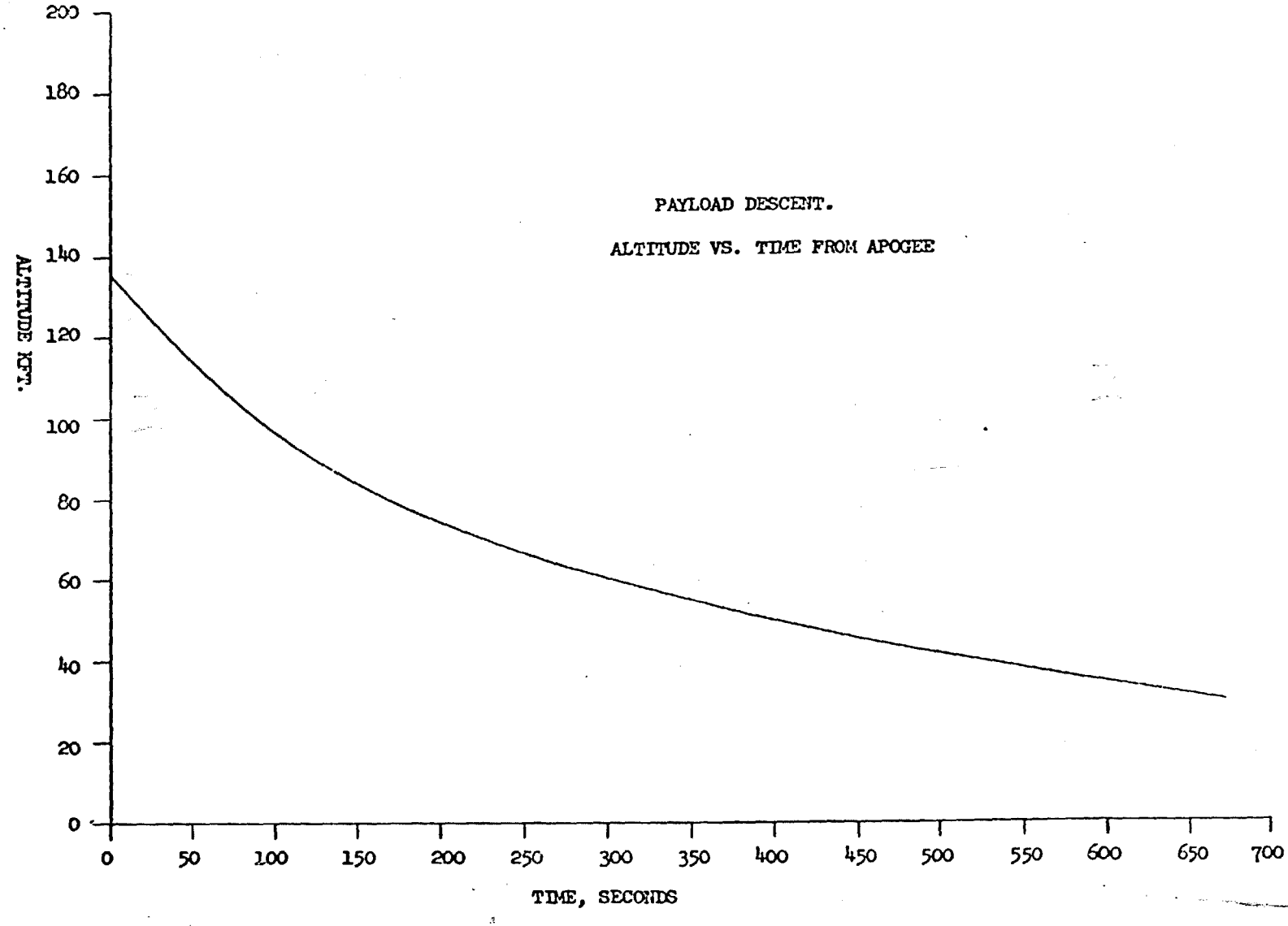

FIGURE 4-22

PAULA I RADIOSONDE ALTITUDE VS. TIME FROM APOGEE

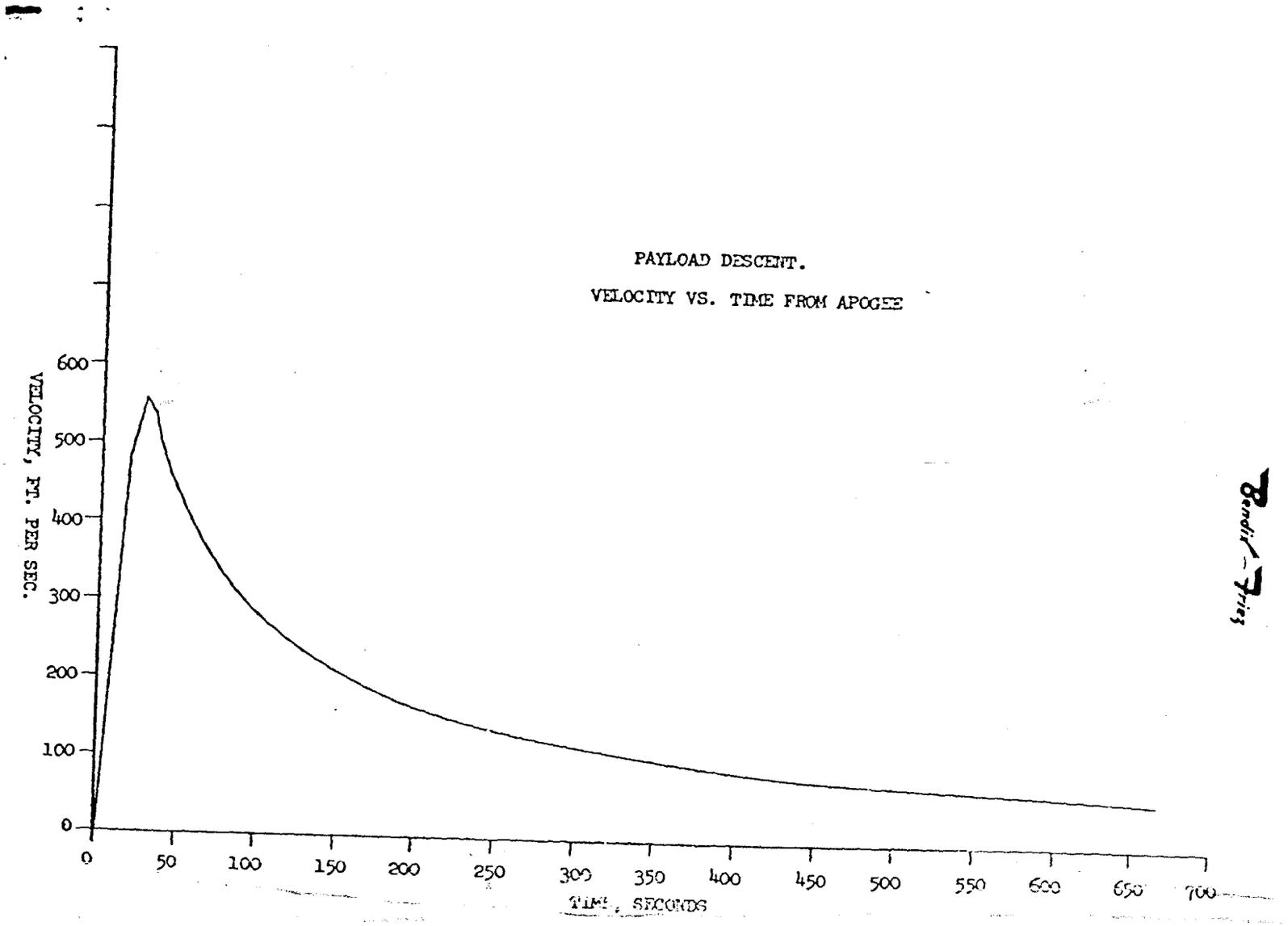

FIGURE 4-23

PAULA I RADIOSONDE VELOCITY VS. TIME FROM APOGEE

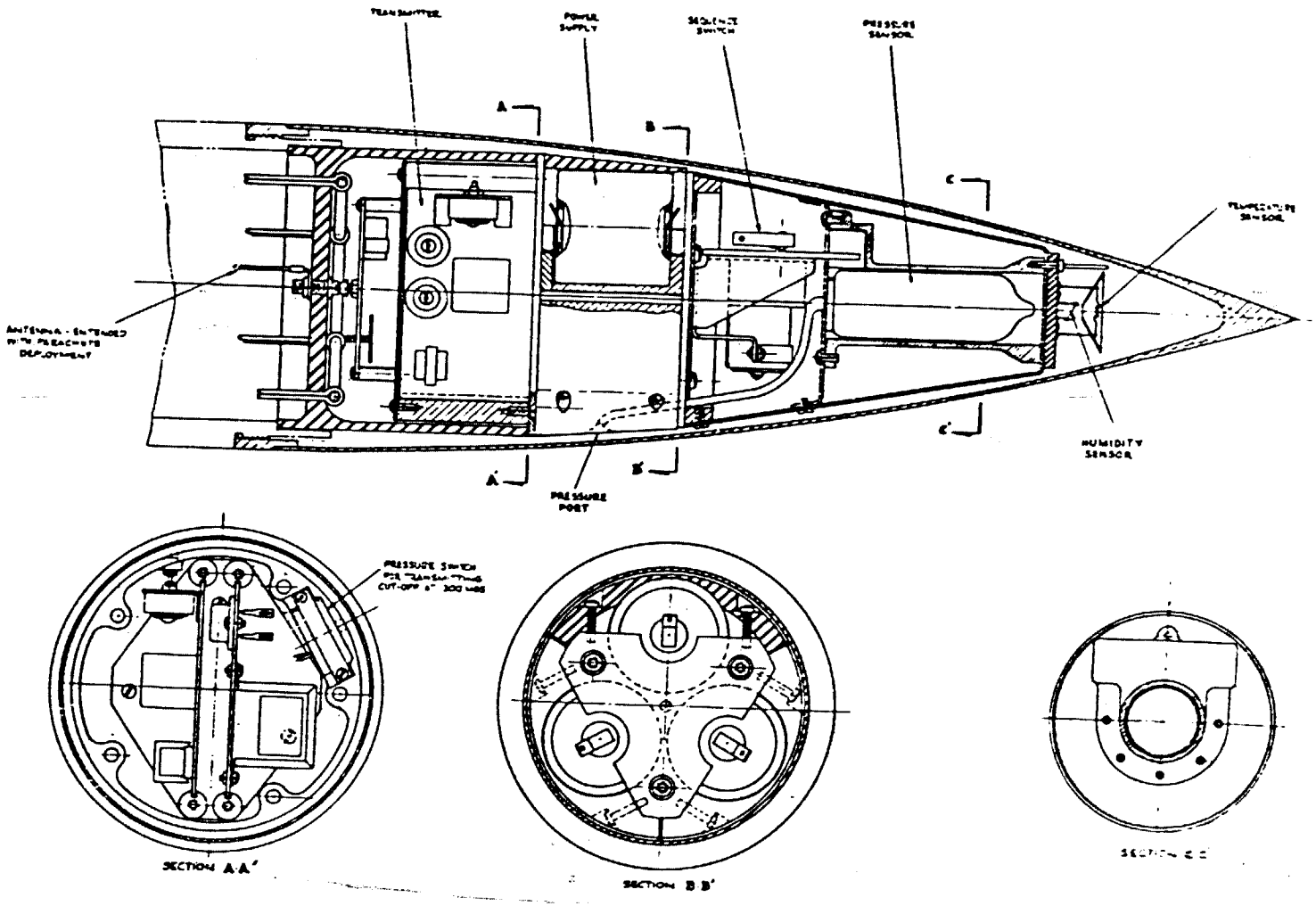

FIGURE 4-24

PAULA I RADIOSONDE
INSTRUMENT PACKAGE CONFIGURATION

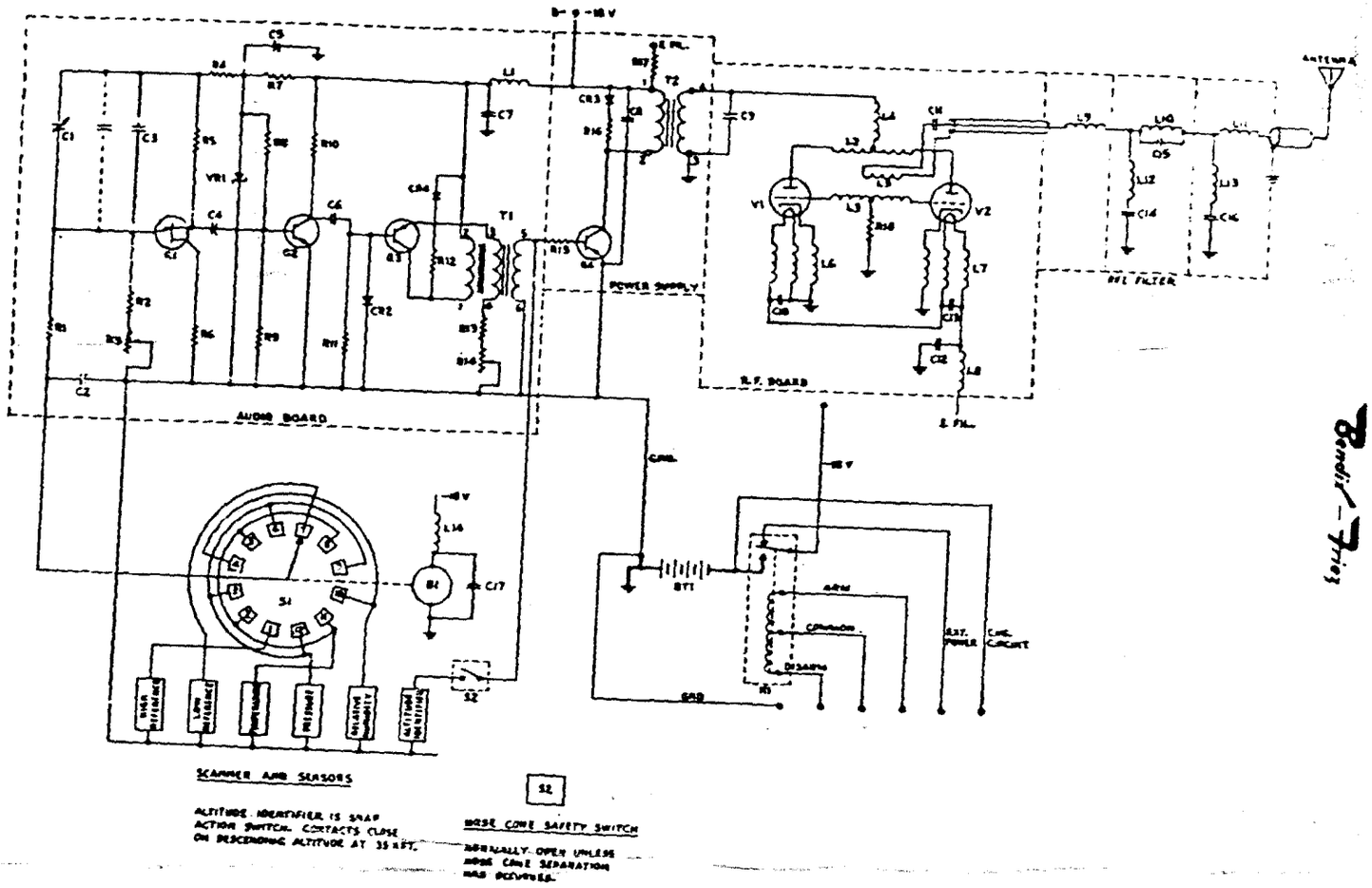

FIGURE 4-25

RADIOSONDE SCHEMATIC DIAGRAM

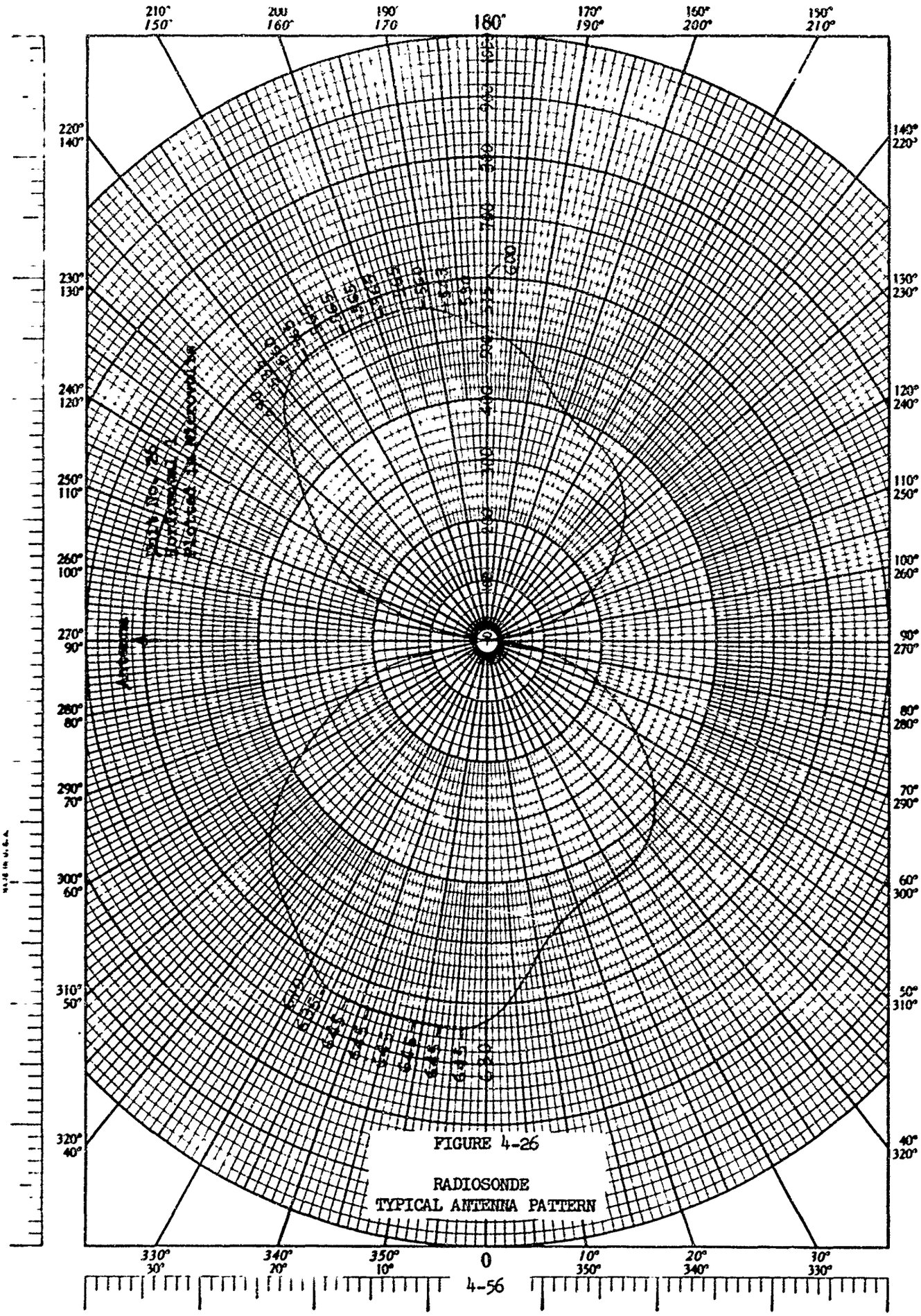

FIGURE 4-26

RADIOSONDE
TYPICAL ANTENNA PATTERN

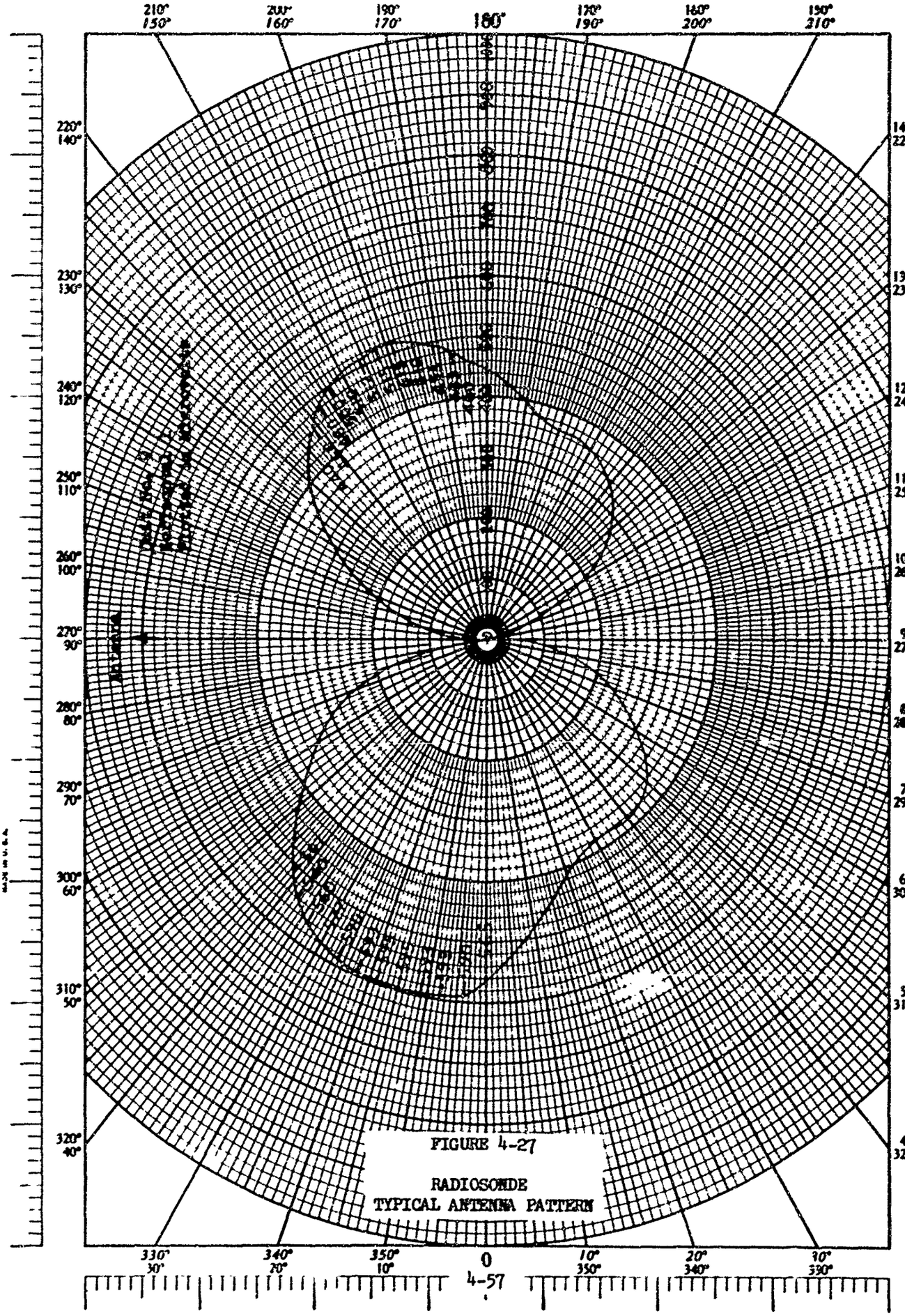

FIGURE 4-27

RADIOSONDE
TYPICAL ANTENNA PATTERN

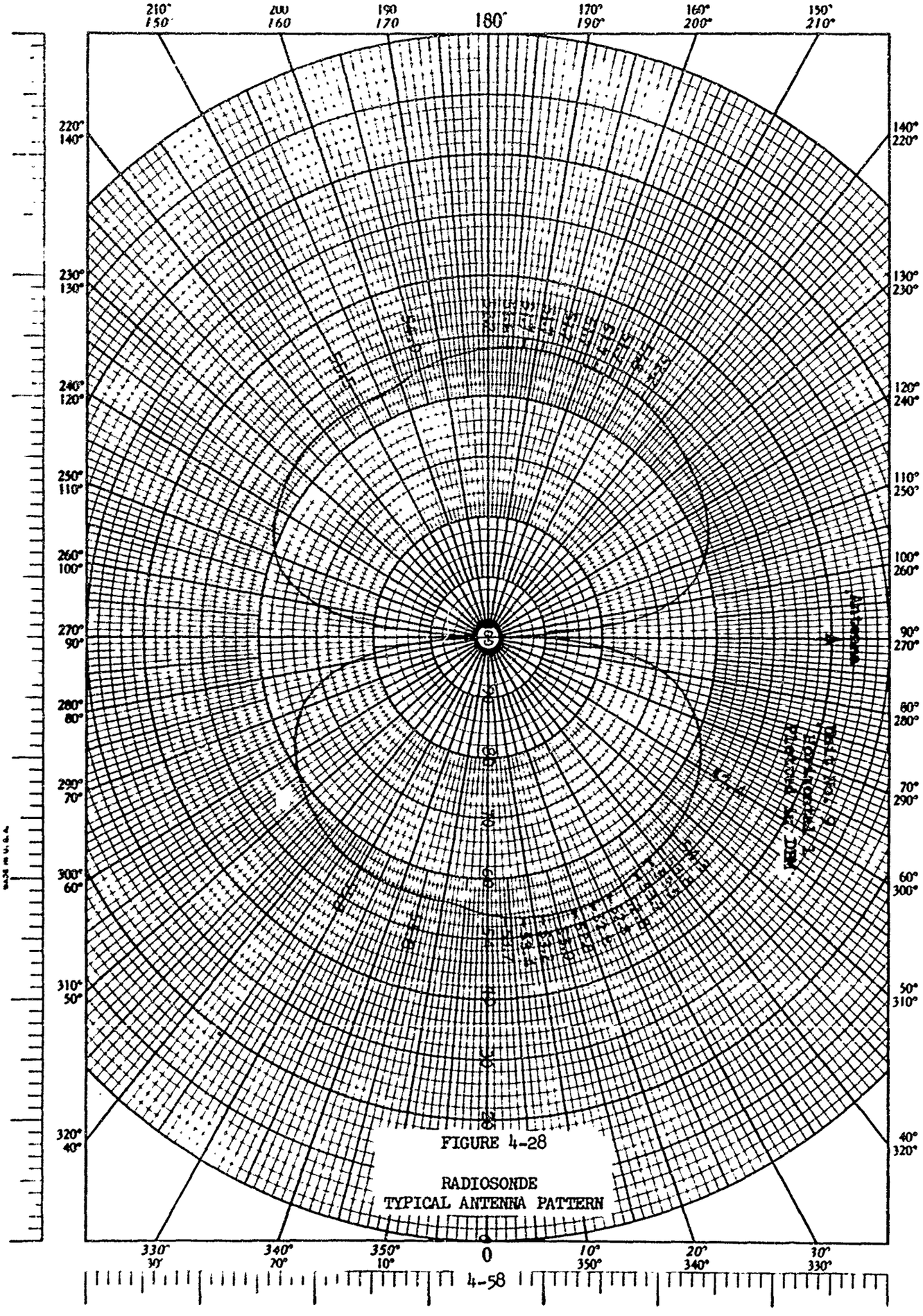

FIGURE 4-28

RADIOSONDE
TYPICAL ANTENNA PATTERN

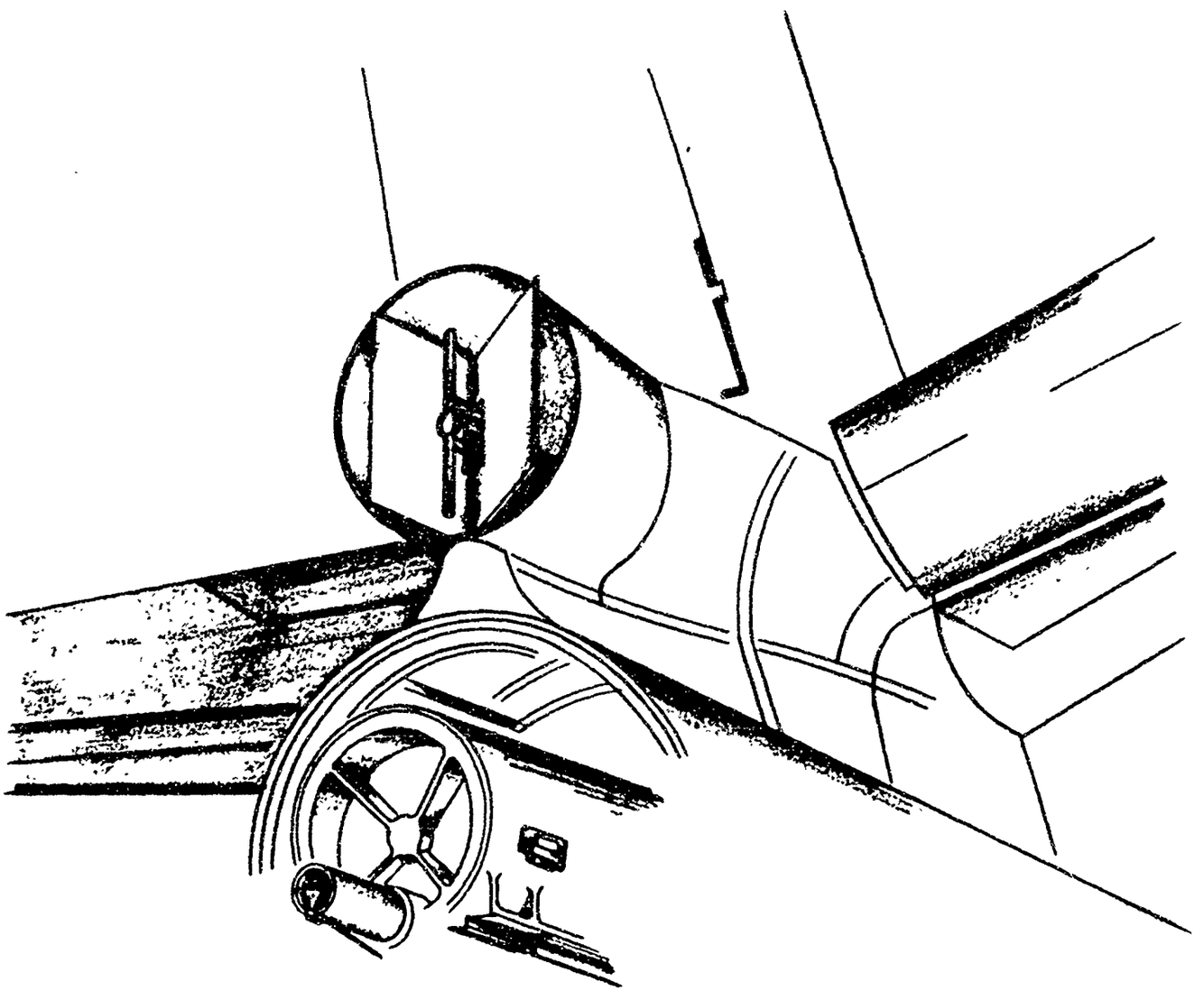

FIGURE 4-29

LOCATION OF UPWARD LOOKING ANTENNA
W-47E AIRCRAFT

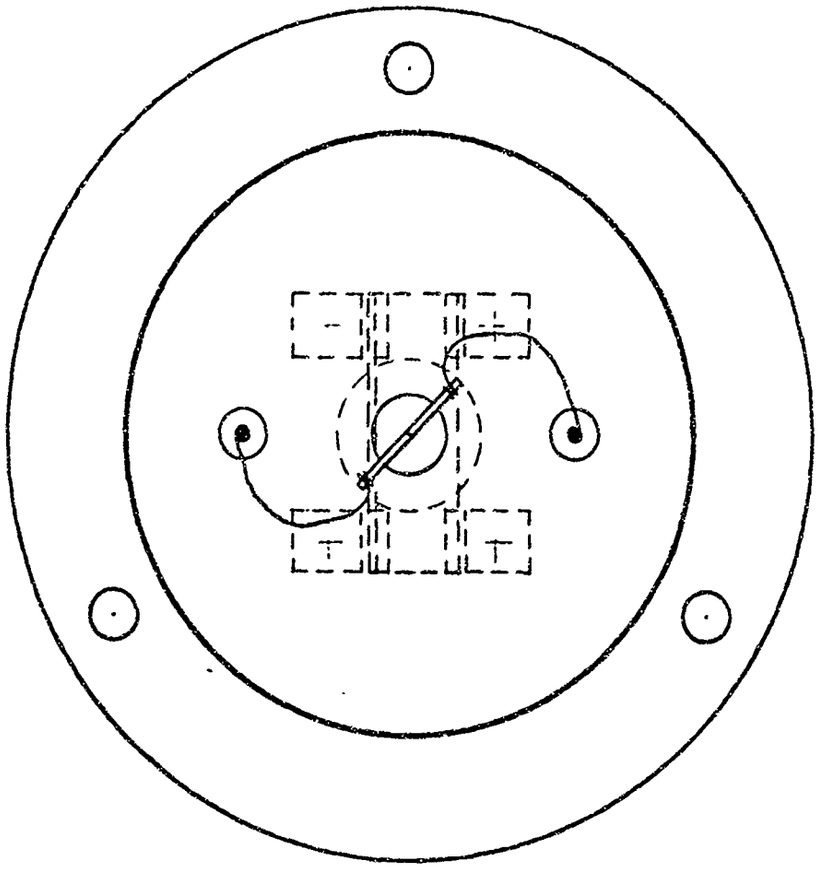

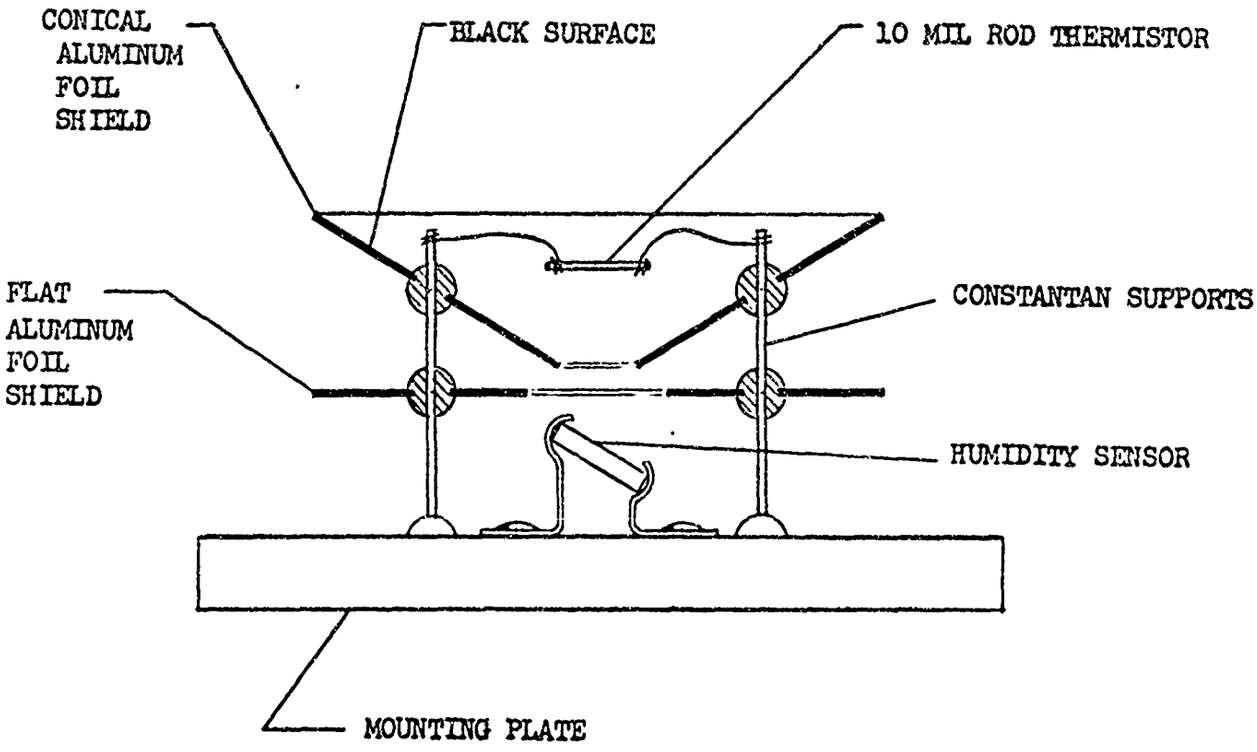

FIGURE 4-30

PAULA I RADIOSONDE
SENSOR MOUNTING

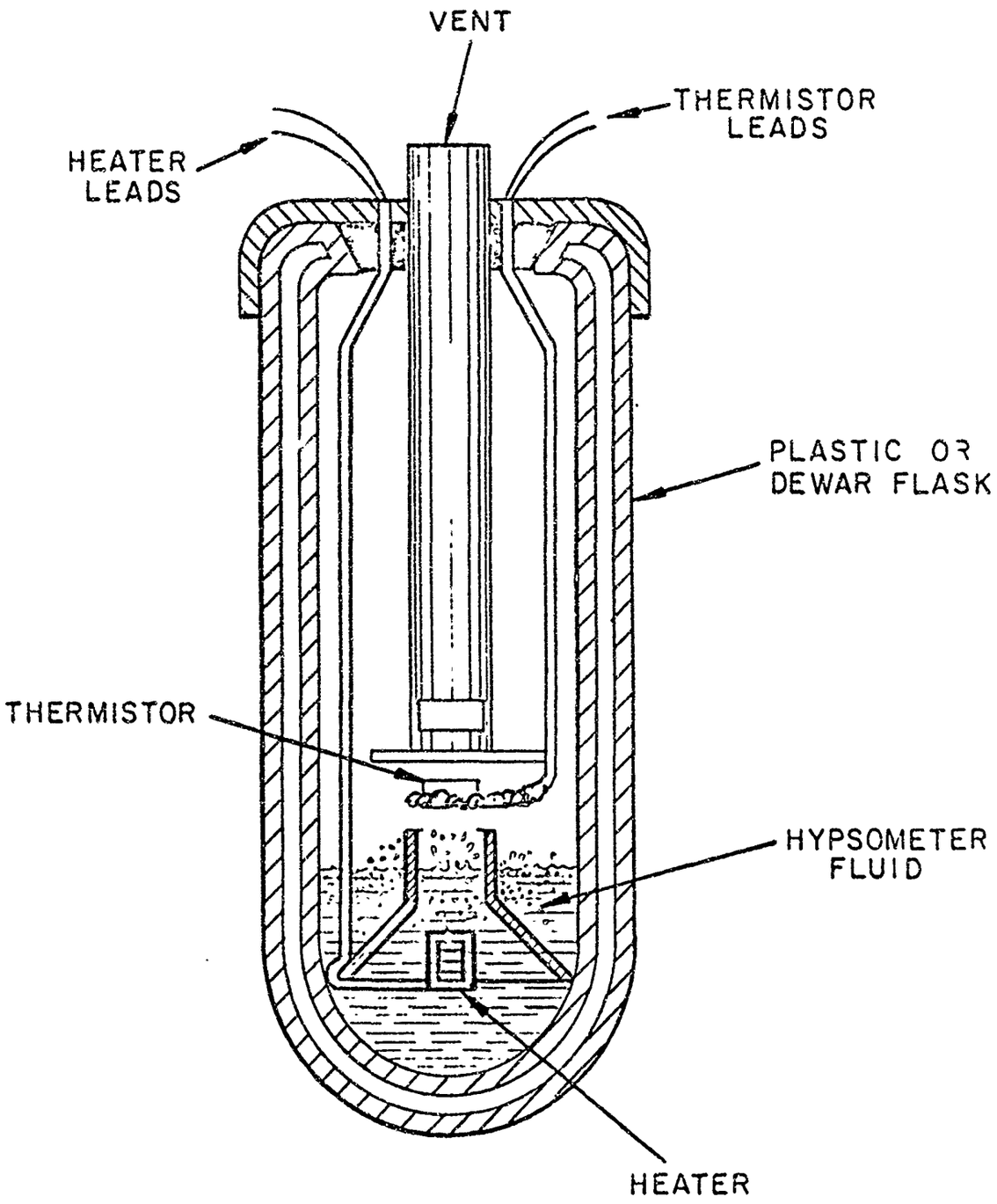

FIGURE 4-31

PAUTA I RADIOSONDE
DETAIL OF HYPSOMETER

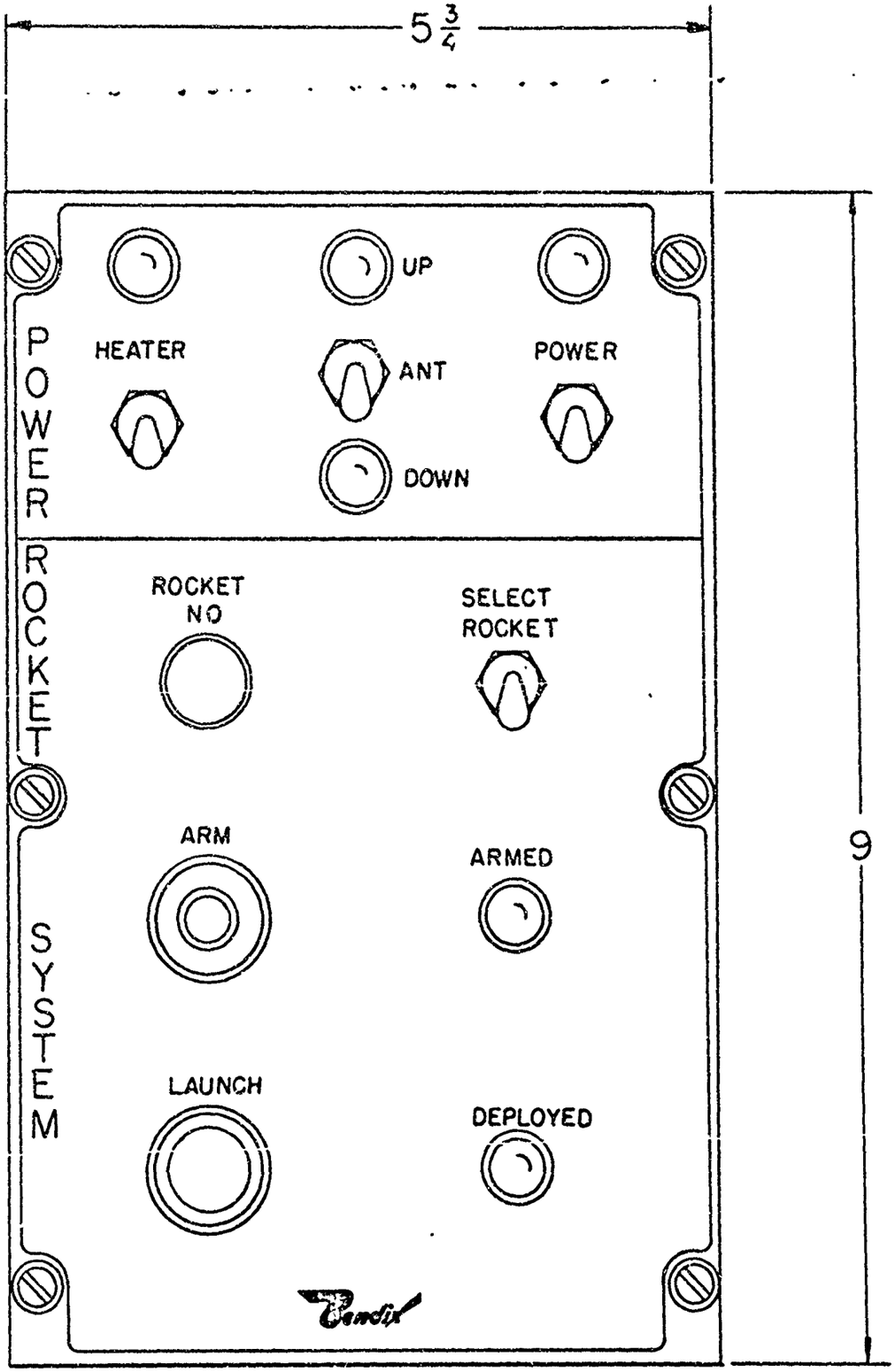

FIGURE 4-32

ROCKETSOUNDING SYSTEM
CONTROL PANEL

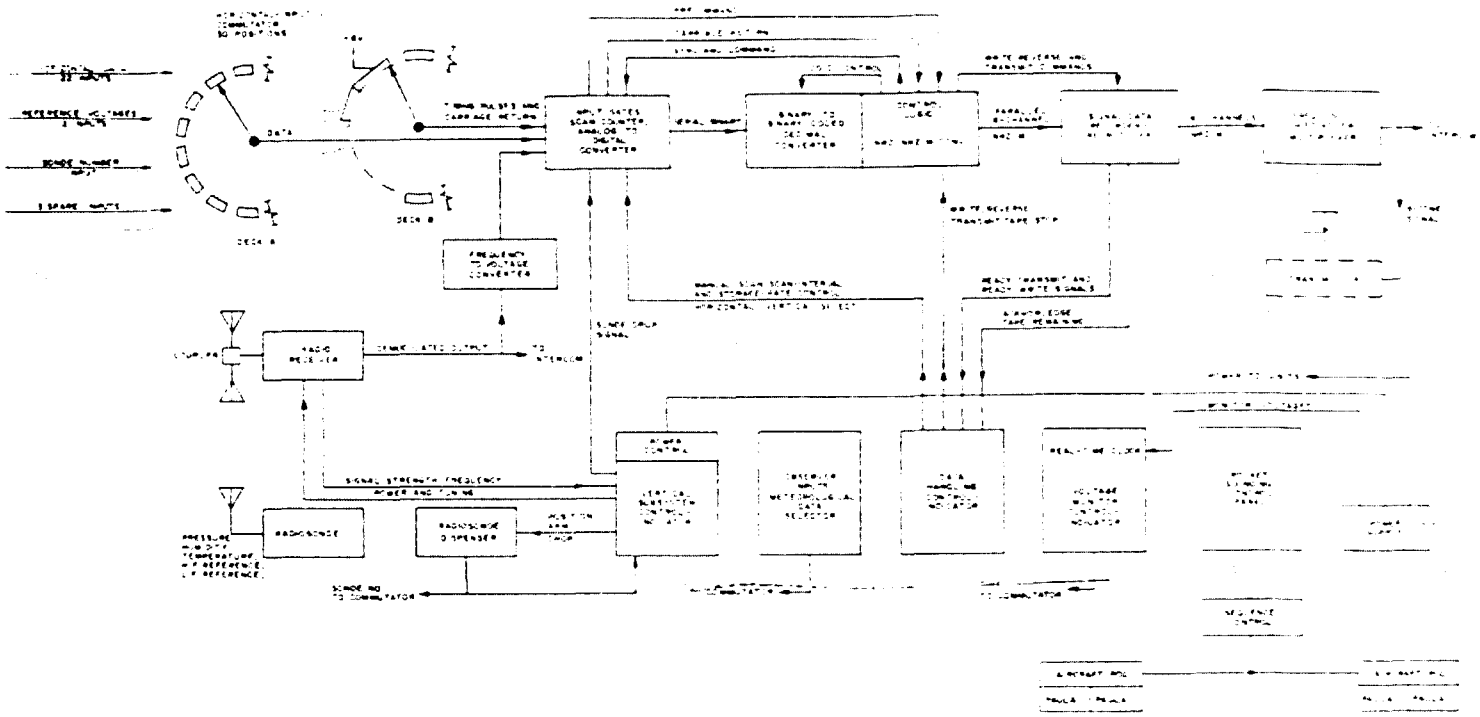

FIGURE 4-33

AN/AMQ-19 SYSTEM MODIFIED
TO INCLUDE ROCKETSOUNDING

SECTION V

SUMMARY OF INVESTIGATIONS

In the course of this study program many appraoches to the problem of deploying a meteorological probe from a moving aircraft to 120,000 feet were considered. In the course of these considerations, careful attention was given to establishing certain basic objectives for the study. Certain encouraging approaches, which are presented in this report were abandoned since they did not fulfill these objectives. The program objectives which were primary considerations are:

1. Aircraft Flight Safety must be considered of paramount importance.

2. The system must be readily adaptable to both the W-47E and the KC/C-135B aircraft with a minimum of structural modification to the aircraft.

3. The telemetering equipment must be compatible with the AN/AMQ-19.

4. The rocket motor used for propulsion of the flight vehicle should be, perferably, aircraft qualified and an Air Force stocked item.

5. The Rocketsounding System should consist of state-of-the-art techniques for use at altitudes of 120,000 feet and be readily expandable to 250,000 feet, and the region between 400,000 feet and 600,000 feet as applicable sensors become available.

Investigation of the configuration of the W-47E and the KC/C-135B airframes indicates three possible areas for installation of upper atmosphere sounding vehicles, these areas are:

1. The fuselage center section.

2. The empannage.

3. External stores under wing pylon.

An internal arrangement may be possible in the fuselage (space permitting) or external packages might be attached to the fuselage. These investigations of areas for storing the flight vehicles aboard the aircraft resulted in study of three methods of initial sounding instrument deployment. These methods can be summarized as follows:

1. Release of the vehicle in a downward direction from the aircraft, followed by an operational sequence to stabilize the unit, then propulsion to the desired altitude. This is the recommended method.

2. Ejection of the vehicle horizontally aft in the manner used with the AN/AMT-13 radiosonde, followed by a stabilization phase and propulsion to altitude.

3. Direct vertical (upward) injection to the desired altitude.

Internal sounding vehicle installation in the W-47E is limited by equipment located in the former bomb bay area and the fuel cell installations. In the case of the KC/C-135B, there are inherent problems in providing openings in a pressurized fuselage. External packages bolted to the fuselage are a possibility with either airframe.

Several additional airframe installations and methods of deploying a sounding instrument into the upper atmosphere were investigated. These investigations are summarized in the following paragraphs.

VERTICAL INJECTION METHOD

A very interesting, and somewhat unusual, approach was considered for injecting a probe into the upper atmosphere. Since the instrument package must be deployed vertically, it was considered very desirable to deploy directly to altitude without the necessity of any additional sequential steps. To accomplish this, the application of the proven ground-based gun-launched probe principle to an aircraft was studied. In the final analysis it would appear that the extremely high breech pressure, very high accelerations, and need for extensive aircraft modification to absorb recoil, result in a conclusion that this method is impractical for a state-of-the-art operation system.

The gun-launched probe system studied, which does offer many beneficial attributes, is illustrated in Figure 5-1 installed in the W-47E aircraft. Launch and deployment of the meteorological package is

shown in Figure 5-2. The most critical characteristics of the system are discussed below and are supported by data in graphs and figures. Some of the information presented herein was established through rather liberal extrapolation of existing gun-launched probe data. The following parameters have been assumed for this discussion.

1. Projectile apogee: 125,000 feet and 250,000 feet.

2. Barrel length: 10 to 15 feet.

3. Projectile diameter: 1/2 barrel diameter.

4. Aircraft forward velocity neglected.

Inspection of the data presented in Figure 5-3 shows the muzzle velocities required to reach the desired altitudes with a gun whose bore is three to six inches. Figures 5-4 and 5-5 show the muzzle velocity capabilities of ten and fifteen feet gun barrels assuming an operating breech pressure of 47,000 pounds per square inch.

Based on the margin of velocity between the muzzle velocity capabilities and muzzle velocity requirements, the following assumptions can be made to determine an approximate breech pressure lower than 47,000 psi. These results are shown in Figures 5-6 and 5-7.

1. Ten foot gun operating to 125,000 feet. (Figure 5-8)

2. Ten foot gun operating to 250,000 feet. (Not possible below 47,000 psi.)

3. Fifteen foot gun operating to 125,000 feet. (Figure 5-9)

4. Fifteen foot gun operating to 250,000 feet. (Operating at 47,000 psi, the following are feasible.)

   a. Four inch gun with five pound projectile.

   b. Six inch gun with twelve pound projectile.

In the case of the fifteen foot gun operating to 250,000 feet, accelerations and muzzle velocities experienced by the projectile are:

1. Four inch gun muzzle velocity 5,500 feet per second (15 pound projectile), peak acceleration 63,000 g.

2. Six inch gun muzzle velocity 5,100 feet per second (15 pound projectile), peak acceleration 54,000 g.

Inspection of this data indicates that extensive changes are necessary in present radiosonde circuitry and meteorological sensors due to the high accelerations involved. As it is the aim of this system to be operational within the limitations of state-of-the-art hardware, this approach was eliminated from consideration early in the study program.

HORIZONTAL EJECTION METHOD

A careful study was also made of the problems involved in installing a sounding vehicle dispensing system in the tail of the aircraft. With the W-47E, this concept appears to be encouraging as the MX-4768/AMQ-19 Radiosonde Set Dispenser is installed in this area and several possible methods can be used. The most promising among these was to nest four "Judi" type rockets, equipped with meteorological instrumentation, in the space available around the dispenser. This rocket motor provides much of the required performance, although primarily used for DART transport and not presently qualified for aircraft use. It has been established that four of these vehicles could be mounted around the dispenser in the W-47E as shown in Figure 5-10. The sounding vehicles would be contained in a tube which also provides storage for the stabilization parachute and timing devices.

The meteorological sounding package would be contained in an ogive-shaped nose cone designed to be deployed at apogee, allowing the meteorological package to descend by parachute. Due to the extreme turbulence experienced at the after end of the aircraft during flight it was felt that the rocket vehicle must be deployed from the aircraft with a "pogo stick" type of launcher rather than a drogue parachute. Figure 5-11 illustrates the rockets and payload packages in their dispenser. When used in this application, the Judi would provide a vehicle displaying the approximate characteristics listed in Table VIII.

TABLE VIII

Weight	38 pounds	38 pounds
Length (approximate)	90 inches	90 inches
Payload Diameter	3 inches	4 inches
Apogee (approximate)	257,000 feet	200,000 feet
Peak Acceleration	120 g's	120 g's
Payload	9 pounds	9 pounds

Selection of this configuration would preclude the use of many existing AN/AMT-13 assemblies due to the small volume available in the nose, and, also, probably due to electrical power requirements, the proven hypsometer for the measurement of pressure altitude.

Additional research and development would be required to support the design of a suitable transmitter. This effort removes the Judi from the realm of state-of-the-art hardware. The major problem involved in the use of this method is the extensive rework to the aircraft and resultant non-interchangeability of the system between the two aircraft (W-47E and KC/C-135B). It is anticipated that PAULA I will require only minor modification to the aircraft involved, the W-47E and the KC/C-135B, to utilize the system presented in Section IV of this report. In addition, a Judi-powered sounding vehicle and dispensing system does not appear to lend itself readily to modification for soundings at 120,000 feet, 250,000 feet, and the area between 400,000 and 600,000 feet. Additional flight vehicle and aircraft modifications would appear necessary to achieve this desired extension to higher altitudes.

EXTERNAL STORES

Following the consideration of various fuselage mounting techniques, study effort was concentrated on the concept of external stores. As the aircraft involved, W-47E and KC/C-135B, are, or can be, equipped to carry external fuel tanks, this offered an ideal location for the mounting of instrumented rocket vehicles. It is highly desirable to have a package which would fit either aircraft, and be readily adaptable to additional types of aircraft. External mounting permits this option. The final configuration of the PAULA I system is presented in the preceding section of this report. Several configurations considered during the evolution of the final package are briefly discussed below. One design parameter established for the program was that four sounding vehicles must be carried aboard the aircraft. One configuration studied is shown in Figures 5-12 through 5-15. The external fins on the pod, as well as the rocket vehicle fins projecting through the pod, were used in combination as a spin stabilization device for the pod to assure separation from the aircraft prior to parachute opening. This finned pod arrangement does not lend itself to side-by-side wing pylon mounting due to the extreme aerodynamic interaction (turbulence) generated. To preclude turbulence affects the pod remained attached to the aircraft and the sounding vehicle deployed aft with its parachute as shown in Figures 5-16 and 5-17. This presented a smooth aerodynamic shape to the air flow but still left the exposed vehicle fins aft. Even though this is an improvement over the previous concept, it still was not a desirable solution to the problem. The concept was modified by installing two wing pods side-by-side with a door which could be opened in the after end for vehicle deployment. This configuration is shown in Figure 5-18. While this represents a usable solution, the cost of design and fabrication plus the resultant loss of aircraft performance, makes it appear undesirable. The step leading to evolution of the PAULA I system was the use of a large pod containing the

sounding vehicle. This pod would be dropped and act as a launching platform for the sounding vehicle after parachute stabilization. This system utilized the PAULA I sounding vehicle but represented a different deployment technique. The sequence of this deployment is illustrated in Figures 5-19 through 5-23. This particular configuration showed sufficient promise to warrant analysis in the IBM 7040 computer. Canted fins were used on the drop pod for spin-up. An integrating accelerometer, mounted on the periphery of the pod and, therefore, actuated by rotation during deployment, was used as the final safety device in the flight safety program. This was considered one type acceleration which could only be experienced after release from the aircraft. Although this system appeared to offer a workable solution, the problem of installing two pods on a common external stores pylon, their large frontal area and proximity to each other, had a deleterious affect on aircraft performance.

The last concept evolved prior to the final PAULA I system consisted of a vehicle powered by the Falcon M-58A2 motor and utilizes a rotary dispenser made from a modified W-47E external fuel tank. This is very close to the final design which is discussed in Section IV. The dimensions and launch sequence are shown in Figures 5-24 through 5-30.

The background information evolved from the configurations presented in this section lead to preparation and study of the final recommendations necessary to assure that an operational state-of-the-art system could be provided. This final PAULA I deployment configuration is presented in Section IV of this report.

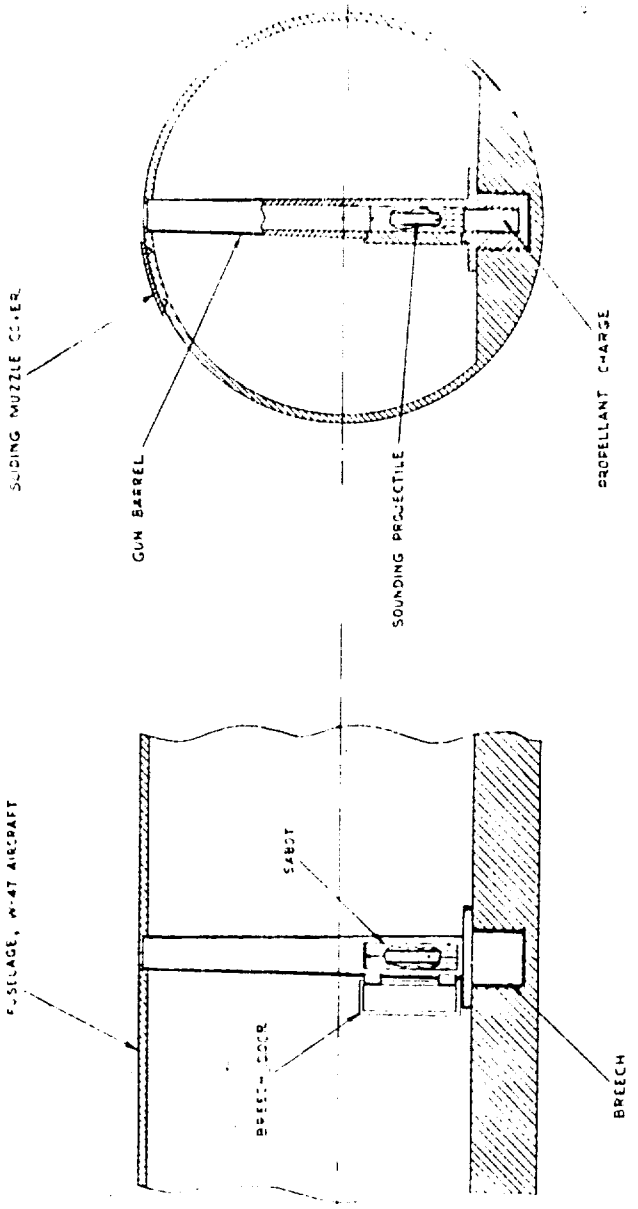

FIGURE 5-1

GUN-LAUNCHED PROBE
AIRCRAFT MOUNTING

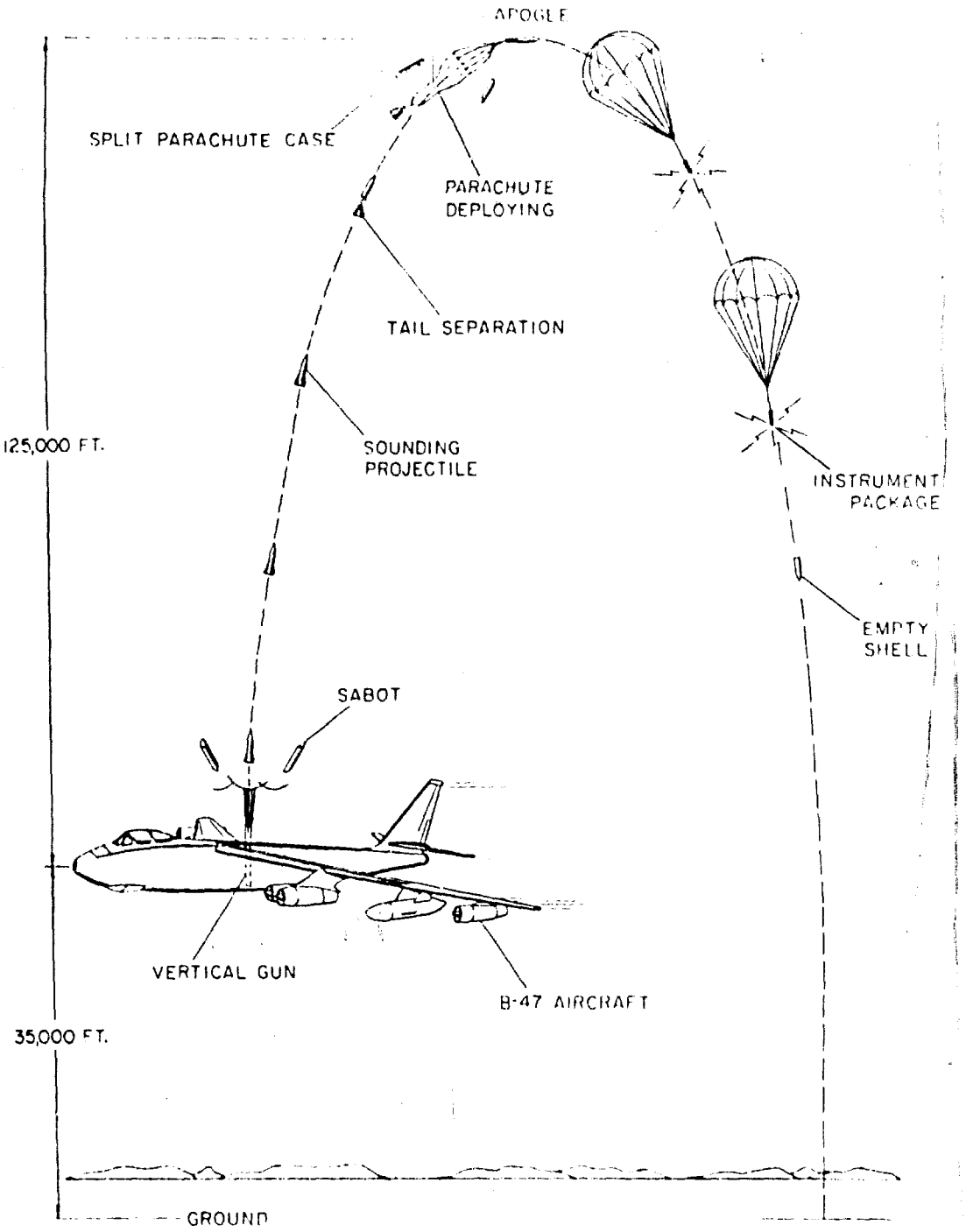

FIGURE 5-2

GUN-LAUNCHED PROBE DEPLOYMENT

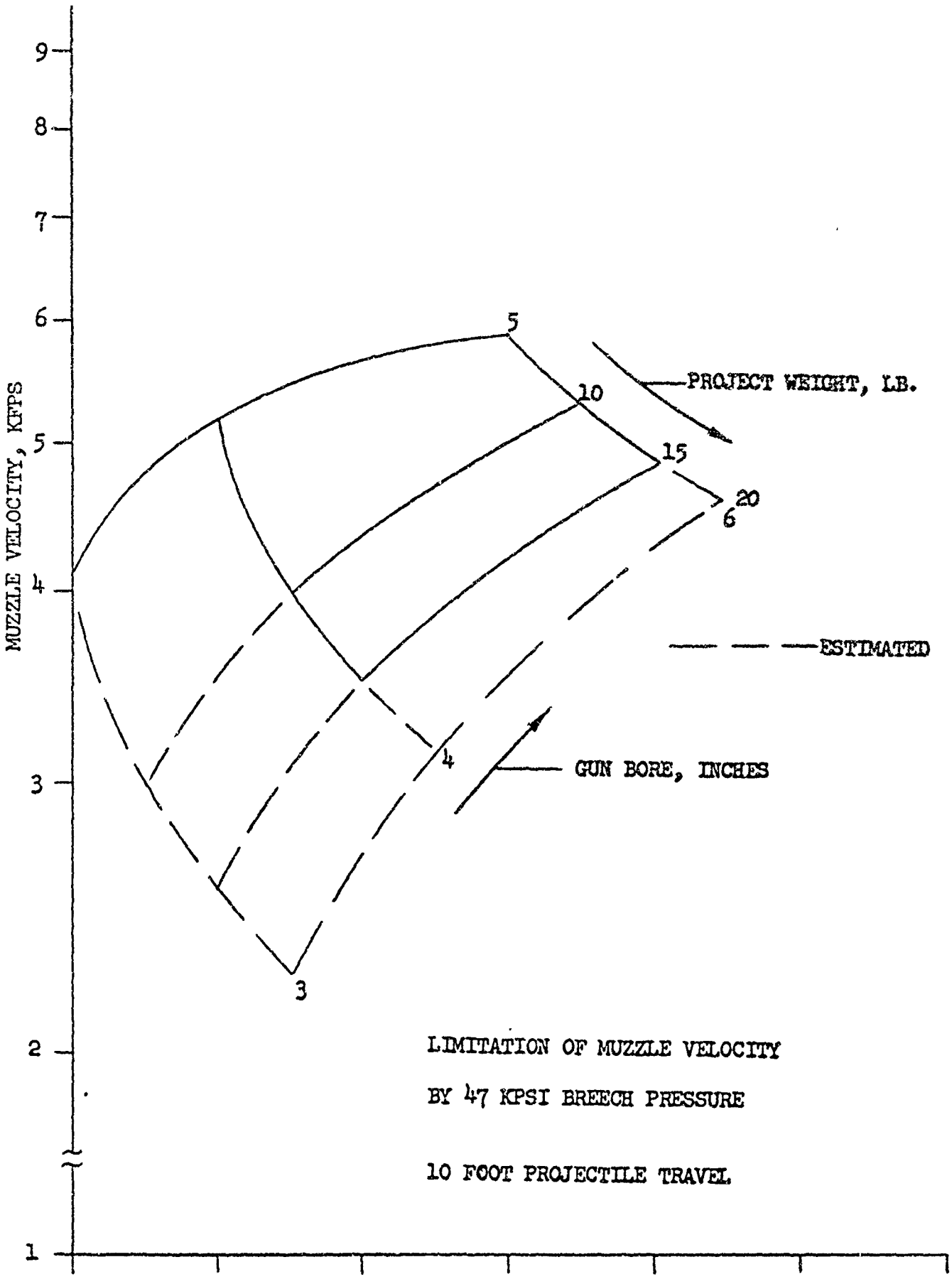

FIGURE 5-3

GUN-LAUNCHED PROBE

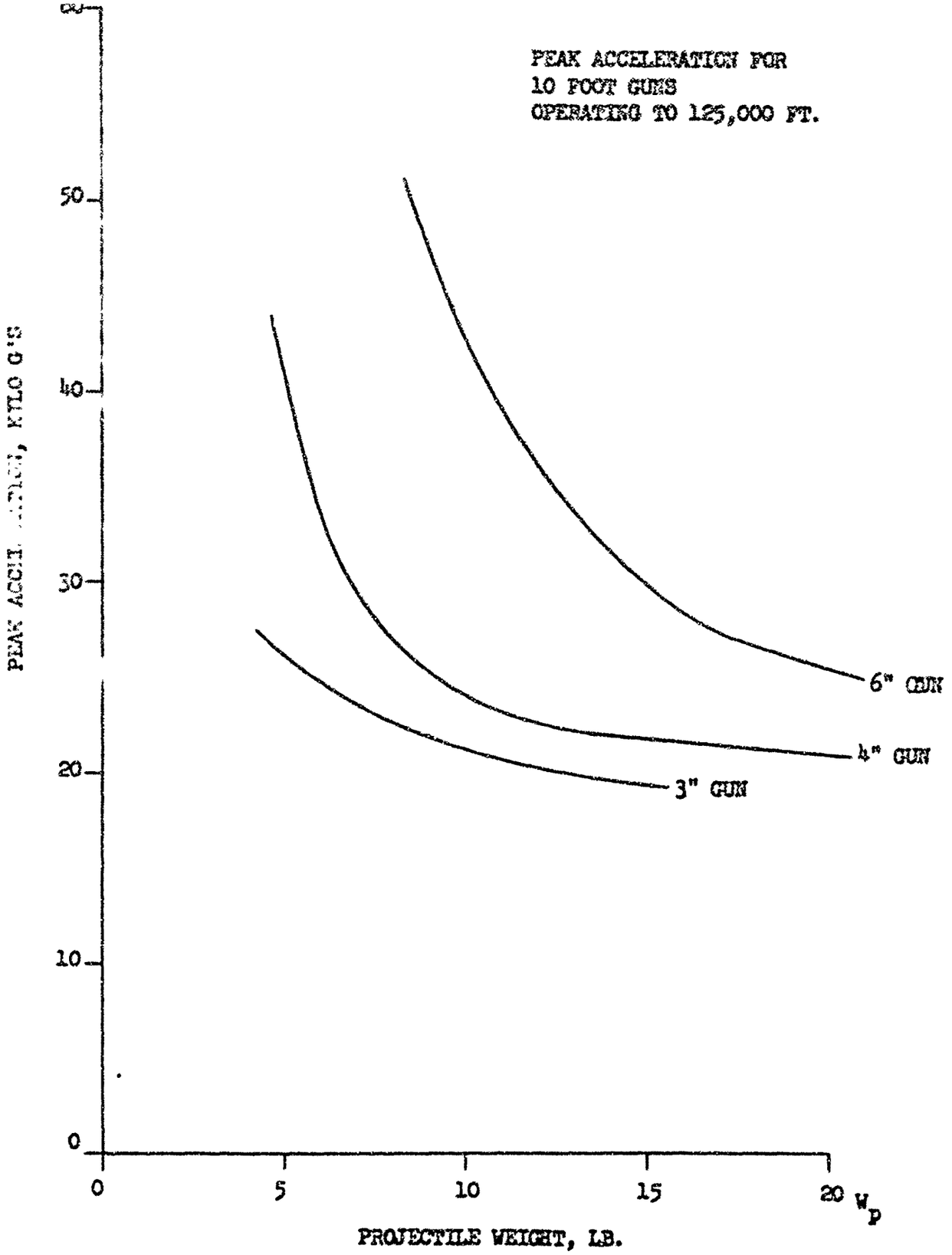

FIGURE 5-4

GUN-LAUNCHED PROBE

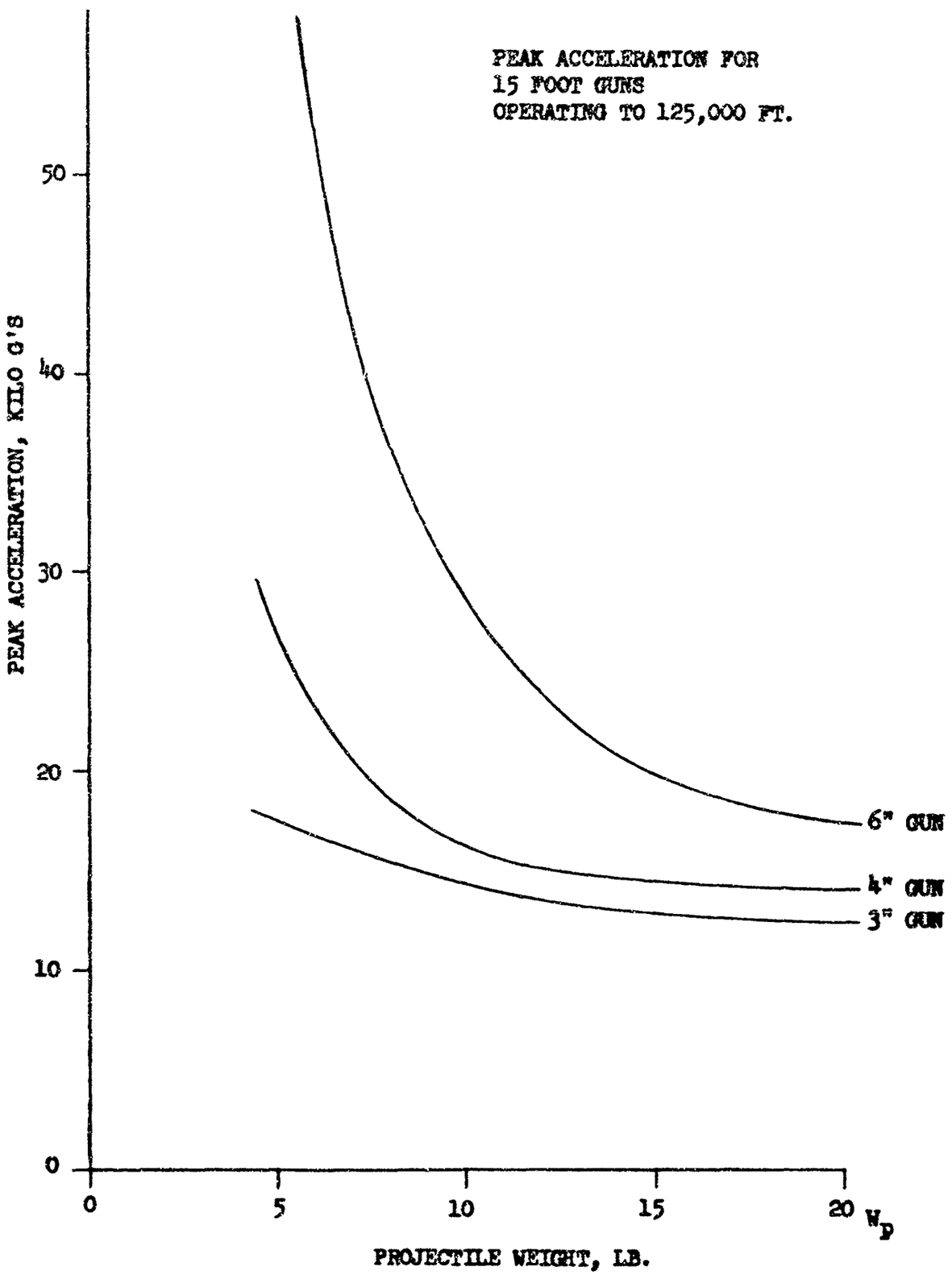

FIGURE 5-5

GUN-LAUNCHED PROBE

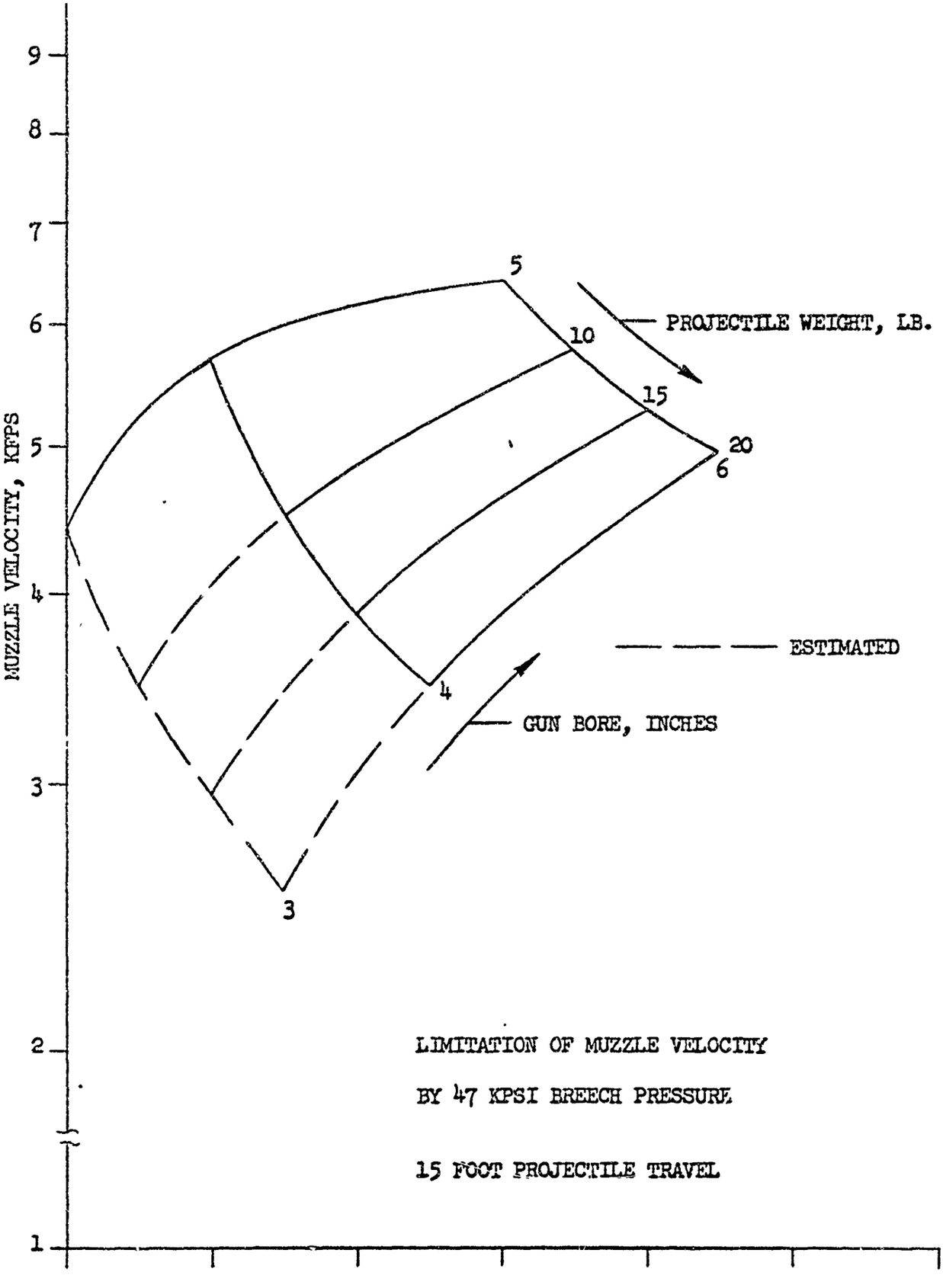

FIGURE 5-6

GUN-LAUNCHED PROBE

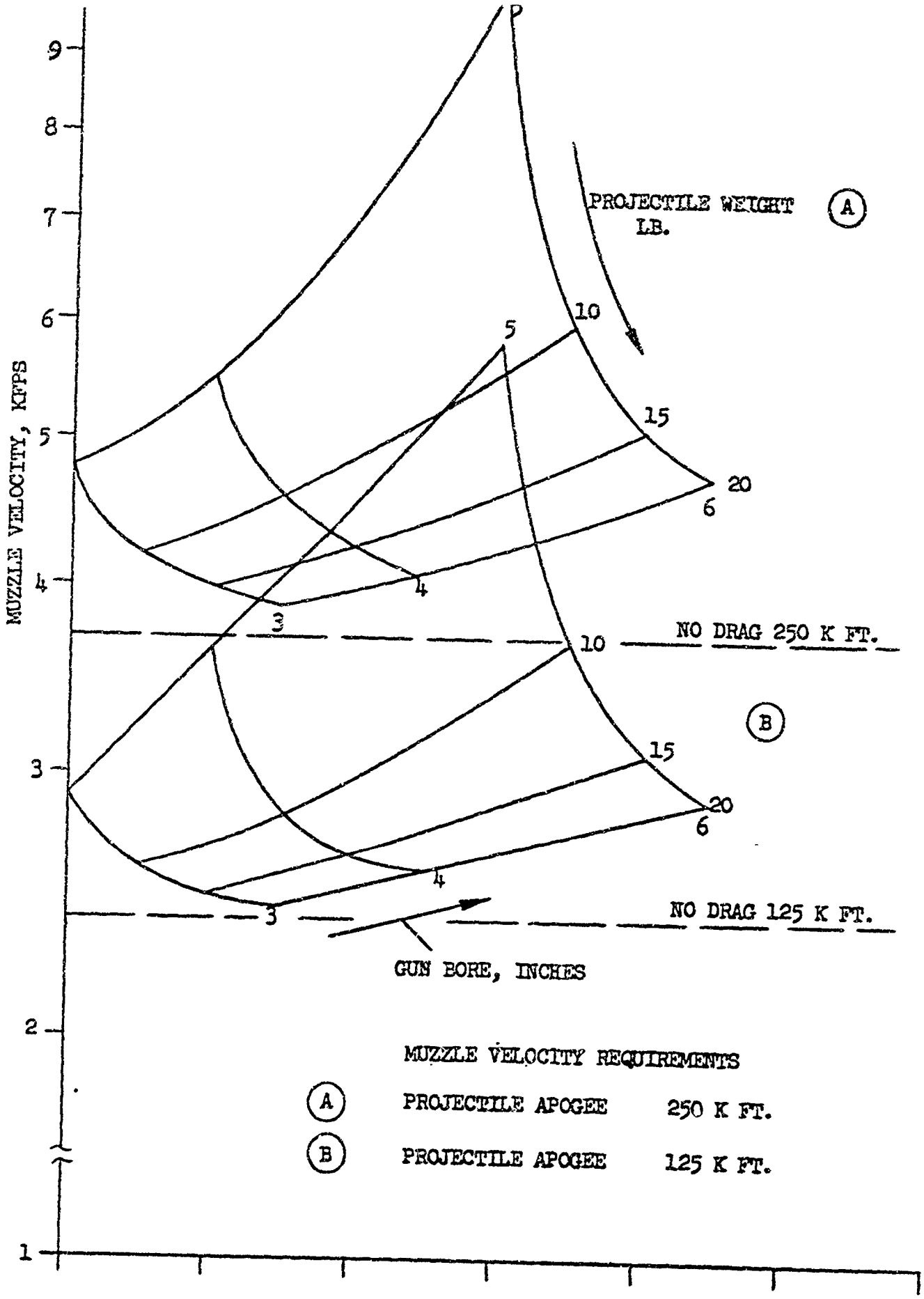

MUZZLE VELOCITY REQUIREMENTS

(A)	PROJECTILE APOGEE	250 K FT.
(B)	PROJECTILE APOGEE	125 K FT.

FIGURE 5-7

GUN-LAUNCHED PROBE

35,000 FT. LAUNCH

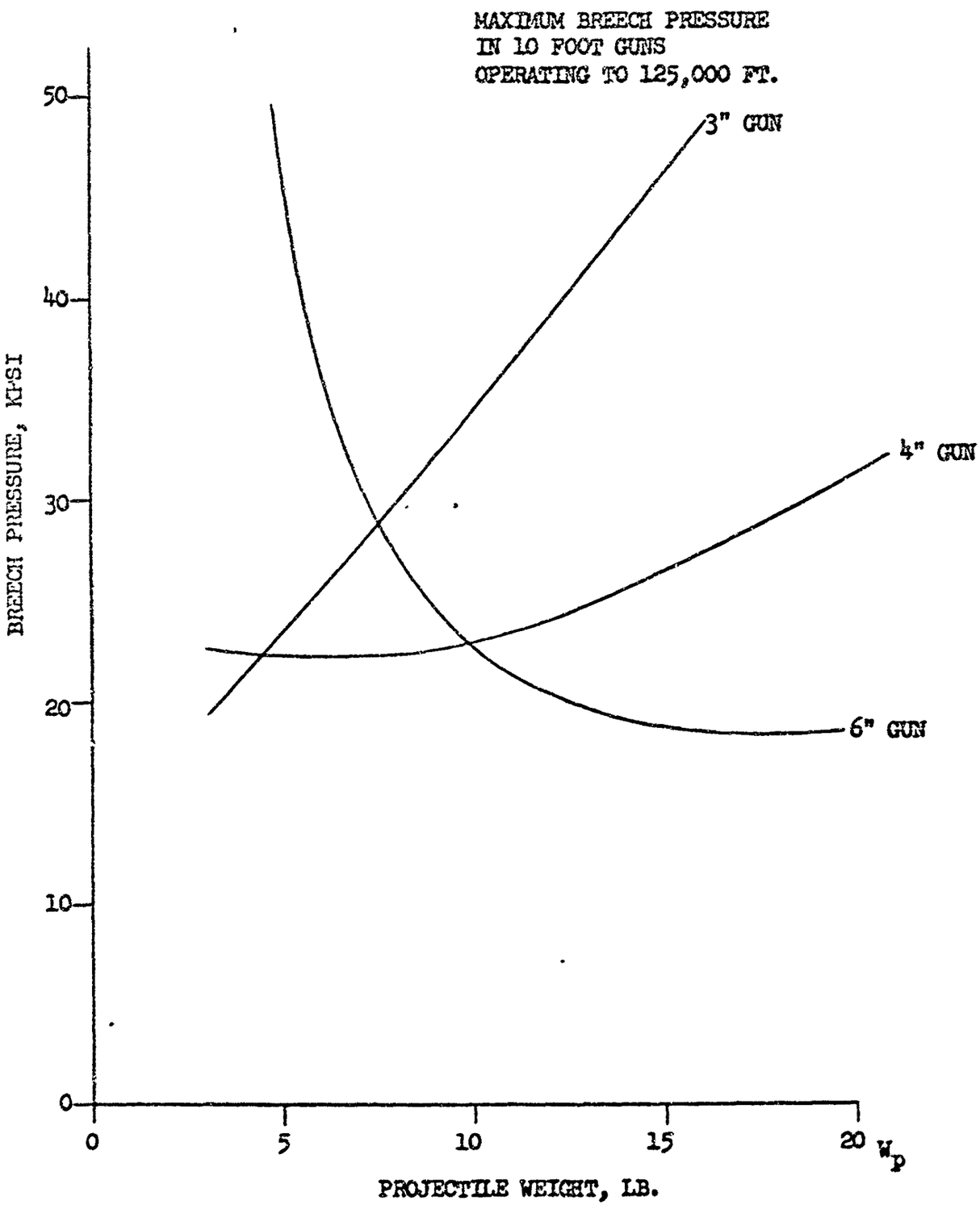

FIGURE 5-8

GUN-LAUNCHED PROBE

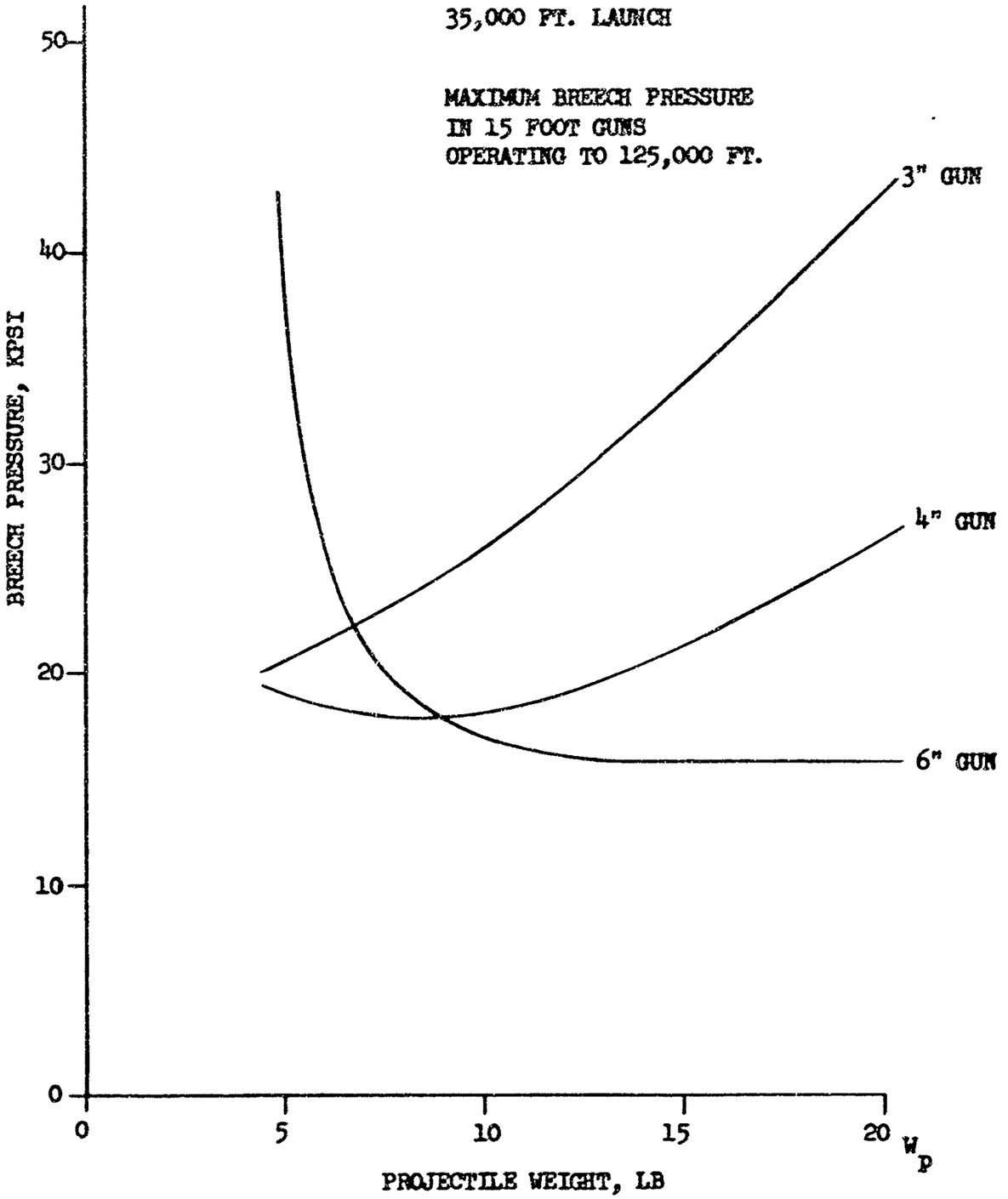

FIGURE 5-9

GUN-LAUNCHED PROBE

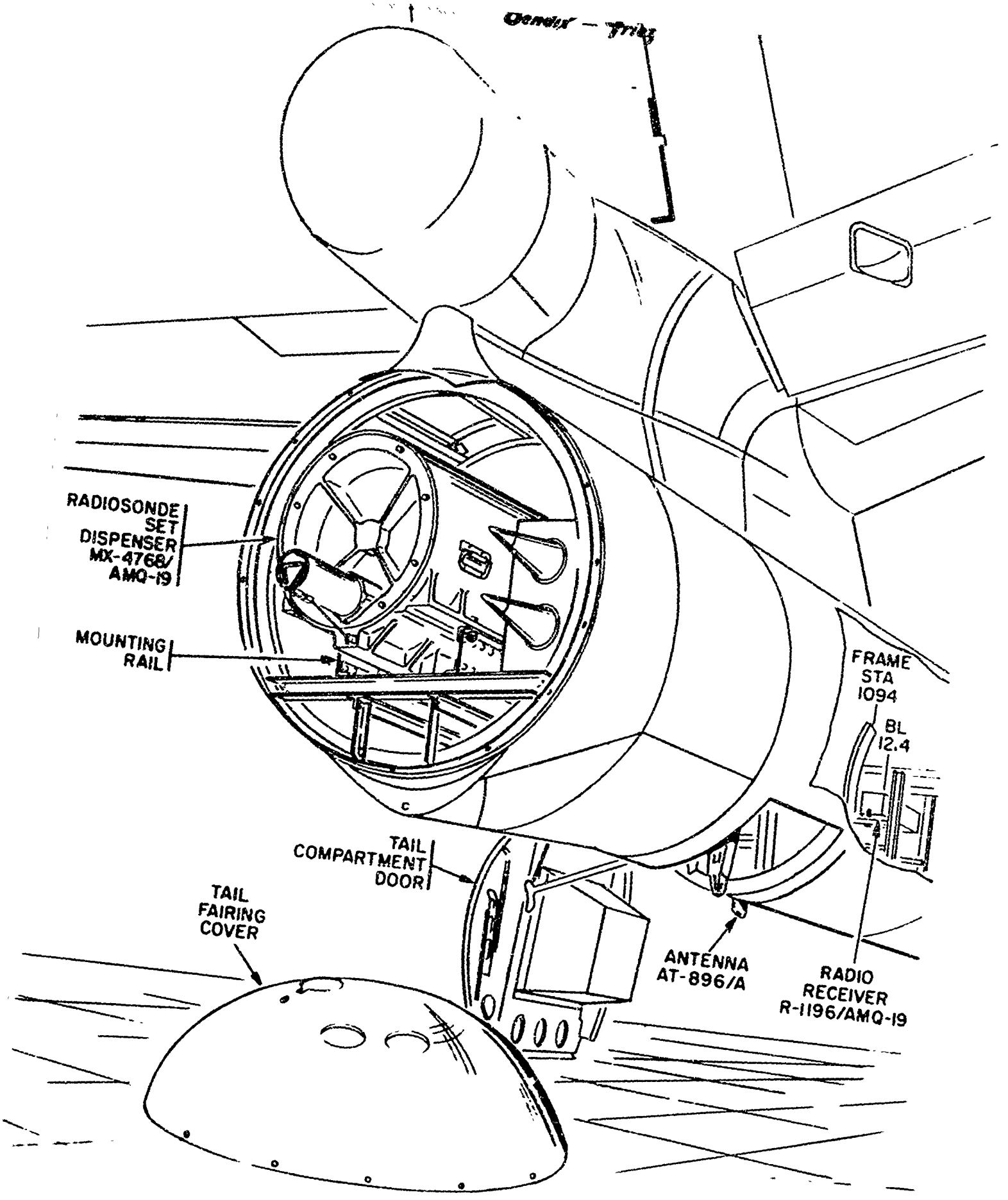

FIGURE 5-10

Aft Mounting Rocket Dispenser

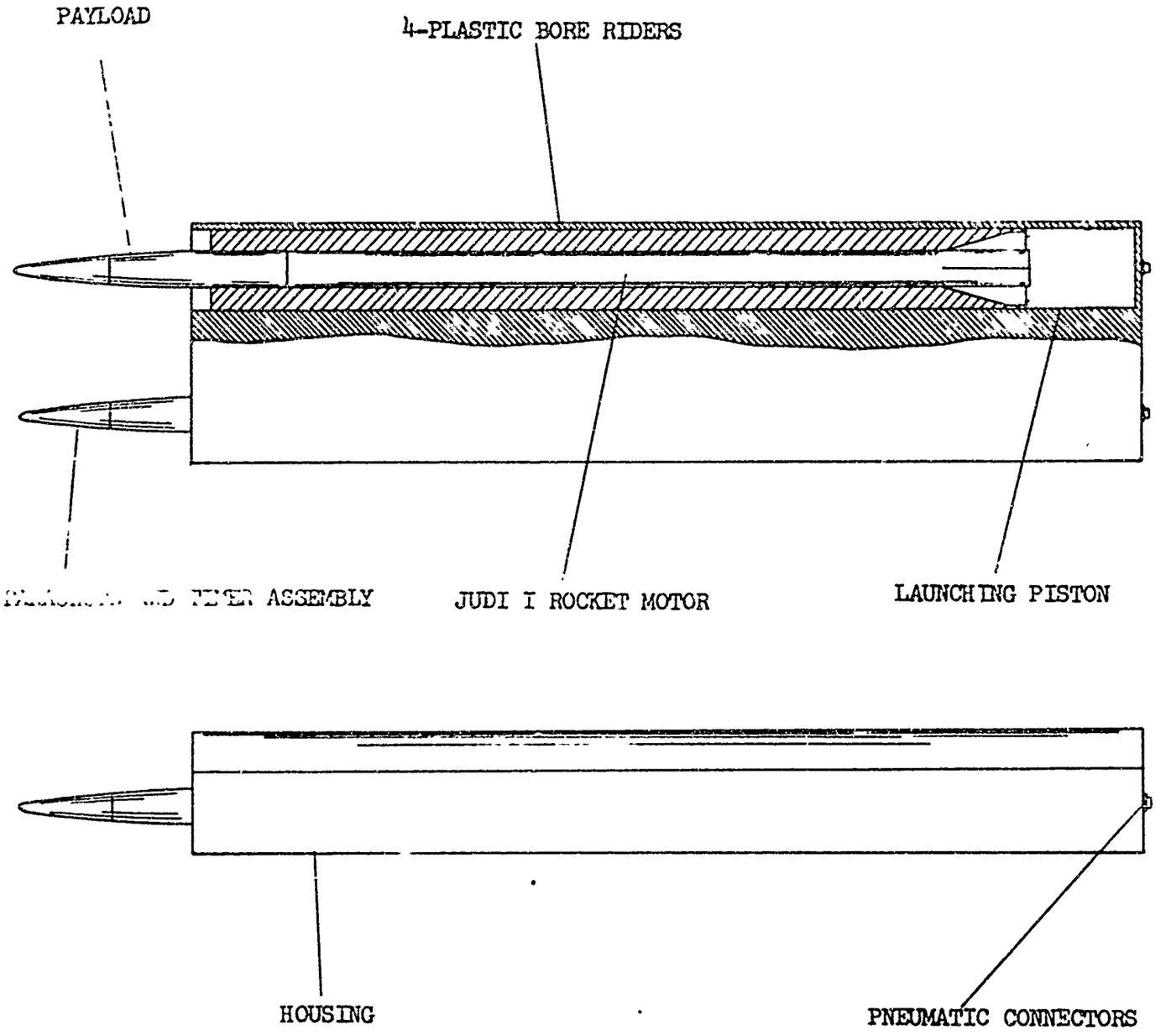

FIGURE 5-11

AFT FUSELAGE
DISPENSER

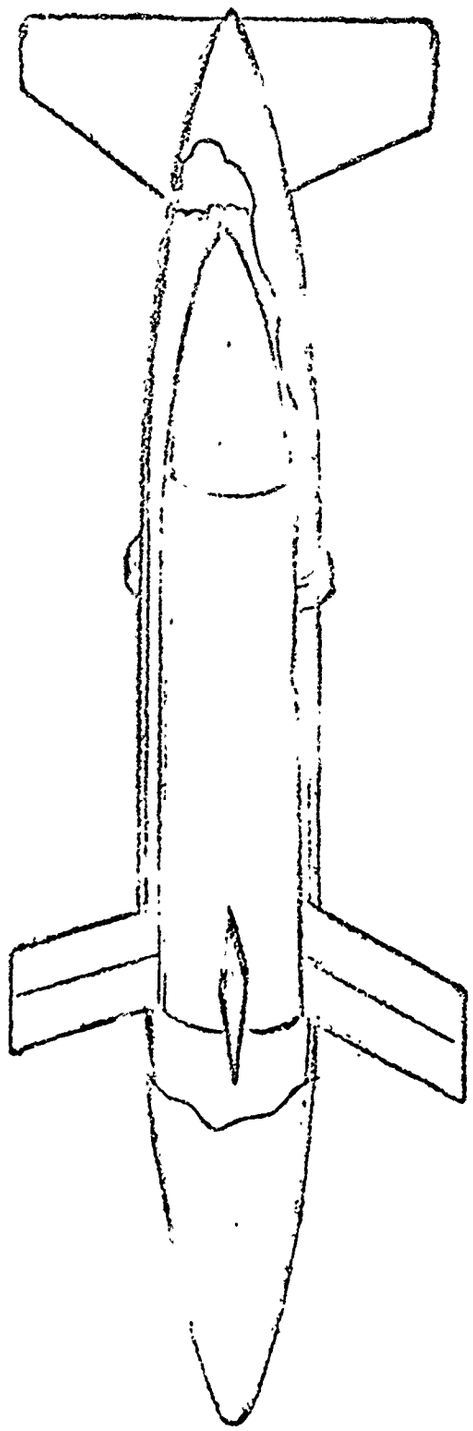

FIGURE 5-12

SOUNDING ROCKET IN POD

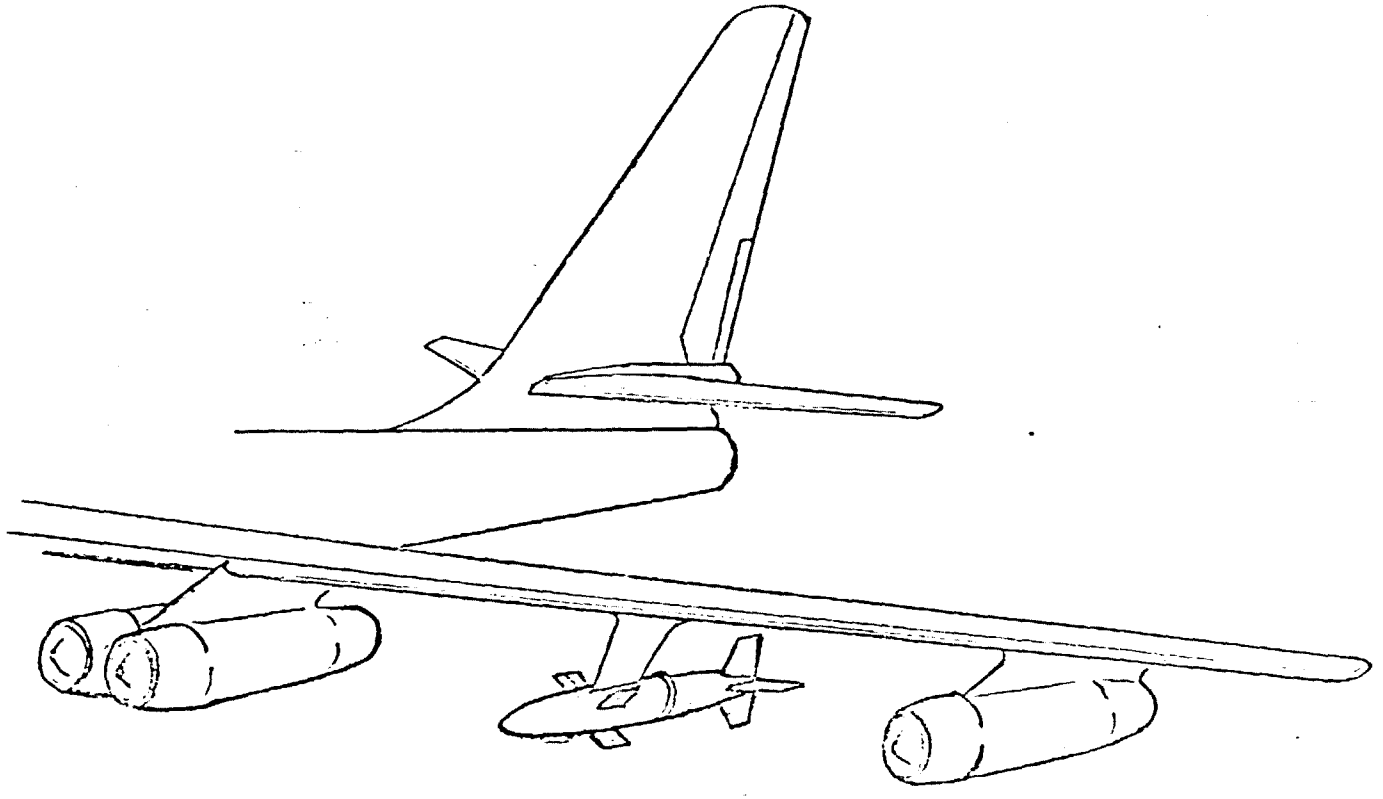

DROP POD INSTALLATION ON
W-47 AIRCRAFT

FIGURE 5-13

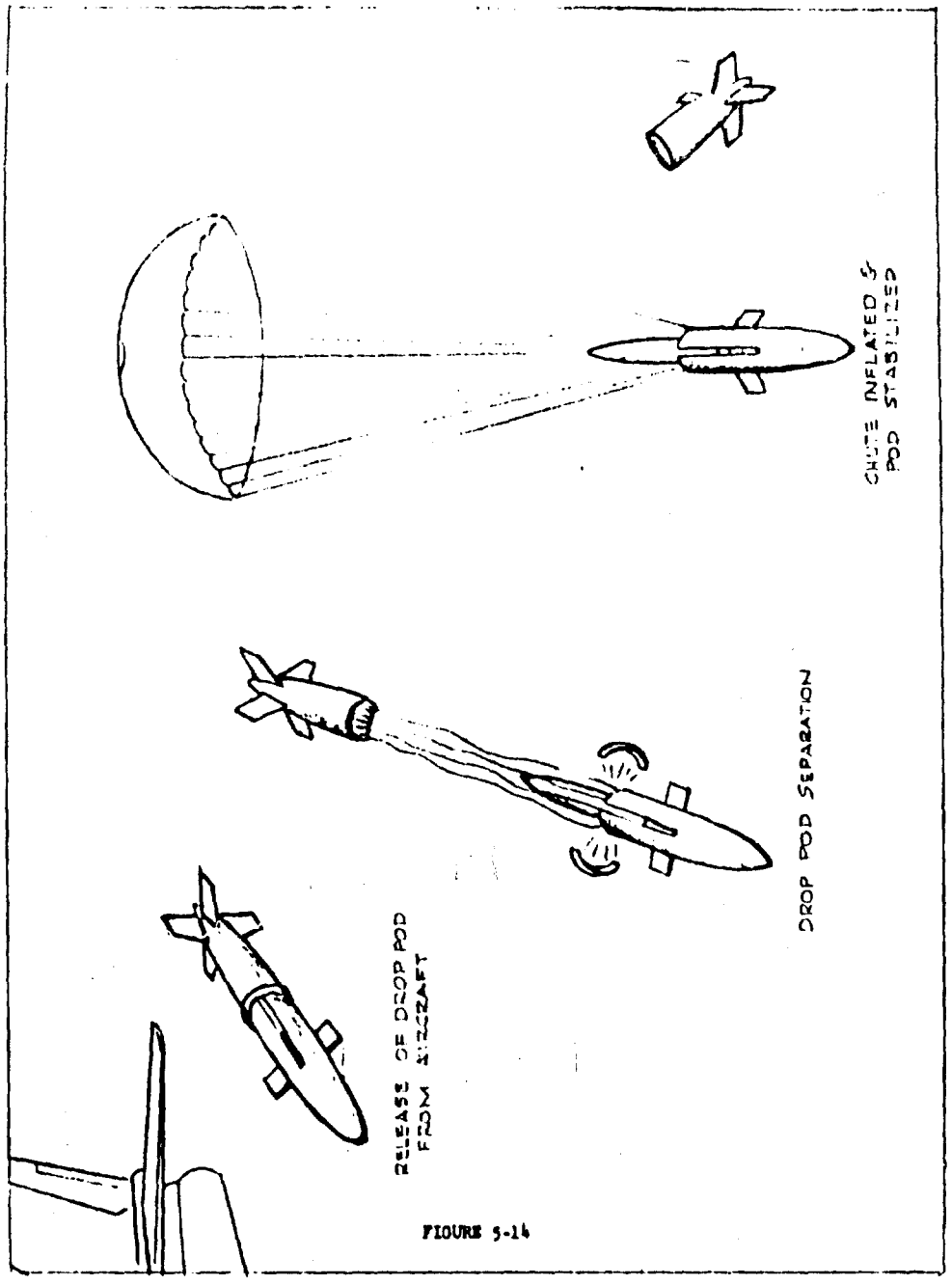
CHUTE INFLATED & POD STABILIZED
DROP POD SEPARATION
RELEASE OF DROP POD FROM AIRCRAFT

FIGURE 5-14

SOUNDING ROCKET
ASCENT

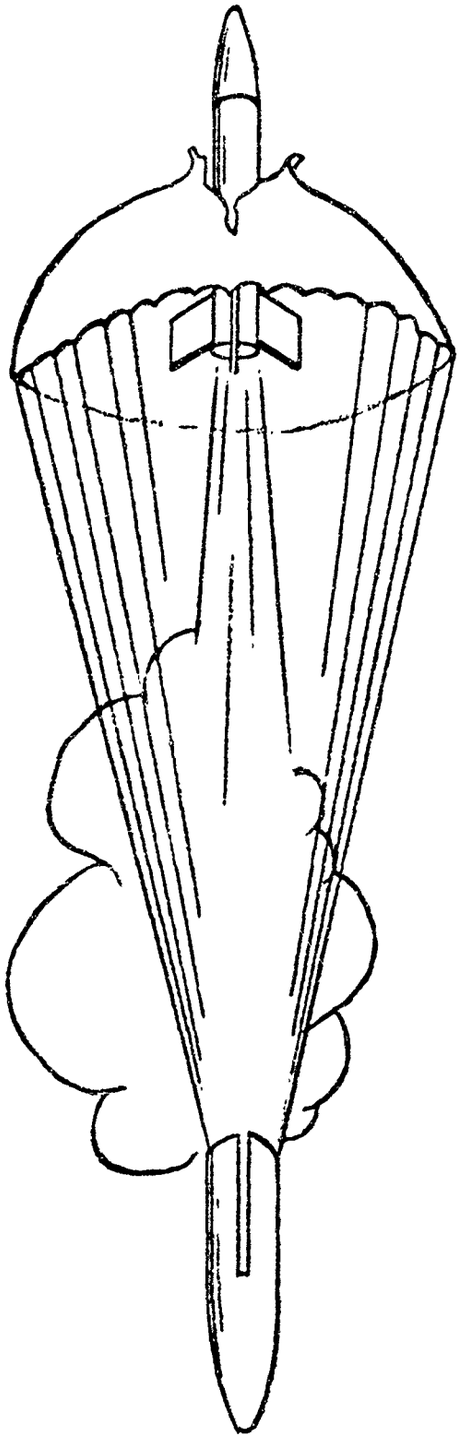

FIGURE 5-15

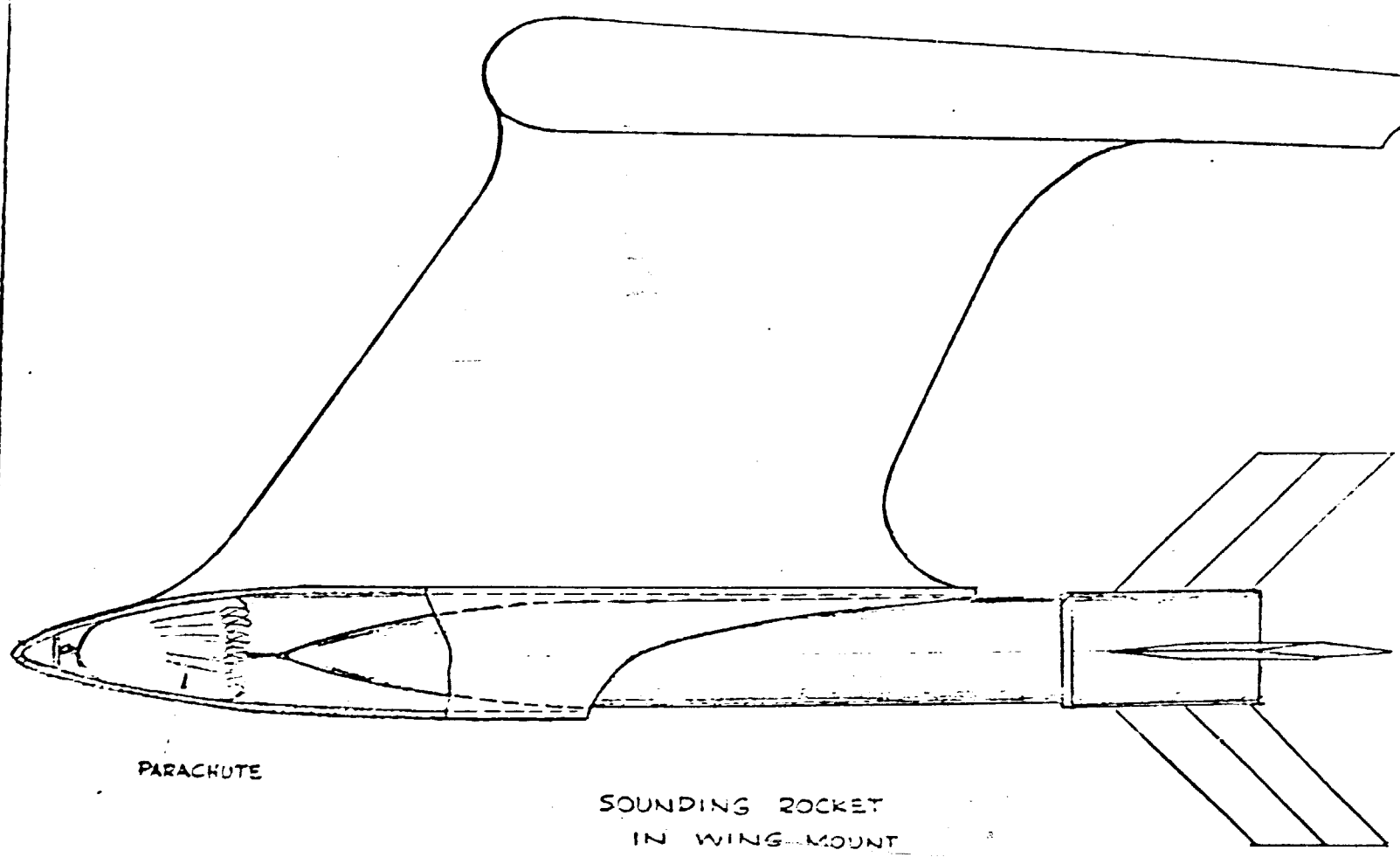

FIGURE 5-16

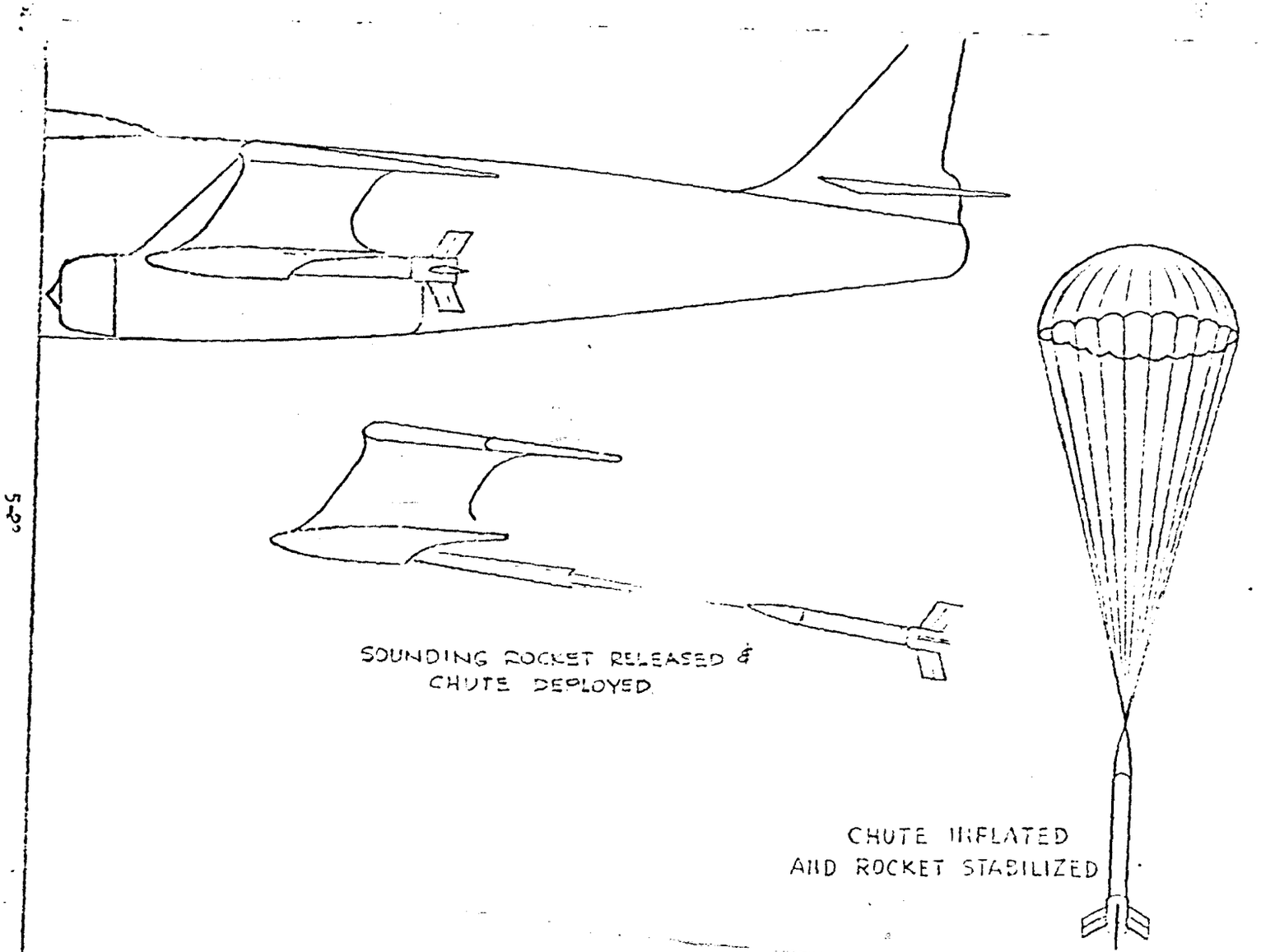
SOUNDING ROCKET RELEASED &
CHUTE DEPLOYED
CHUTE INFLATED
AND ROCKET STABILIZED

FIGURE 5-17

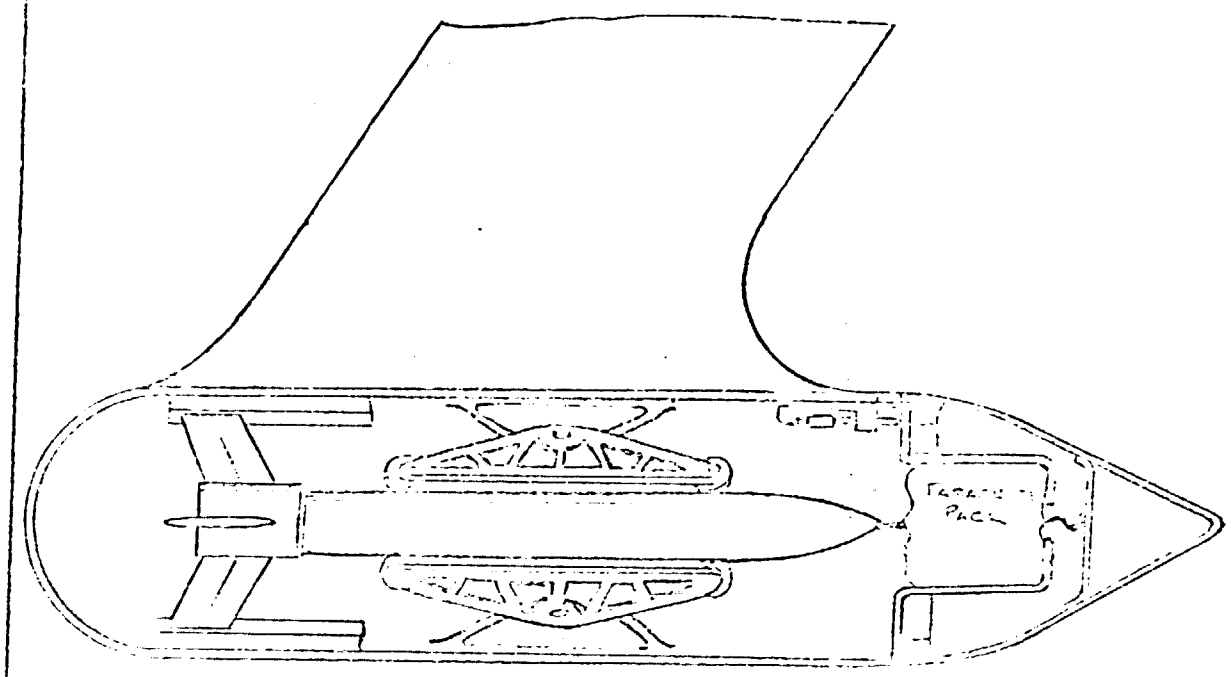

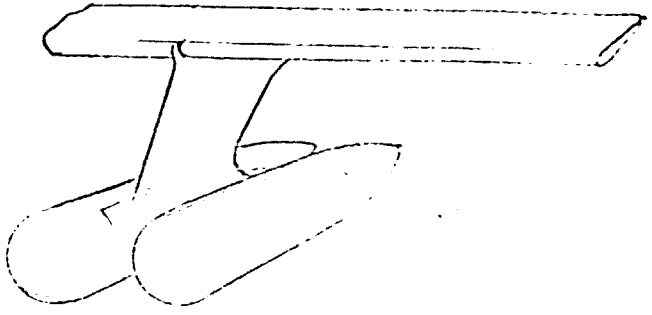

SOUNDING ROCKET IN PERMANENT WING MOUNTED DUAL PODS.

FIGURE 5-18

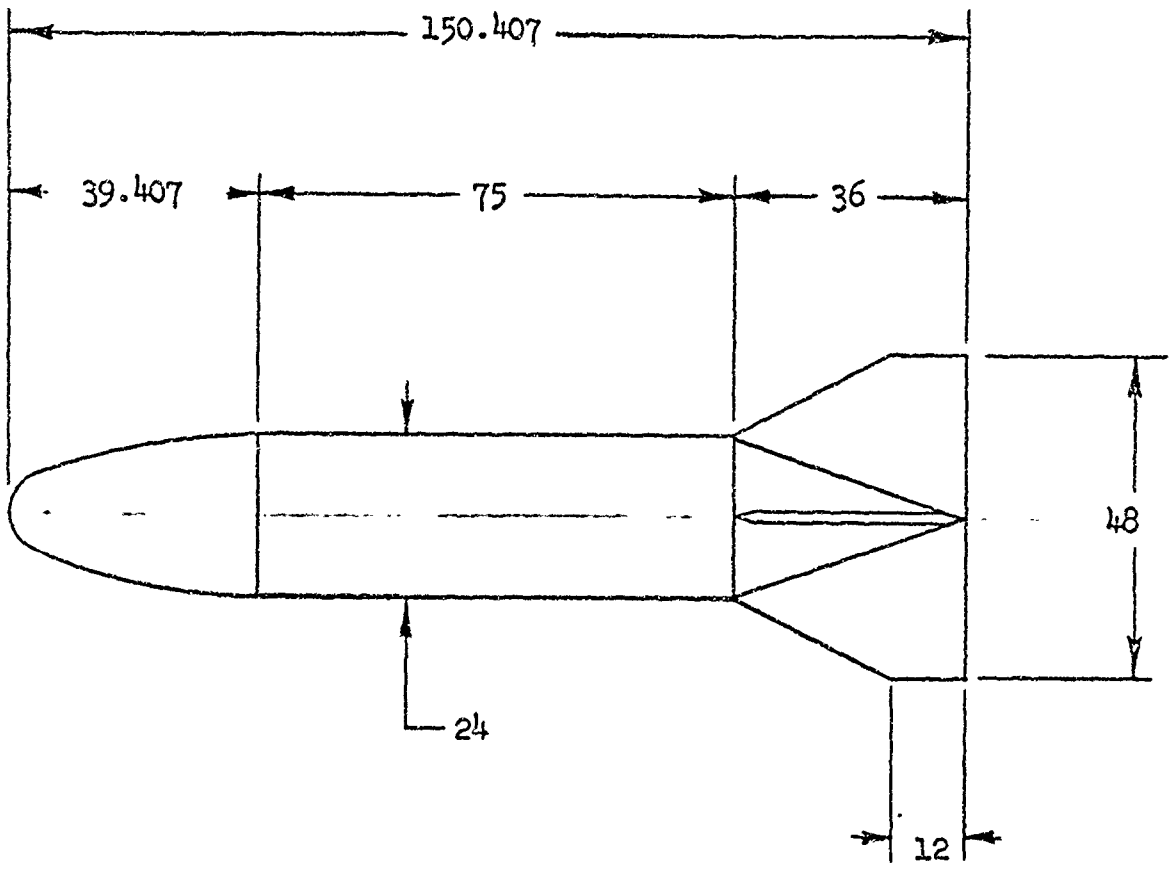

FIGURE 5-19

SOUNDING ROCKET DROP POD

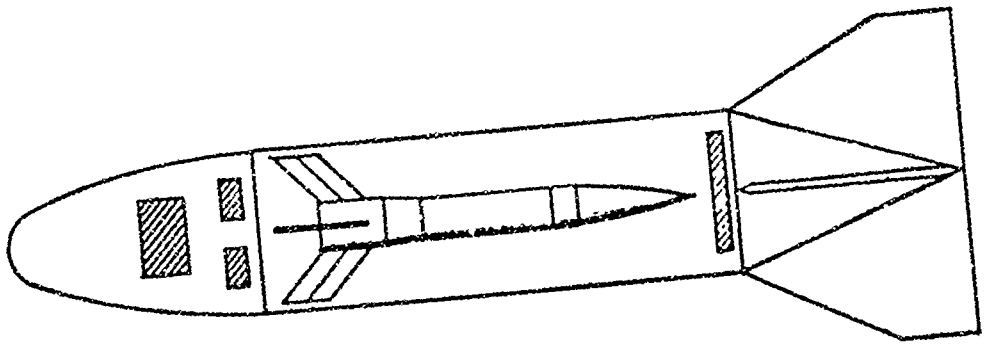

CROSS SECTION OF DROP POD SHOWING SOUNDING ROCKET, FIRING MODULES AND PARACHUTE.

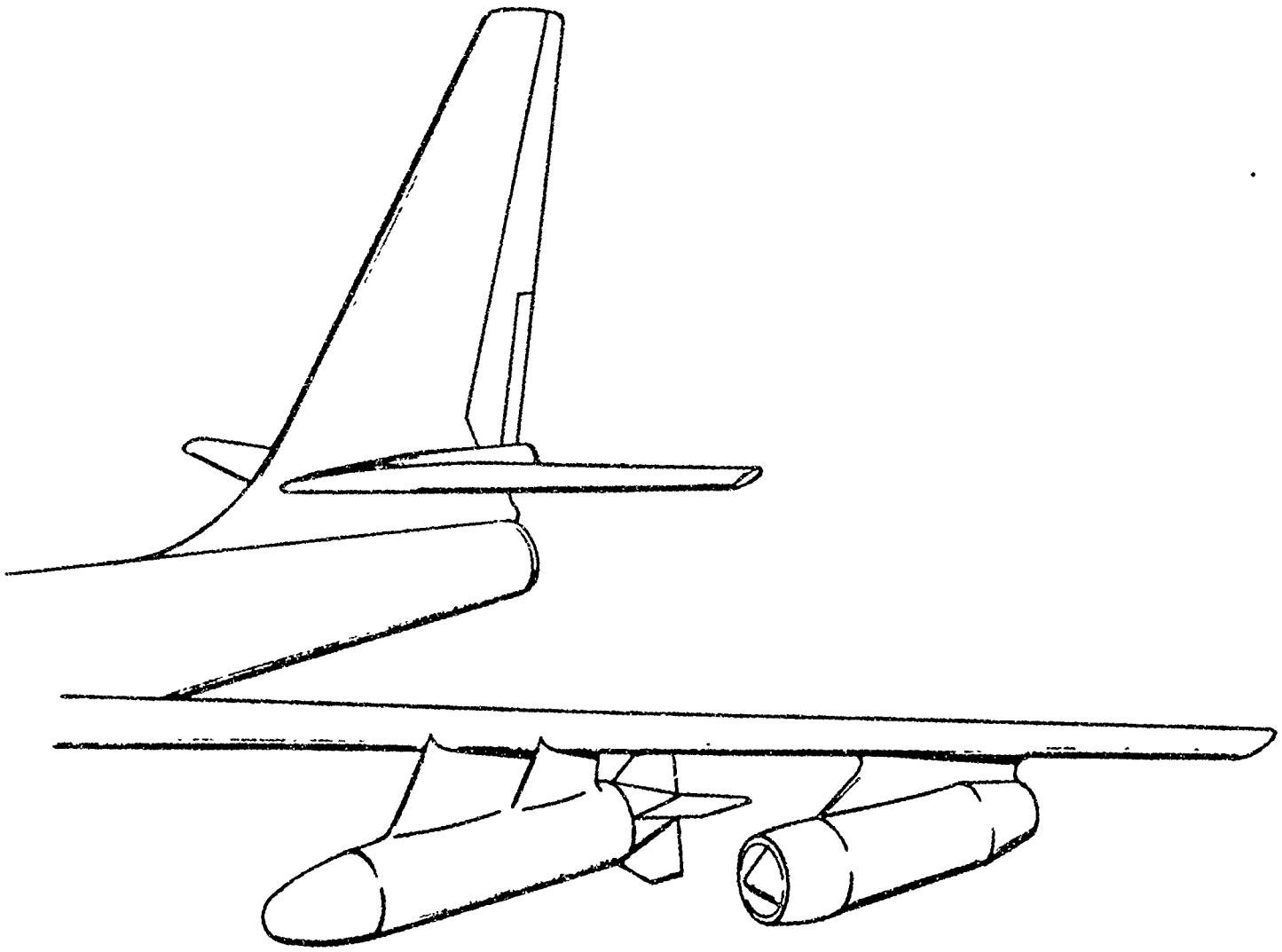

DROP POD INSTALLATION ON W-47 AIRCRAFT.

FIGURE 5-20

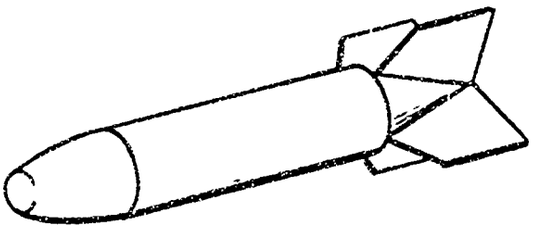

RELEASE OF DROP POD FROM AIRCRAFT

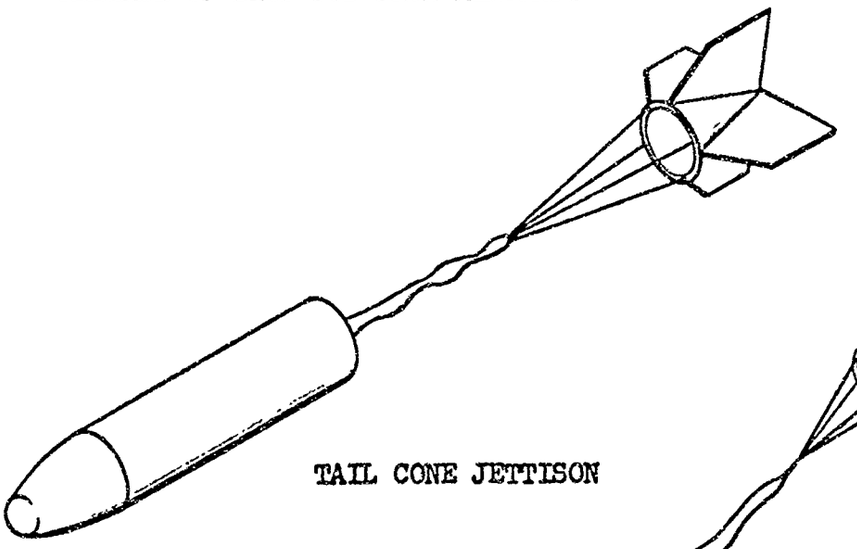

TAIL CONE JETTISON

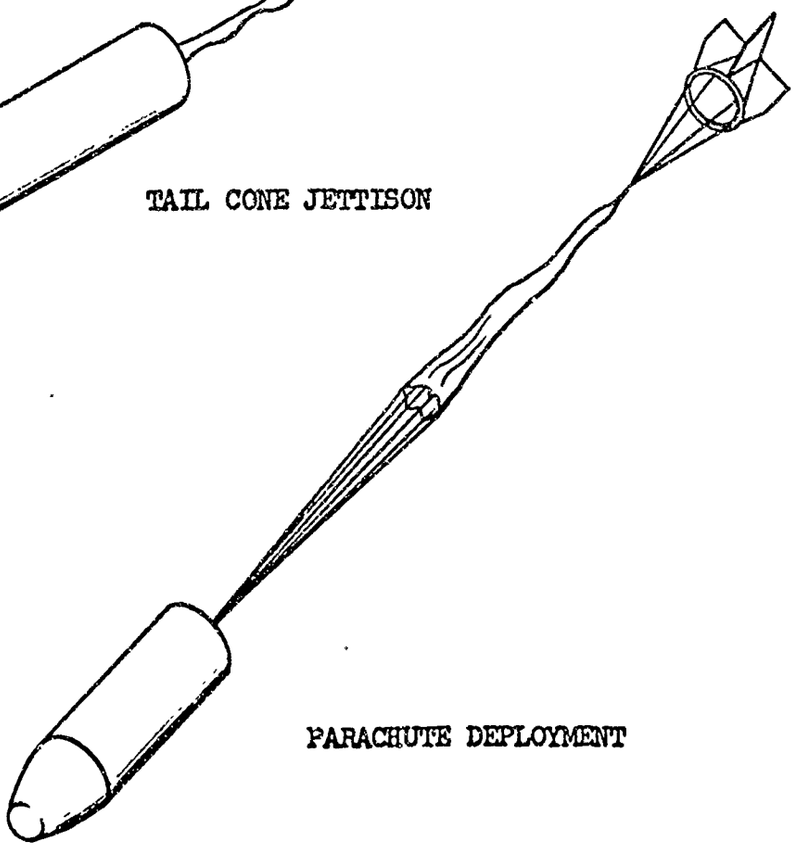

PARACHUTE DEPLOYMENT

FIGURE 5-21

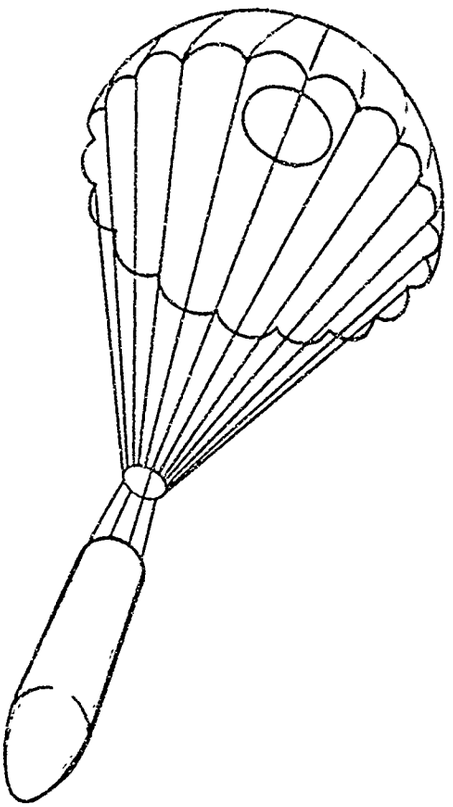

PARACHUTE INFLATION
AND POD STABILIZATION

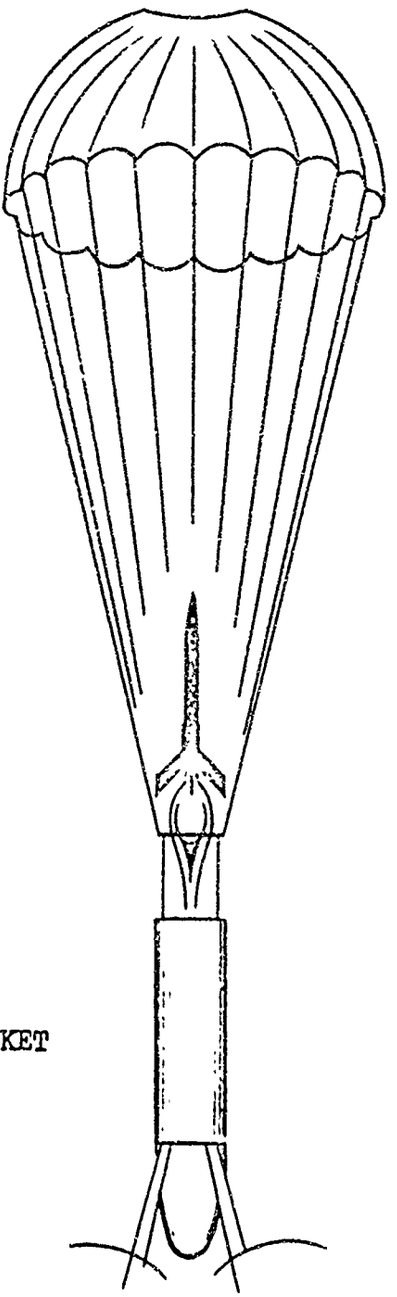

SOUNDING ROCKET
IGNITION

FIGURE 5-22

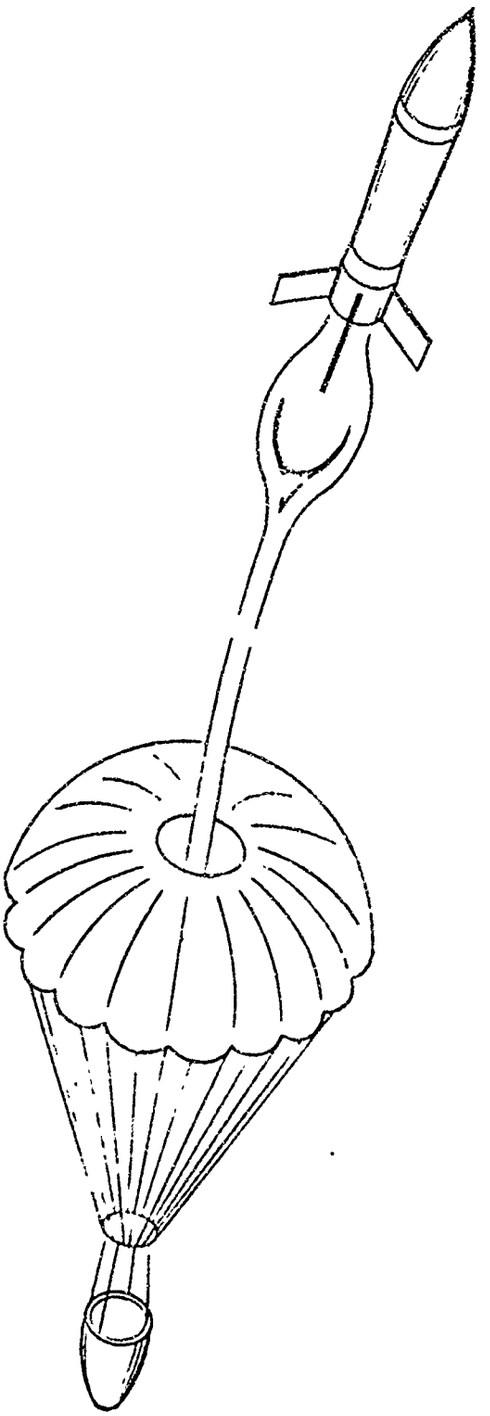

SOUNDING ROCKET ASCENT

FIGURE 5-23

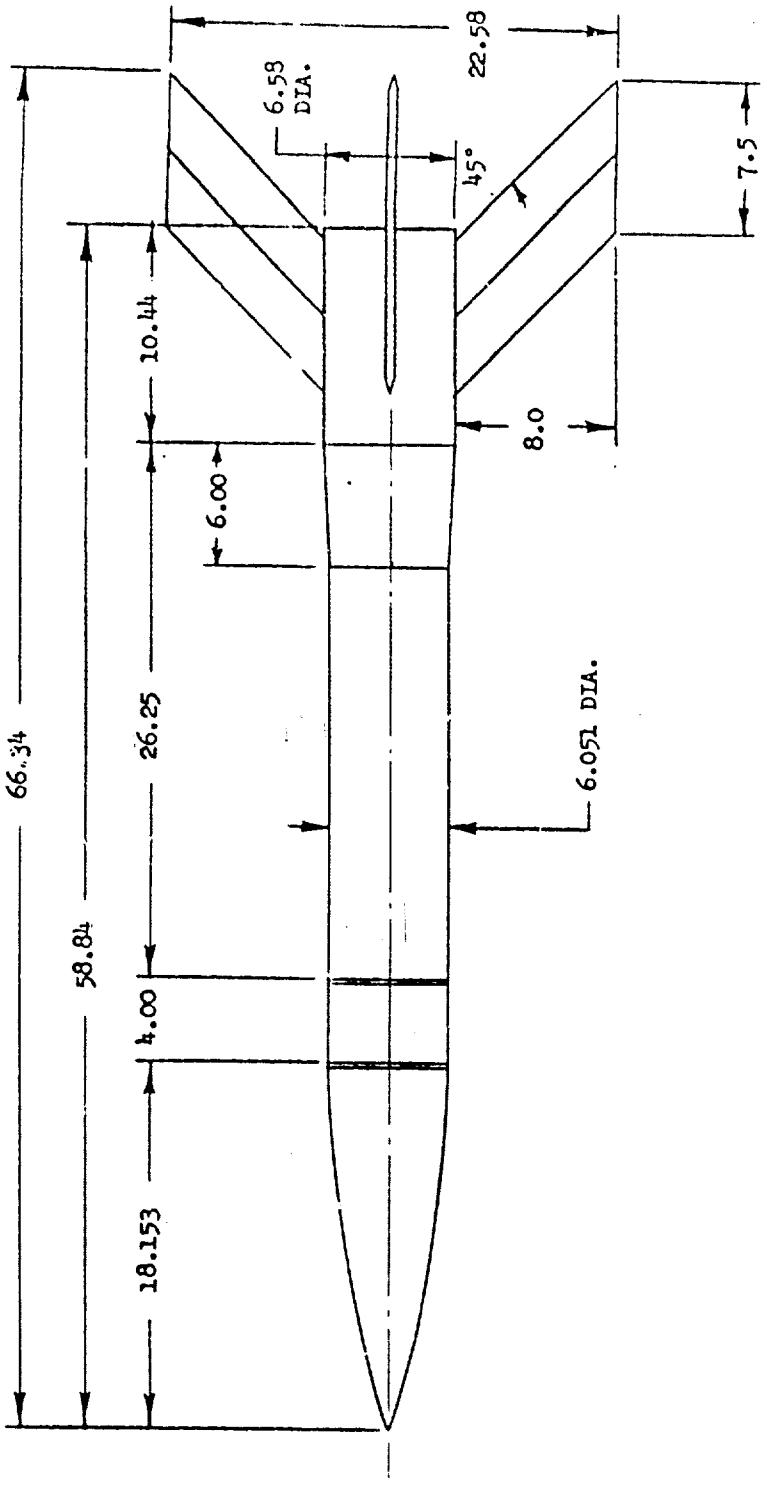

FIGURE 5-24

AIR LAUNCHED METEOROLOGICAL SOUNDING VEHICLE

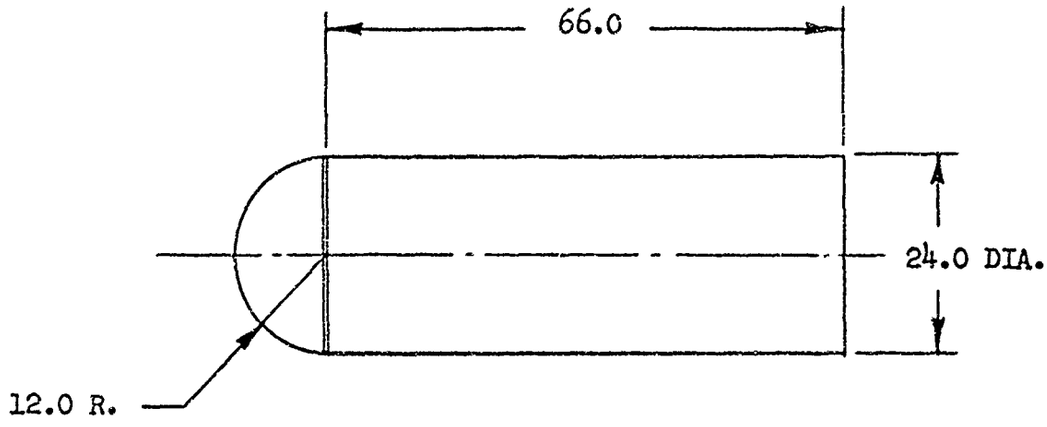

SOUNDING ROCKET DROP POD

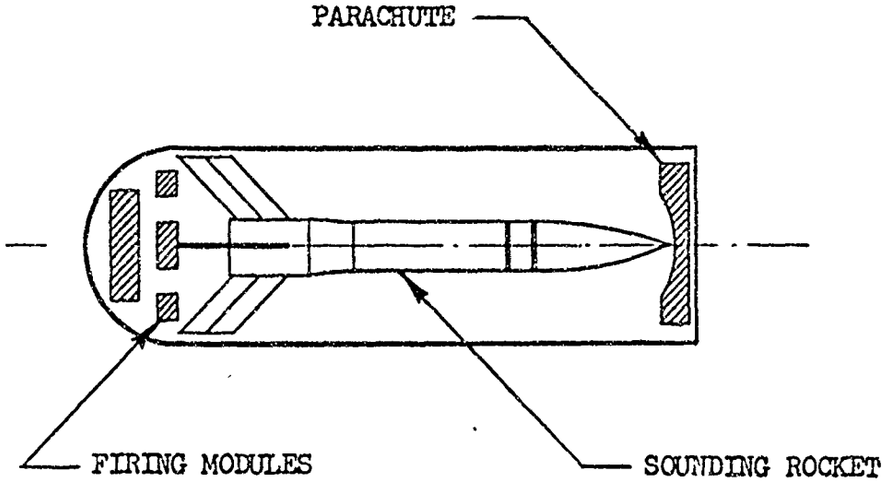

CROSS SECTION OF DROP POD

FIGURE 5-25

SOUNDING ROCKET DROP POD

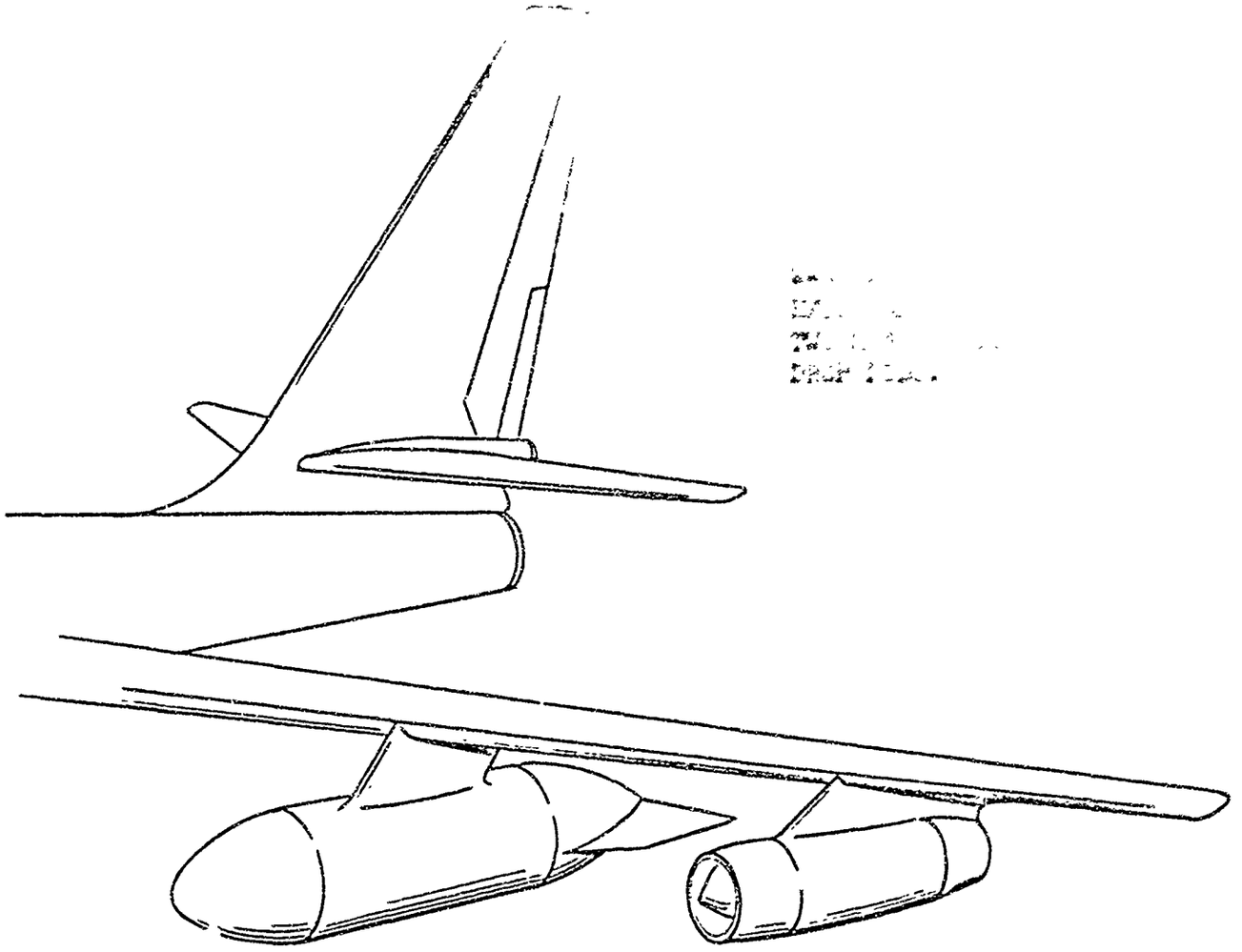

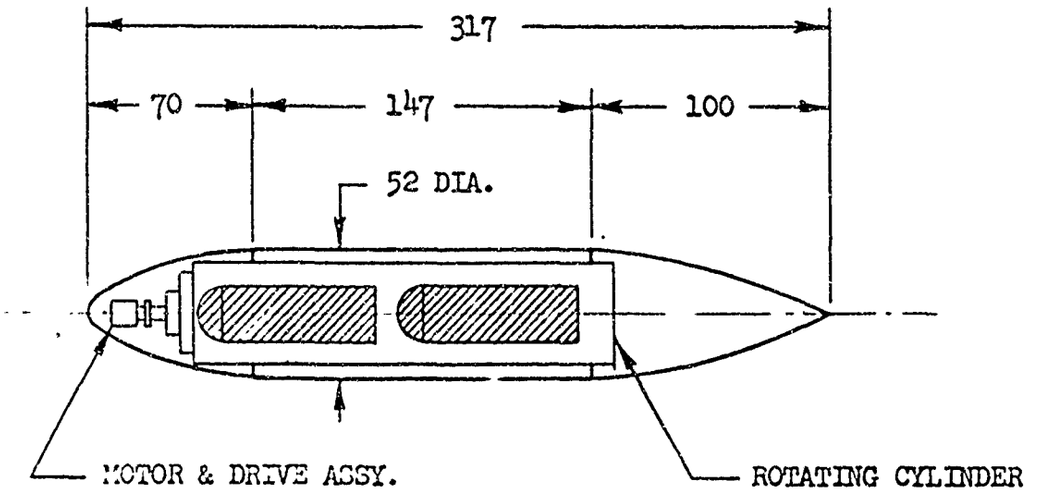

CROSS SECTION OF W-47 EXTERNAL STORE

FIGURE 5-26

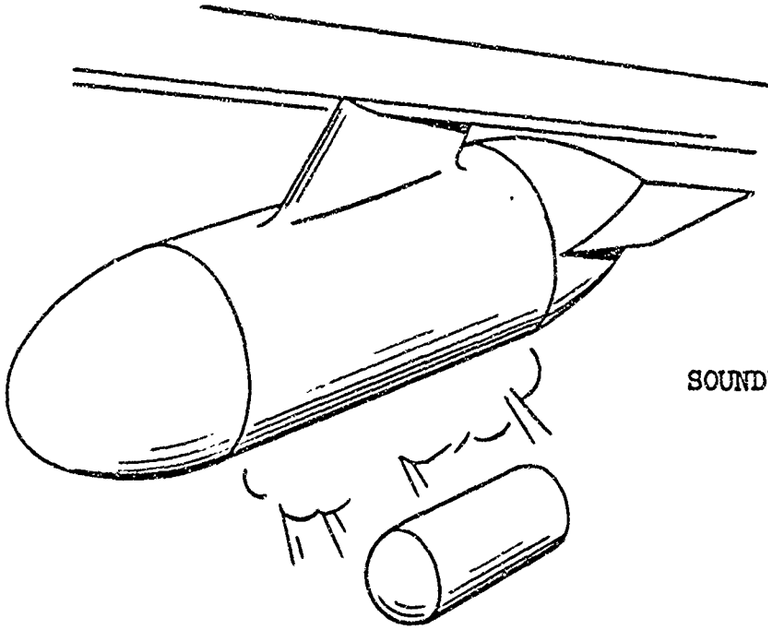

SOUNDING ROCKET DROP POD JETTISON

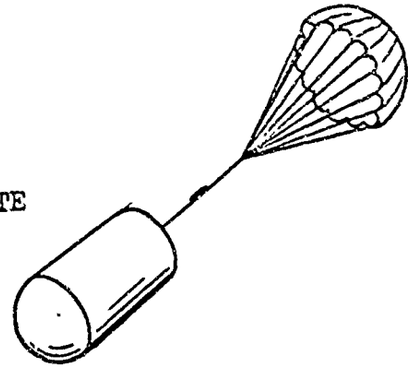

DROGUE PARACHUTE
DEPLOYMENT

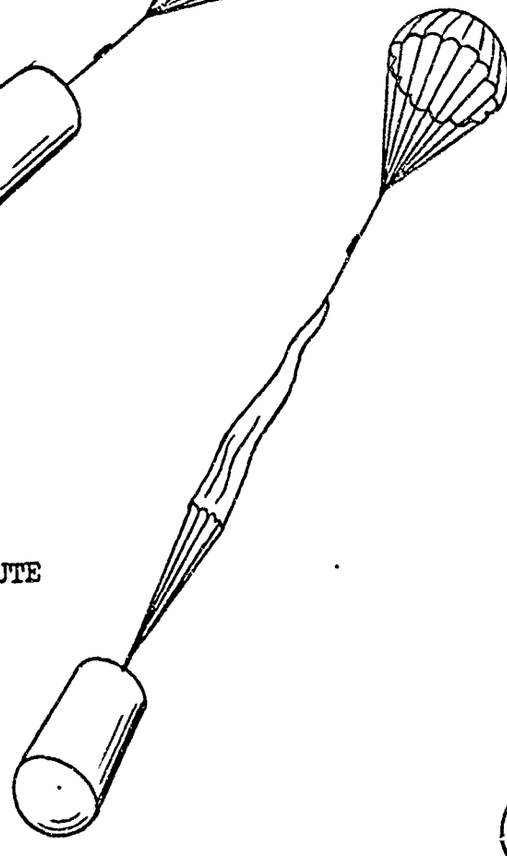

MAIN PARACHUTE
DEPLOYMENT

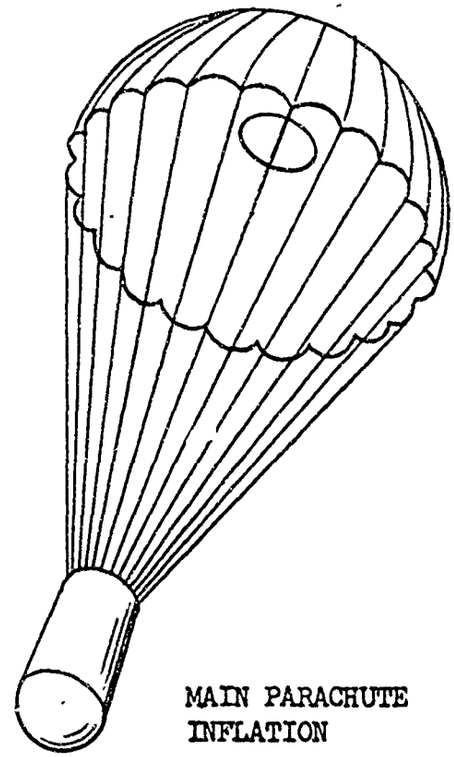

MAIN PARACHUTE
INFLATION

FIGURE 5-27

LAUNCH SEQUENCE

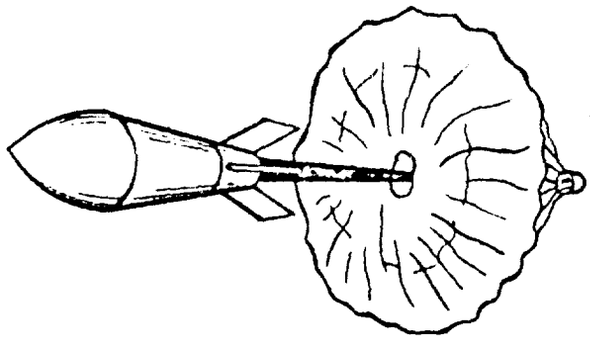

SOUNDING ROCKET ASCENT

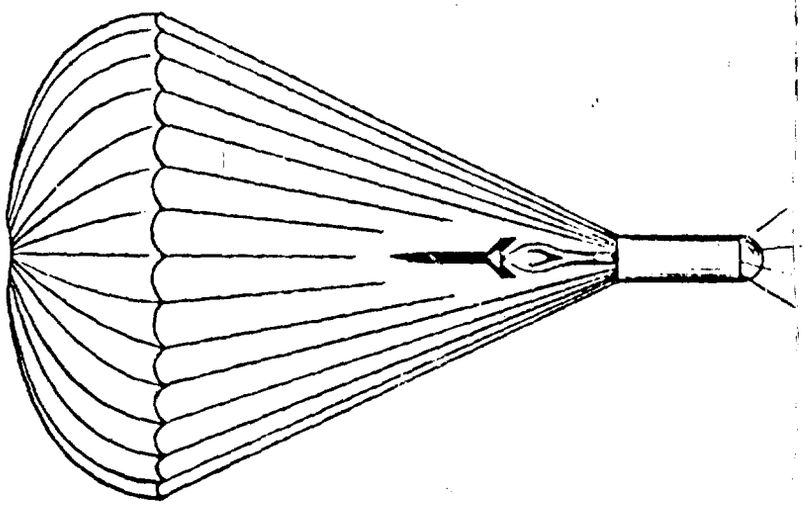

SOUNDING ROCKET IGNITION

FIGURE 5-28

SOUNDING VEHICLE DEPLOYMENT

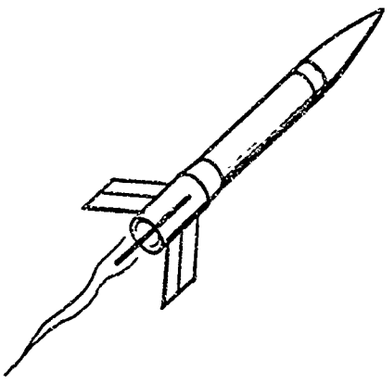

SOUNDING ROCKET IMMEDIATELY
PRIOR TO APOGEE

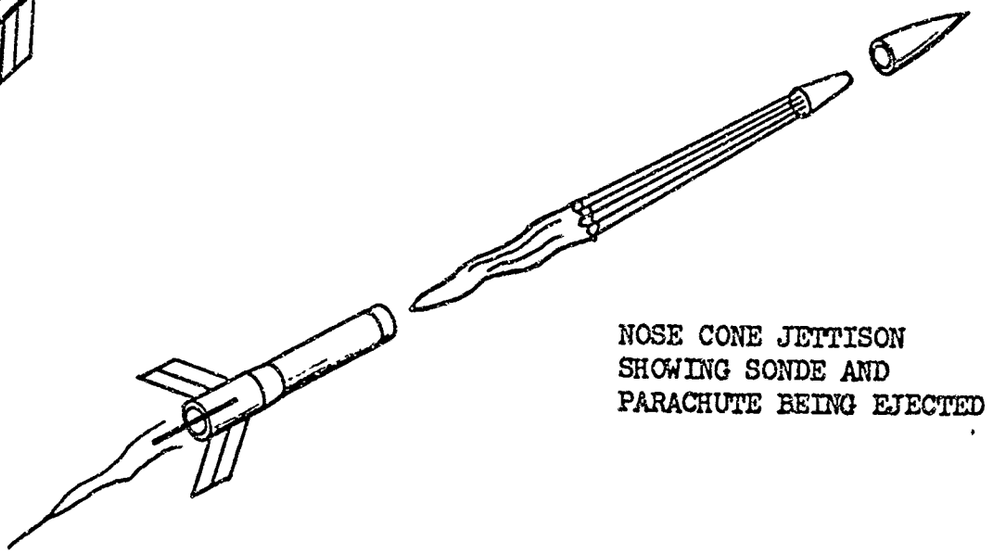

NOSE CONE JETTISON
SHOWING SONDE AND
PARACHUTE BEING EJECTED

PARACHUTE INFLATION
AND STABILIZATION

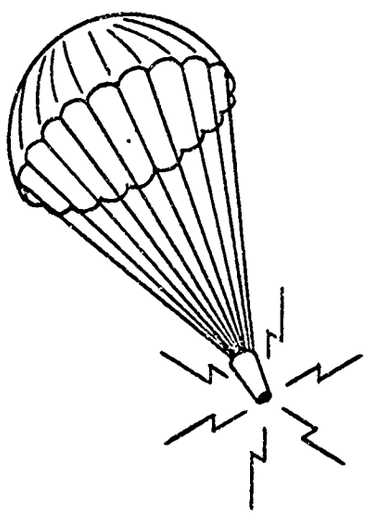

SONDE DESCENDING
ON PARACHUTE

FIGURE 5-29

APOGEE TO RADIOSONDE DEPLOYMENT

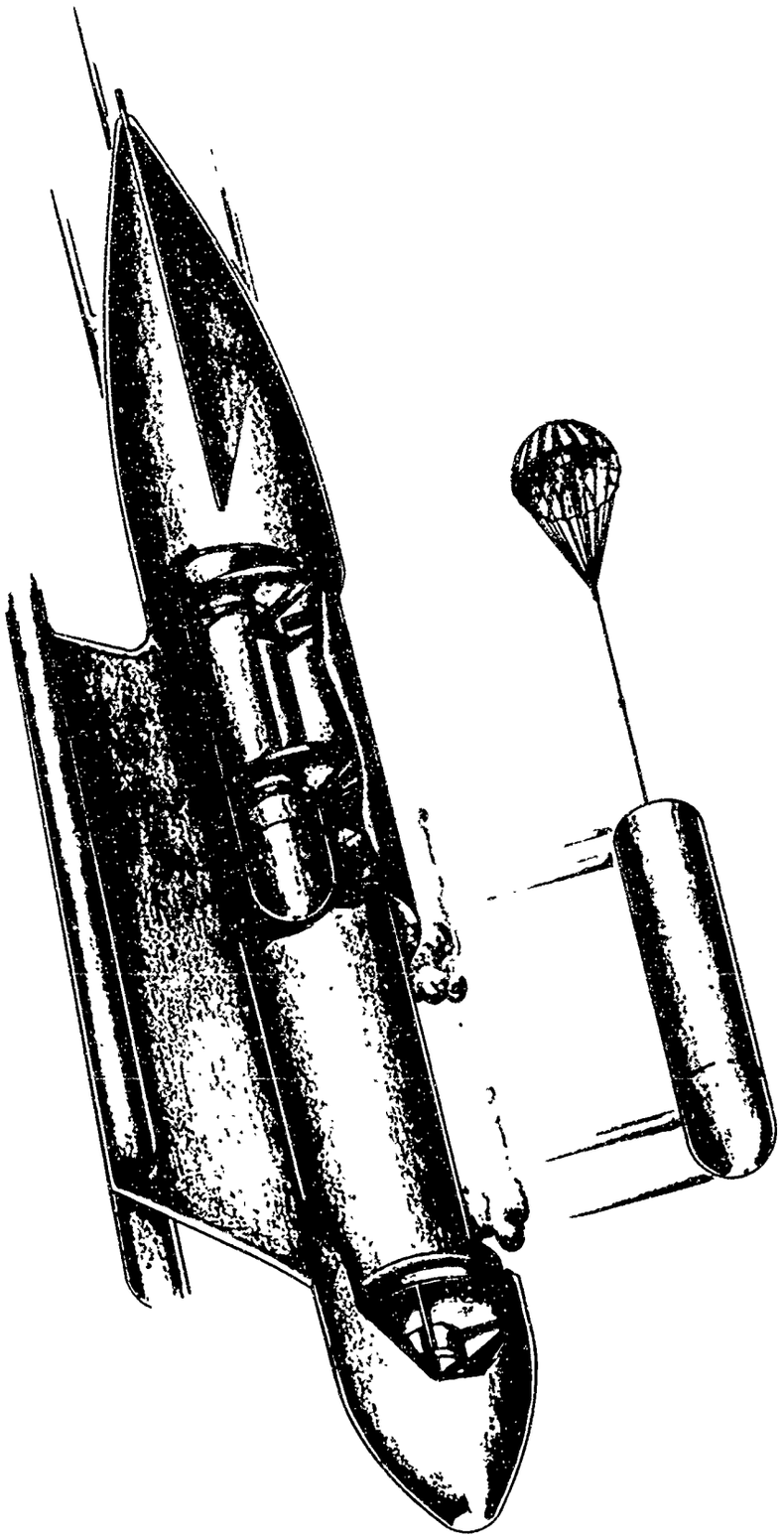

FIGURE 5-30

DISPENSER OPERATION

SECTION VI

THE AN/AMQ-19 AUTOMATIC METEOROLOGICAL SYSTEM

The AN/AMQ-19 Meteorological System, produced by Bendix Friez, includes three subsystems. These are Vertical, Horizontal and Data Handling. In addition, a Ground Data Handling system is used to process the data transmitted by the collecting aircraft. A Functional Diagram of the AN/AMQ-19 System is shown in Figure 6-1.

The following components are contained in the AN/AMQ-19 system:

Radiosonde, AN/AMT-13

Radio Dispenser, MX-4768/AMQ-19

Antenna, AT-896/A

Receiver, Radio, R-1196/AMQ-19

Converter-Scanner, Signal Data, CV-1523/AMQ-19

Generator, Control Signal, O-1113/AMQ-19

Power Supply, PP-3768/AMQ-19

Control Panel, Vertical Subsystem Control-Indicator

Control Panel, Observer Inputs Selector

Control Panel, Data Handling Control-Indicator

Control Panel, Voltage Monitor Control-Indicator

Recorder-Reproducer, Signal Data, RD-253/AMQ-19

Frequency Shift Keyer-Multiplexer, KY-494/AMQ-19

VERTICAL SUBSYSTEM

The vertical subsystem consists of those components (Radiosonde, Dispenser, Antenna, and Receiver) needed to collect, process, and provide vertical sounding inputs to the data handling subsystem. This equipment can be described as follows:

A. AN/AMT-13 Radiosonde

The AN/AMT-13 Radiosonde is a meteorological sensing and telemetering package designed for ejection from high performance aircraft flying at speeds up to Mach 0.85 and at altitudes up to 50,000 feet. The radiosonde senses the characteristics of the atmosphere (pressure, temperature, and humidity) through which it passed during parachute descent from altitude. The meteorological data measured during descent are encoded into analog pulse repetition rates in the nominal range between 2450 and 6050 pulses per second. The encoded data is transmitted to a radio receiver aboard the aircraft by a 403 megacycle carrier.

The AN/AMT-13 Radiosonde, as shown in Figure 6-2, consists of a cylindrical instrument package containing the sensors, electronics, and power supply which is supported during descent from altitude by a parachute. The cylindrical instrument package is 3.5 inches in diameter and 18 inches in length. The covering tube is open and slotted at the forward end to permit the free flow of air to temperature and humidity sensors. Ports for the barometric pressure sensor are located around the cylinder at the midpoint in length. A compartment for storage of the parachute is located at the aft end of the unit. The descent parachute is a nylon hemispherical canopy 12 inches in diameter, which is attached to the instrument package by nylon risers. This parachute configuration results in descent from 40,000 feet in nine minutes, from 35,000 feet in seven minutes, and from 10,000 feet in 2.5 minutes. The radiosonde weighs 4.75 pounds.

The AN/AMT-13 Radiosonde, together with the R-1196/AMQ-19 Radio Receiver aboard the aircraft, provides a reliable communications link of approximately 210 nautical miles with the aircraft flying at 40,000 feet (line of sight transmission limitation). The radiosonde transmitter operates in the 400-406 megacycle meteorological band with a peak power output in excess of 18 watts. The active elements in the sonde electronics are solid state devices with the exception of the carrier oscillator which uses an electron tube. The transmitter antenna is a flexible half-wave dipole which is extended upright and rigid at parachute deployment. The antenna is attached to, and supported by, the parachute canopy.

The sonde electronics is powered by three 6 volt nickel-cadmium rechargeable batteries. This type of power supply permits charging to maximum capacity just before use for maximum efficiency and reliability.

The sensors used for data collection are sampled during descent by a programmer assembly. The programmer consists of a flush type

commutator board, rotating contact arm, and motor and gear assembly. The DC motor, with its attendant gear train, provides a commutation rate of 10 scans per minute (one commutator sweep each six seconds). Twelve conducting segments are provided on the commutator. The contact arm dwells on a segment for a period of 450 milliseconds and is interrupted for a period of 50 milliseconds between segments. Data is available at the segments in the following order during one scan of commutator: 1) High Frequency Reference, 2) Humidity, 3) Temperature, 4) Pressure, 5) Humidity, 6) Temperature, 7) Low Frequency Reference, 8) Humidity, 9) Temperature, 10) Pressure, 11) Humidity, 12) Temperature.

The pressure sensor is also a part of the programmer assembly. This design feature permits the programmer motor to drive the programmer contact arm and also to actuate the pressure contact arm at preset time intervals. The pressure sensor consists of an aneroid capsule which drives a contact arm through an appropriate linkage and provides motion across a wire-wound resistance card, providing a pressure versus resistance relationship. Humidity measurements are obtained with an ML-476/AMT carbon humidity element. An ML-405A/AMT-11 rod thermistor is used for measuring temperature. An internal view of the AN/AMT-13 radiosonde is presented in Figure 6-3.

The technical characteristics of the AN/AMT-13 radiosonde are as follows:

1. Range of Measurement

   a) Atmospheric Pressure: 100 millibars to 1060 millibars

   b) Temperature: +55°C to -90°C

   c) Relative Humidity: 5% to 100%

2. Dimensions

   a) Diameter: 3.5 inches

   b) Length: 18 inches

   c) Weight: 4.75 pounds

3. Transmitter

   a) Preset R.F. Frequency: 403 $\pm$ 2 megacycles

   b) Signal: Pulse time modulated

c) Pulse Repetition Frequency: Variable between 2400 and 6100 cycles per second

d) Pulse Width: 16 ± 3 microseconds

e) Peak Pulse Power Output: 18 watts minimum

B. Dispenser, Radiosonde Set, MX-4768/AMQ-19

The dispenser is designed to carry and eject nine radiosondes at altitudes up to 50,000 feet, from an aircraft flying at speeds up to Mach 1. The ejection path is aft and parallel to the axis of the aircraft. Exit velocities between 20 and 30 feet per second are obtained.

The dispenser is a drum-shaped aluminum alloy assembly approximately 48 inches long by 22 inches in diameter. It weighs approximately 180 pounds. It has an ejection port at one end and a dust-and moisture-proofing cover at the other. An access cover, running longitudinally on the drum, provides means for visual inspection and space for adjusting the indexing motor and arming mechanisms.

Nine individual tubes (barrels) house the radiosonde sets. Thermostatically controlled heaters maintain the temperature of the radiosondes at approximately 25°C when the ambient temperature is below this level.

The tubes are held in position by two rigid end plates and stainless steel braces to form a cylinder. This assembly, which resembles the cylinder of a revolver, rotates within a housing to position a radiosonde for ejection when the operator depresses the eject button.

A special pneumatic actuator ejects the radiosonde. The actuator consists of a free piston which moves in a slotted cylinder. A shoulder on the piston extends through the slot and provides a means for taking out the power of the piston. The slot is sealed by a thin metal ribbon threaded through the piston and fixed at each end of the cylinder. Air pressure, moving the piston through the cylinder, forces the ribbon against a flat surface beneath the slot. As the piston moves, it contacts the radiosonde, accelerates and thrusts the radiosonde aft.

The special features of the actuator are:

1. A slow approach to the radiosonde.

2. A momentary hesitation upon contact with the radiosonde, then, full line pressure ejection of the radiosonde.

3. Automatic piston return, which readies the actuator for the next stroke.

The pneumatic power is supplied from a rechargeable air or gas bottle (100 cubic inches volume, 2500 psi pressure) mounted on the outside rear bulkhead of the dispenser.

Access to the dispenser is through the W-47E tail compartment door or by removal of the tail dome cover. Radiosondes are loaded in the dispenser through the radiosonde eject port. A solenoid-powered linear actuator rotates the cylinder one position at a time. An indexing mechanism automatically aligns the barrel with the eject port.

Controls and indicators for the dispenser are located on the Vertical Subsystem Control-Indicator at the observer's operating position. These are:

1. Sonde Number meter (identifies the barrel aligned with the ejection port, 1 through 9).

2. Index switch (rotates the cylinder one position).

3. Arm switch (turns on the radiosonde).

4. Drop switch.

C. Antenna

The AT-896/A Antenna is a 403 megacycle (nominal) stub antenna designed for aircraft use. The antenna operates in conjunction with the radiosonde receiver and is located on the lower aft fuselage in close proximity to the receiver.

D. Radio Receiver

The radiosonde receiver is a double-conversion superheterodyne with a bandpass RF amplifier, a crystal-controlled first local oscillator, a bandpass first IF amplifier, a voltage-controlled second local oscillator, a narrow bandpass second IF amplifier, and a detector section. The detector section contains a pulse or intelligence detector, a peak detector for automatic gain control, and a frequency discriminator for automatic frequency control.

The controls and indicators for the receiver are located on the control panel. Prior to arming a radiosonde, the frequency meter will sweep as it follows the AFC circuit in seeking a signal. The

AN/AMT-13 radiosonde is armed by depressing the switch in its forward end (as shown in Figure 6-2). At this ne the frequency meter will indicate the radiosonde transmitting frequency. The signal strength meter should indicate a strong signal due to its proximity to the receiver and antenna. After the radiosonde is ejected from the dispenser, the frequency and signal strength meters will continue to indicate until the end of the flight at which point the frequency meter will again begin to sweep. Audio monitoring will also indicate flight termination.

If at any time during the radiosonde flight the signal becomes too weak for the receiver to remain locked on, or if a fault occurs in the AFC circuit, the Automatic-Manual switch may be thrown to the Manual position and the receiver tuned with the Manual Tuning Control. It may also be necessary to tune the receiver manually if it has locked onto an unwanted signal, such as that from an AN/AMT-13 launched by another aircraft. After the desired signal has been tuned in, the switch may be returned to the Automatic position.

Receiver characteristics:

1. Tuning Range: 400 to 406 megacycles

2. Input impedance: 500 ohms

3. Sensitivity:

    a) Automatic Tuning: 10 microvolts at 403 mc

    b) Manual Tuning: 8 microvolts at 403 mc

    c) Performance Monitoring: Frequency, Signal Strength, Audio

The output of the receiver is fed to the Frequency to Voltage Converter (data handling subsystem) and processed. This operation is described in a subsequent paragraph.

HORIZONTAL SUBSYSTEM

The horizontal subsystem includes the data inputs from the various aircraft systems and meteorological sensors selected to provide a complete flight level history. These inputs, and their effect upon the basic AN/AMQ-19 System, can be described as follows:

A. Wind Speed and Direction

The outputs of the AN/APN-102 Doppler Radar, the N-1 Compass, and the other navigational instruments are used by the Wind Vector Computer, CP-721/AMQ-19, to provide wind speed and direction as Potentiometer outputs.

B. Position (Latitude and Longitude)

The outputs of the AN/APN-102 Doppler Radar and the N-1 Compass are used by the AN/ASN-6 Dead Reckoning Computer to provide latitude and longitude data. The synchro outputs of the AN/ASN-6 are converted in the Synchro Assembly into outputs across potentiometers.

C. Radar Altitude

This is given by the AN/APN-42 Radar Altimeter, used in accordance with present military practices. The output of the AN/APN-42 set is converted to a potentiometer output in a Bendix supplied Synchro Assembly, CV-1393/AMQ-19.

D. Total Temperature Measuring System

The temperature sensor is a probe which utilizes a resistance element connected in one leg of a self-balancing (motor-driven) bridge. The error voltage, sensed at the bridge is applied through a servo amplifier which operates the balancing motor, and drives the output potentiometer. The temperature indicator is geared to the potentiometer shaft. The range of temperature measurement is plus 40°C to -85°C, with an installed accuracy of plus or minus 1°C.

E. Observer Inputs

The meteorological operator inserts observed weather data in RECCO Code by means of the controls on the Observer Inputs Meteorological Data Selector.

F. Pressure Altitude and Air Speed

Both Pressure Altitude and Air Speed are measured with standard pressure-sampling probes, which position potentiometers as inputs.

G. Time of Day

Time of day is recorded as part of each horizontal data scan. The clock provides analog signals on two channels representing time of day from zero to 2400 hours.

DATA HANDLING SUBSYSTEM

The data handling subsystem of the AN/AMQ-19 Meteorological System receives the information generated in the vertical and horizontal subsystems, provides for conversion to digital form, and relays the digitized data to a buffer storage unit. This subsystem also provides frequency shift keying of the air to ground radio transmitter. The weather information collected is stored in this subsystem in eight parallel channels in field data code format. The transmission of data to the ground is accomplished over the aircraft single sideband radio as a multiplexed audio signal. These components can be described as follows:

A. Signal Data Converter Scanner

The signal data converter scanner is a component from the data handling subsystem. It receives inputs from both horizontal and vertical subsystems, processes the information and converts from analog to a digital signal. A two-deck commutator receives inputs from the horizontal subsystem, vertical subsystem inputs are received in a frequency to voltage converter. The three sections of the converter scanner can be described as follows:

1. Horizontal Input

The horizontal subsystem input consists of up to 30 channels of analog DC voltage signals whose level ranges between -2.5 and +2.5 volts. The 30 channels are scanned by a commutator at a rate of 15 channels per second. The analog voltages are not distorted by more than .01 volts during scanning. The second deck of the commutator adds timing pulses and teletype carriage return information signals to the data. Commutator output is applied to the Analog to Digital Converter portion of the converter scanner.

2. Vertical Input

The vertical subsystem input is the pulse repetition rate between 2450 and 6050 pulses per second relayed from the radiosonde receiver. The frequency to voltage converter transforms the pulse repetition rates received into voltage signals whose level ranges between -2.5 and +2.5 volts DC. These signals are also applied to the Analog to Digital Converter. The A to D converter will not receive signals from the commutator and F to V converter simultaneously.

3. Analog to Digital Converter

The analog to digital converter receives input voltages ranging between -2.5 and +2.5 volts DC from either the horizontal or vertical subsystem. The converter utilizes a capacitive charge transfer technique to accomplish a successive approximation conversion process. The output of the analog to digital converter is a ten bit serial binary number which includes a parity bit.

B. Converter Signal Generator

The Control Signal Generator's function is to convert the binary information supplied by the analog to digital converter into a binary coded decimal signal in field data format for storage in an eight channel tape recorder.

This is accomplished by interplay of the following three sections:

1. B to BCD Conversion

The binary to binary coded decimal converter takes the ten bit serial binary words and converts them to a three decimal, binary coded decimal signal. The information is read in at a 250 kc rate and is read out at 83 cps in NRZ code.

2. Logic Control

The logic control provides the necessary switching and timing signals for reading the information in and out of the BCD converter. It also generates the characters which converts the binary coded decimal information into the field data code form as well as special characters such as line feed, carriage return; space and data identification signals.

All buffer storage control signals such as read, write and reverse are also generated in this section.

3. NRZ to NRZI

The NRZ information coming from the BCD converter, four logic control sections, must first be converted to NRZI form before the recorder can use it. This is accomplished with a flip-flop in each of the eight channels.

C. Power Supply

The components comprising the data handling subsystem portion of the meteorological system receive the voltages required for their operation from a central supply.

This power supply uses 115 VAC, 3 phase, 400 cycle as its primary source of power and supplies -18 VDC, -12 VDC, -6 VDC, -2.5 VDC, +14 VDC, +12 VDC, +6 VDC and +2 VDC to the various components in the data handling portion of the system.

These voltages are regulated by temperature stable transistorized regulators which have built-in over current protection.

The power supply is turned on at the control panel which is used as the distribution point for the +28 VDC and 115 VAC 400 cycle power used by the data handling instruments.

D. Control Panels

Four control panels are used to monitor and control the system. They are as follows:

1. Vertical Subsystem Control-Indicator

This control panel includes those functions needed to monitor and control radiosonde receiver performance, as noted above, and the main power switch. The control panel also includes the horizontal and vertical subsystem power controls.

2. Observer Inputs Selector

This control panel includes provisions for the observer to manually insert weather data in RECCO code.

3. Data Handling Control-Indicator

The data handling control panel contains the controls and selectors necessary for operation of the Signal Data Recorder-Reproducer. The operator can select the interval at which the horizontal data inputs are scanned and the rate at which data is recorded. The selector for determining which subsystem's data is to be recorded, horizontal or vertical is also located here. Atop the panel are located the recorder-reproducer command controls (Write, Reverse, Ready, Transmit).

4. Voltage Monitor Control-Indicator

This control panel provides a means for monitoring the various voltage outputs of the power supply. This panel also contains the time-of-day analog clock.

E. Signal Data Recorder-Reproducer

The Signal Data Recorder-Reproducer has a capacity of at least 600,000 words of eight parallel bits each (8 channels). It records the digital words at a rate of 45 bits per channel per second. When commanded to transmit, the storage unit automatically reads out, without gaps between words, at a rate of 75 bits per second per channel. The output of the Recorder-Reproducer is in non-return to zero form and is used to drive the Keyer-Multiplexer. The output is 0 or 11 volts, representing binary 0 or 1.

F. Frequency Shift Keyer-Multiplexer

The Keyer-Multiplexer accepts inputs from the Signal Data Recorder-Reproducer on eight separate channels. The output for each channel is either of two frequencies, depending on whether the input is 0 or 1. The converter is capable of switching frequencies at a rate compatible with the 75 word per second per channel transmission rate. The output of the Keyer-Multiplexer is compatible with aircraft single sideband transmitters. Reception and processing of the multiplexed audio signal transmitted from the aircraft is described in the following paragraph.

GROUND DATA PROCESSING

Processing of the weather data transmitted from the aircraft as a multiplexed audio signal must be accomplished through equipment installed at a communications ground station. This equipment, a ground data handling system, provides an automatic processing link between the communications single sideband receiver and a teletype system used to display the data and relay the information to other locations. The ground data handling equipment is the AN/GMH-4 Analysis Data Central produced by Bendix Friez.

The receiving set used with the AN/AMQ-19 and the AN/GMH-4 systems must be capable of accepting single sideband type signals in the frequency range from two to 30 megacycles. The detected sideband must have a three kilocycle bandpass to accommodate the eight parallel channels of the frequency shift tone keyer controlling transmission from the aircraft. The receiver must also have the necessary sensitivity to receive the signals of the airborne transmitter, which has peak output of approximately 400 watts.

The output of the single sideband ground receiver must be demodulated (demultiplexed) prior to further processing. This demodulation involves a frequency shift converter and an NRZI to NRZ converter. The signal is then passed to a Code Converter and Adapter for additional processing wherein conversion from field data to serial Baudot code is accomplished. The salient features of the AN/GMH-4 system are as follows:

1. Demodulates, converts, and presents the raw weather data on a teletype page printer.

2. Provides for storage of the received data at the ground station for processing or re-transmission at a later time (up to a maximum of six transmissions).

3. Provides for conversion of the digital message format from parallel NRZI field data code through parallel NRZ field data code to serial Baudot code format.

The AN/GMH-4 System is shown in Figure 6-4.

The components used in the AN/GMH-4 Data Analysis Central and the functions they perform are presented in the following paragraphs:

A. Frequency Shift Converter

The ground single sideband receiver output signal is a duplicate of the signal developed by the Frequency Shift Keyer-Multiplexer which is used to modulate the aircraft transmitter. It is a multiplexed signal consisting of a number of modulated audio frequencies. This signal contains eight (8) parallel channels of information. When demodulated, the frequency identifies the information as a binary 0 or 1. The function of the Frequency Shift Converter is to detect each frequency and convert it to its original DC voltage form of 0 or -12 volts. In this form the ground signal corresponds to the information output of the airborne buffer storage unit.

B. NRZI to NRZ Converter

In NRZI (non-return to zero - IBM format) code, a logic "one" is defined as a change from one voltage level, in either the positive or negative direction, and a logic "zero" is defined as no change in level. NRZI code is the same as NRZ(M). In NRZ (non-return to zero), "one" is defined as one of two voltage levels, and a logic "zero" as the other level. To convert from NRZI to NRZ format, a timing pulse will be derived from the output of the Frequency Shift Converter. This pulse, delayed to preclude skew error, is used to control the temporary storage. The temporary storage consists of

a bank of flip-flop circuits, each corresponding to a particular channel of the Frequency Shift Converter. The flip-flops corresponding to channels that contain logic "ones" are triggered "ON" and those corresponding to channels containing "Zeros" are flipped "OFF". In addition, another pulse is generated by the outputs of the channels, and it provides the system with two control pulses, which are utilized in the Code Converter.

C. Power Supply

The power requirements for operation of the NRZI to NRZ Converter, the Adapter and Control Unit, and the Code Converter are approximately 40 watts (nominal). The output of the Power Supply is +6 VDC, -6 VDC, and -12 VDC. The Power Supply has a voltmeter and selector mounted on the panel so that outputs may be monitored. The Buffer Storage units have internal power supplies.

D. Code Converter and Adapter

The input to the Code Converter and Adapter in NRZ field data from the NRZI to NRZ Converter. Conversion from NRZ field data code to Baudot code is performed by means of decoding gates and a matrix consisting solely of solid state devices. The output of the matrix is five parallel channels of Baudot coded information. A strobe pulse is generated to time the output of Baudot coded information to the buffer storage unit in the Write mode. It is necessary to differentiate numbers from letters by upper and lower case on the teletypewriter keyboard. In the case of meteorological data, upper case signal is actually initiated when the frequency selector switch on the Control Panel is depressed. A parity error counter is provided to count the erroneous data that may be received during a transmission, and the percentage of error will be indicated by the setting of the selector switch, an indicator light, and an alarm buzzer at the Control Panel. In addition, a question mark is transmitted whenever an error is detected.

E. Buffer Storage Unit

The buffer storage unit consists of two Digi-Store units. Although each individual unit has Read/Write capability, the two units will be mounted side by side in the rack with one operating in the Write mode and the other in the Read mode as required. Provisions have been made for the difference in read and write speeds. The buffer storage units utilize magnetic tape which is perforated for a sprocketed wheel, and stepping motor is used for positive indexing. The units use 100% transistorized circuitry and a minimum of moving parts. The input and output speeds are asynchronous to 300 characters per second, and the units are compatible with the teletype

machines with no external adaptation.

Utilization of two complete Digi-Store units as a buffer storage enables faster transmission of messages and less time lost in maintenance, if one unit malfunctions. In addition, if one unit does go out, the other unit can be utilized for recording and transmitting. However, under normal conditions one unit will always be in write mode and the other unit in read mode. The buffer storage receives the input signal from the Code Converter and Adapter as five parallel bits of Baudot code at a rate of 75 characters per second and produces an output in serial Baudot with a start and stop pulses added. The readout of the buffer storage units is compatible with standard teletype machines.

F. Control Panel

The Control Panel of the Ground Data Handling System will be placed at an operator's console in the single sideband Communication Center. The Control Panel includes frequency selector switches, a power enable switch and indicator light, an error indicator light and percentage error selector switch, an error alarm switch, and a system reset switch and indicator light.

G. Self-Test Equipment

The Self-Test Equipment consists of a tape transport, an NRZI Converter, and a Frequency Shift Keyer. The output of the system will be fed into the Frequency Shift Converter. The equipment will be mounted in the rack with the Analysis Data Central equipment. A pre-programmed test tape will be provided to test each channel of the Analysis Data Central System individually, and to check the effectiveness of the parity check circuitry, percentage of error counters, percentage of error alarm, and the system reset function.

Operation of the AN/GMH-4 equipment is essentially automatic; however, certain switches, panel lights, and monitoring circuits are provided at the Control Panel. A power control switch and an indicator light permits energizing the system from the console position. The power to the system is supplied through a main circuit breaker at a power distribution panel.

Six frequency selector switches are provided at the Control Panel to permit the operator to select the single sideband receiver to receive the transmission. Although six switches are provided, it does not necessarily mean that six receivers will be connected. When a transmission is to be received, the operator will push a switch corresponding to the single sideband receiver or frequency desired for the transmission, and an indicator light which is a part of the switch will be illuminated. The buffer storage units should

already be set in the write and read modes of operation, so that when the power is turned on the system will be ready to receive the input signal.

The system reset switch is provided to enable the operator to return the System digital devices to a pre-determined state before operation or before a self-test check-out. This feature improves the performance of the system and eliminates the possibility of misleading operation during a system check-out. The reset indicator light functions in conjunction with the system reset switch and the parity error circuitry, and, the light is illuminated whenever the first erroneous data is received. The system should be reset after a transmission, if the reset light is illuminated, even though the error light may not have come on.

A selector switch and error indicator light are provided at the control panel to enable the operator to monitor the quality of the transmission. The operator will probably be listening to the incoming signal also. A counter is provided in the circuitry to count the errors received in the transmission. The percentage of error as indicated by the selector switch is defined as the number of erroneous characters expressed as a percentage of 6000 characters (considered to be the length of an average transmission). The operating principle is simple in that the selector switch is preset at the predetermined level of permissible error, and when the counting circuit receives sufficient error counting pulses the indicator light on the Control Panel will light.

A buzzer-type alarm works in conjunction with the error detecting circuitry, and it buzzes when the preset percentage of errors is received. A switch is provided to disable the alarm buzzer if the operator so desires, either after it sounds or to prevent it from sounding. The error light (not the system reset light) illuminates coincident with the sounding of the alarm buzzer. The normal setting of the alarm switch permits the buzzer to operate upon receiving a signal from the error counters.

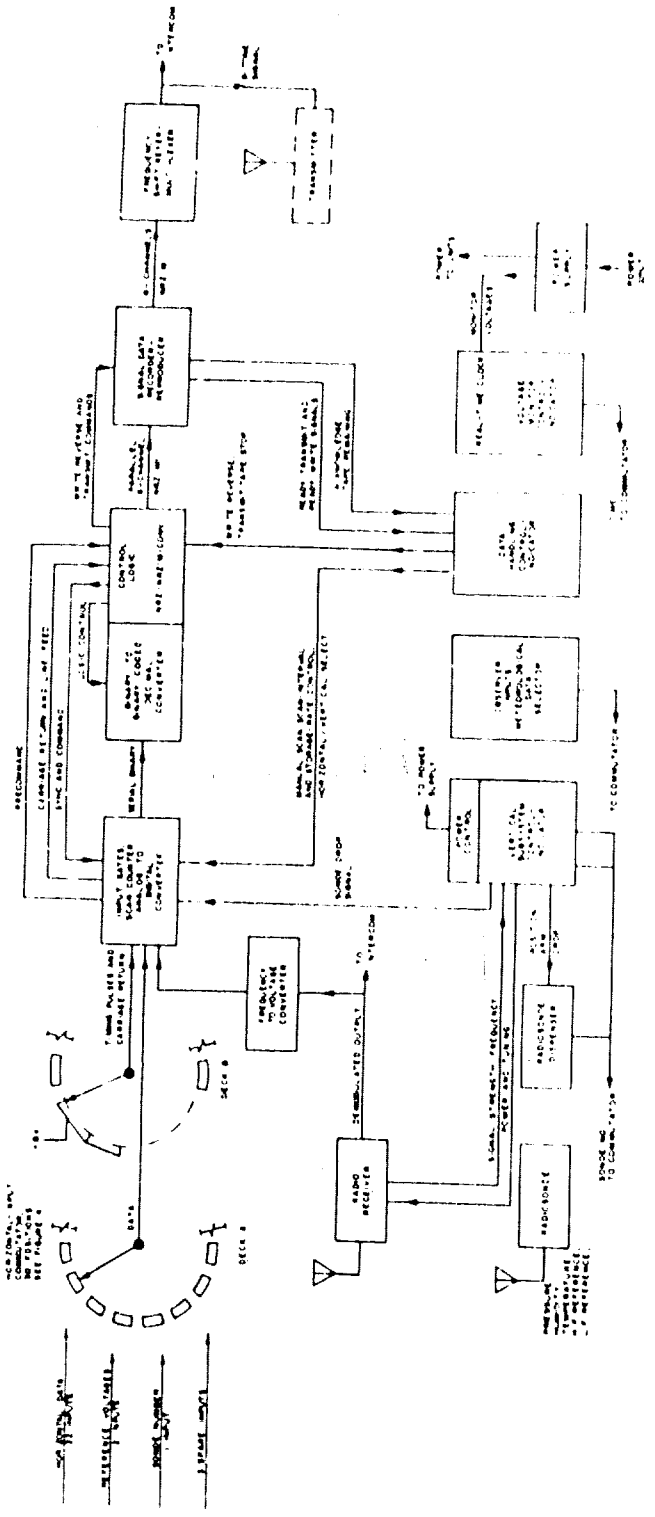

Figure 6-1

FUNCTIONAL BLOCK DIAGRAM OF ..../AIR-19 SYSTEM

Bendix-Friez

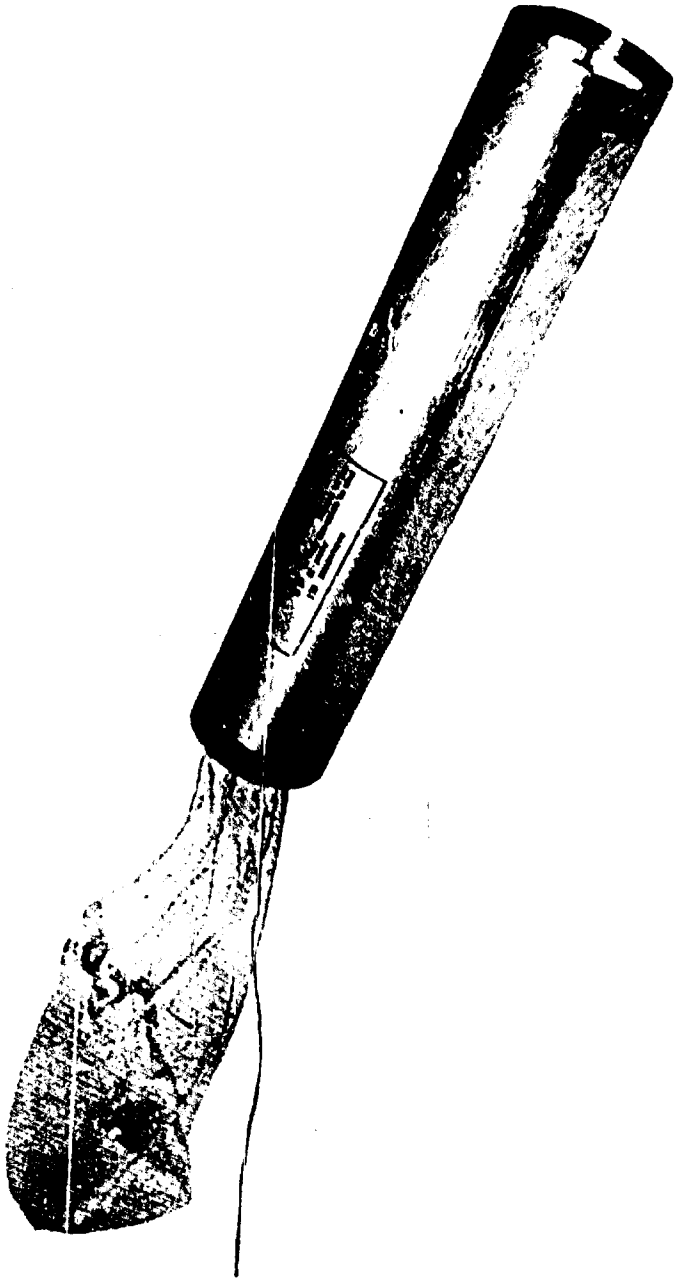

FIGURE 6-2

THE AN/AMT-13 RADIOSONDE

Benoit Fries

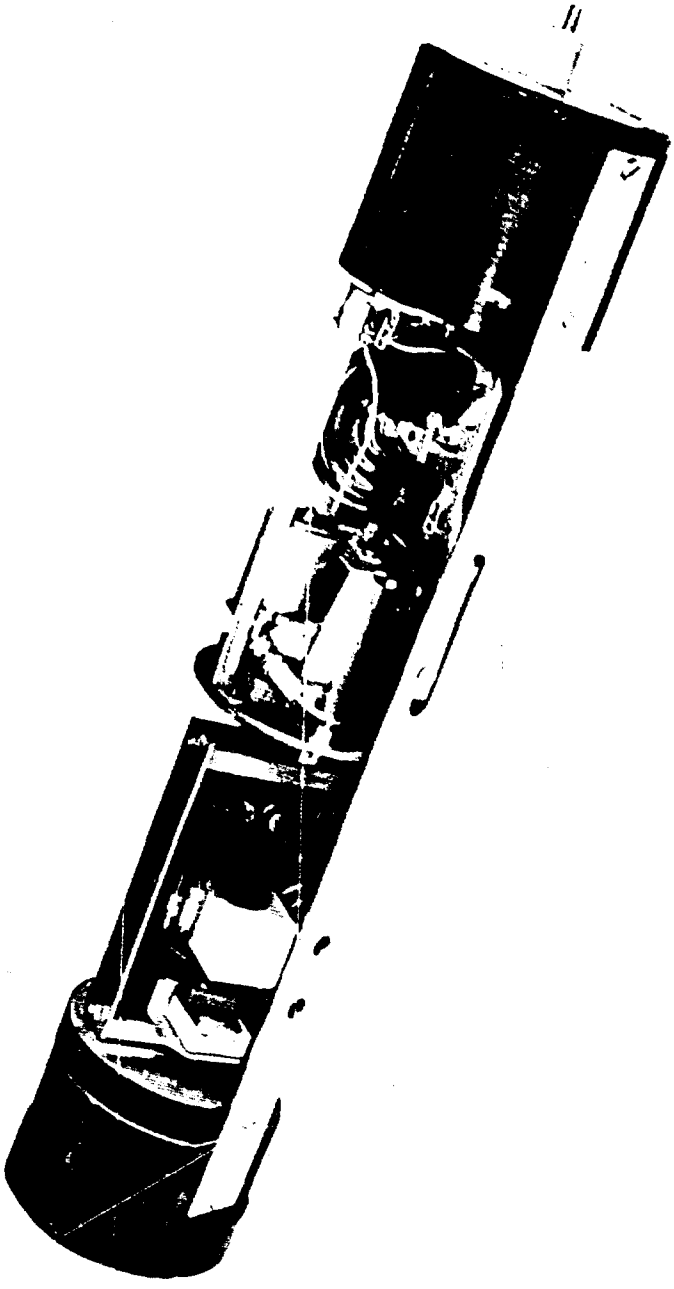

FIGURE 6-3

COMPONENTS OF THE AN/AMT-13 RADIOSONDE

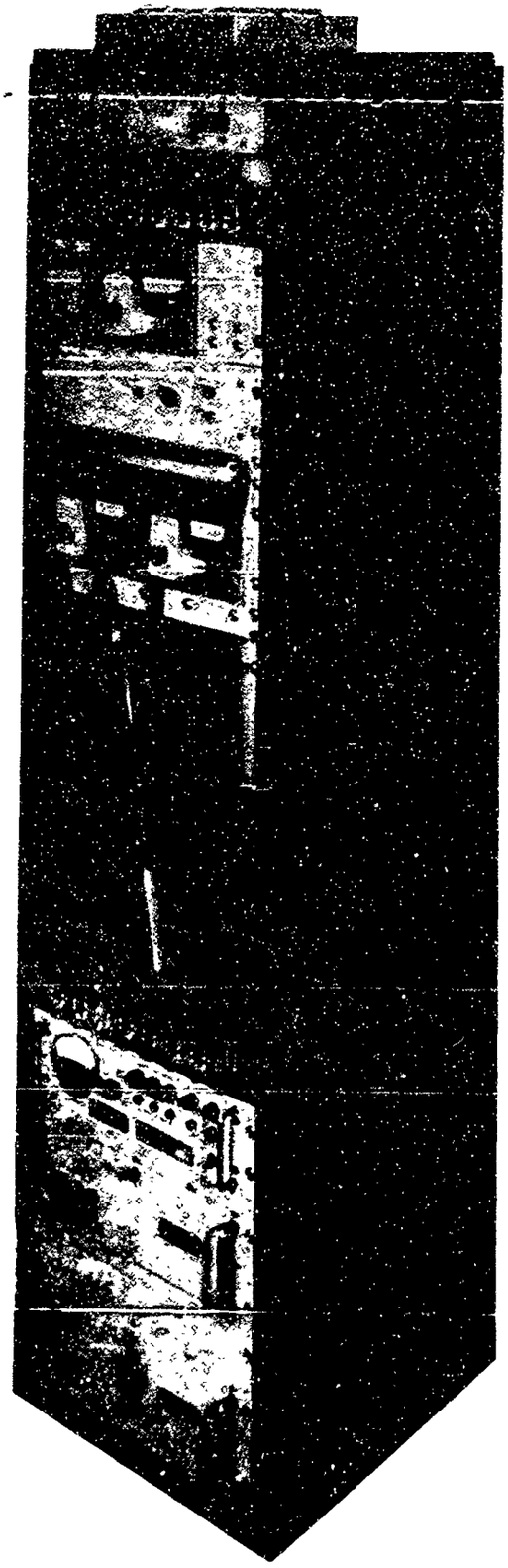

FIGURE 6-4

THE AN/GMH-4 ANALYSIS DATA CENTRAL

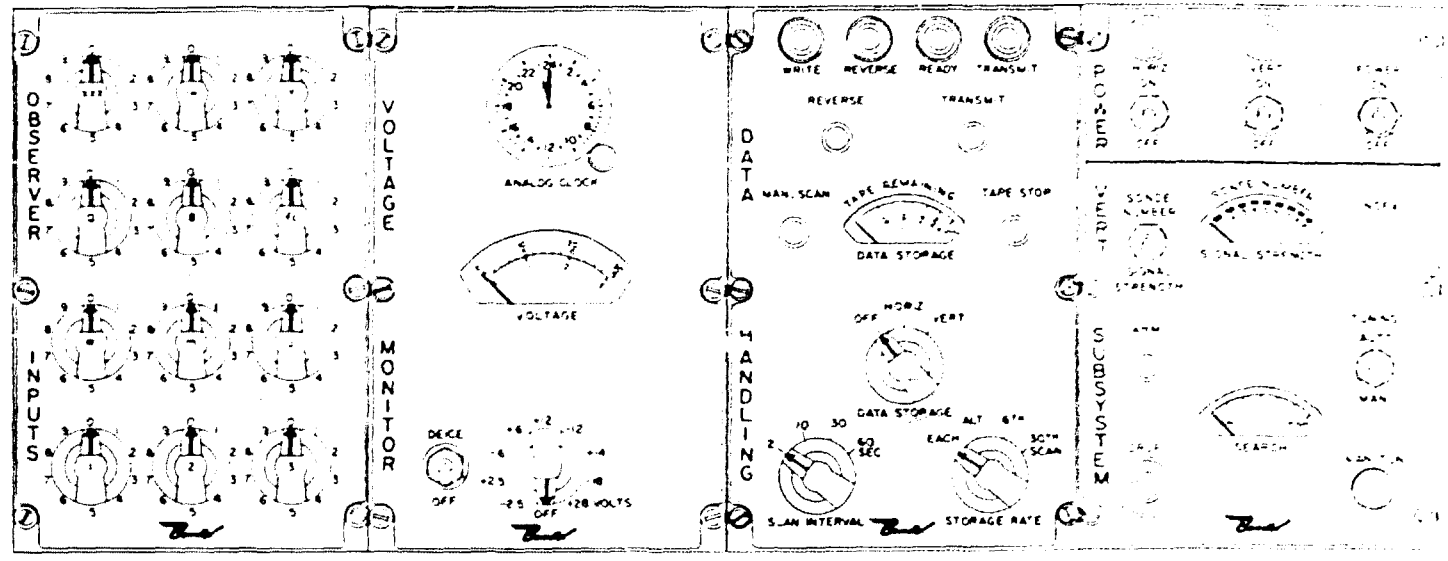

FIGURE 6-5

AN/AMQ-19 CONTROL PANELS

APPENDIX I

EQUATIONS OF MOTION

TRAJECTORY EQUATIONS AND COMPUTER PROCEDURES

The trajectory data included in this report were obtained from a digital computer program. The equations used in the program are given below in vector form.

1. Coordinate Systems Definitions

1.1 Launcher coordinate system, l_i

origin	at launcher
l_1 axis	east
l_2 axis	north
l_3 axis	up

The earth forces, the wind, and the atmosphere are defined in the l_i system. The trajectory position and velocity data are computed in this system.

1.2 Principal axis system, p_i

origin	at rocket c.g.
p_1	along long axis of rocket
p_2, p_3	normal to p_1

p_1, p_2, p_3 are along the principal axes of inertia. The differential equations of translation and rotation are expressed in the principal axis system.

1.3 Reference axis system r_i

origin	the geometric center of the motor exit plane
r_1	along long axis of airframe
r_2, r_3	normal to r_1, defined by fin positions

The thrust force vector, the center of gravity and the inertia tensor are defined in the reference system.

1.4 Airframe axis system a_i

origin	at rocket c.g.
a_1, a_2, a_3	parallel to r_1, r_2, r_3

The aerodynamic forces and moments are functions of the angles of attack and the angular rates of the airframe axis system.

1.5 Relative wind axis system w_i

origin	at rocket c.g.
w_1	along relative wind vector
w_2	normal to w_1 in the plane defined by w_1 and a_1
w_3	normal to w_1 and w_2

The lift and drag forces are defined in the w_i system.

2. Coordinate Conversion Equations

2.1 The transformation between the l_i and the p_i system is

$$\vec{V}^p = \left[a_{ij}\right] \vec{V}^l$$

$\left[a_{ij}\right]$ is obtained in computation by integration of the differential equations of rotation, using the components of the angular velocity vector $\vec{\omega}^p$.

2.2 The transformation between the p_i system and the a_i system

$$\vec{V}^p = \left[b_{ij}\right] \vec{V}^a$$

The inertia tensor in the a_i system is

$$I^a = \begin{bmatrix} I_{11}{}^a & I_{12}{}^a & I_{13}{}^a \\ I_{12}{}^a & I_{22}{}^a & I_{23}{}^a \\ I_{31}{}^a & I_{32}{}^a & I_{33}{}^a \end{bmatrix}$$

and is furnished as part of the input data. The matrix $\left[b_{ij}\right]$ is a matrix such that

$$\left[b_{ij}\right] \; I^a \; \left[b_{ji}\right] = I^p$$

is a diagonal tensor.

$\left[b_{ij}\right]$ will be assumed to be constant, and is pre-computed and stored for a given trajectory.

2.3 The transformation between the airframe system and the wind system is

$$\vec{V}^w = \left[c_{ij}\right] \vec{V}^a$$

The elements of $\left[c_{ij}\right]$ are computed from the components of the relative wind

$$\vec{U} = \vec{V} - \vec{W}$$

$$\left[c_{ij}\right] = \left[R_3(\alpha)\right] \left[R_2(\beta)\right]$$

$$\sin\beta = U_3 \Big/ \sqrt{U_2^2 + U_3^2}$$

$$\cos\beta = U_2 \Big/ \sqrt{U_2^2 + U_3^2}$$

$$\sin\alpha = \frac{\sqrt{U_2^2 + U_3^2}}{|U|}$$

$$\cos\alpha = \frac{U_1}{|U|}$$

2.4 The transformation between the reference axis system and the airframe axis system is a translation

$$\vec{R}_x^{\,a} = \vec{R}_x^{\,r} - \vec{R}_p^{\,r}$$

where $\vec{R}_p^{\,r}$ is the center of gravity position vector in the r_i system.

3. Trajectory Equations

The force equation is

$$\vec{V}^P = \frac{1}{M}\sum F^P = \omega^P \times V^P \qquad (1)$$

The moment equation is

$$I^P \vec{\omega}^P = \sum M^P - \vec{\omega}^P \times I^P \vec{\omega}^P - I^P \vec{\omega}^P \qquad (2)$$

The velocity equation is

$$\dot{\vec{R}}_m^{\,1} = \left[a_{ij}\right] \vec{V}^P \qquad (3)$$

The rotation equation is obtained by using

$$\left[a_{ij}\right] = \left[R_1(\phi)\right] \left[R_2(\theta)\right] \left[R_3(\psi)\right] \qquad (4)$$

yielding

$$\begin{bmatrix} \dot{\phi} \\ \dot{\theta} \\ \dot{\psi} \end{bmatrix} = \begin{bmatrix} 1 & \sin\phi\tan\theta & \cos\phi\tan\theta \\ 0 & \cos\phi & -\sin\phi \\ 0 & \sin\phi\sec\theta & \cos\phi\sec\theta \end{bmatrix} \begin{bmatrix} \vec{\omega}_1^{\,P} \\ \vec{\omega}_2^{\,P} \\ \vec{\omega}_3^{\,P} \end{bmatrix} \qquad (5)$$

Equations (1), (2), (3) and (5) are a set of twelve first order scalar differential equations which will describe the motion of a rigid body. Equation (4) is a functional relationship between variables. The force sum, ΣF^P in equation (1) and the moment sum, ΣM^P in equation (2) can be described in other functional equations which will complete the mathematical model of the simulation.

4. Force and Moment Equations

4.1 Gravity

$$\vec{G}^1 = -|G| \vec{1}_3$$

$$|G| = -g_o \left(\frac{R_o}{R_o + A_m^1}\right)^2$$

$$\vec{G}^P = [a_{ij}] G^1$$

4.2 Thrust

$$|T| = T_s + A_e (P_s - P_a)$$

$$\vec{T}^a = |T| \vec{t}^a$$

$$\vec{T}^P = [b_{ij}] \vec{T}^a$$

$$\vec{M}_t^a = \vec{R}_t^a \times \vec{T}^a$$

$$\vec{M}_t^P = [b_{ij}] \vec{M}_t^a$$

4.3 Jet Damping

$$\vec{J}^a = \dot{M}\vec{\omega}^a \times \vec{R}_t^a$$

$$\vec{J}^P = [b_{ij}] \vec{J}^a$$

$$\vec{M}_J^a = \vec{R}_t^a \times \vec{J}^a$$

$$\vec{M}_J^P = [b_{ij}] \vec{M}_J^a$$

4.4 Drag

$$\vec{D}^W = -|D| \vec{w}_1$$

$$|D| = qd^2 C_D$$

$$C_D = C_{Do} + C_{Di}\ \alpha^2$$

$$\vec{D}^a = \left[c_{ij}\right] \vec{D}^w$$

$$\vec{D}^p = \left[b_{ij}\right] \vec{D}^a$$

$$\vec{M}_D{}^a = \vec{R}_p{}^a \times \vec{D}^a$$

$$\vec{M}_D{}^p = \left[b_{ij}\right] \vec{M}_D{}^a$$

4.5 Lift Force and Moment

$$\vec{L}^w = -\left|L\right| \vec{w}_2$$

$$\vec{L} = qd^2 C_{L\alpha} \sin\alpha \cos\alpha$$

$$\vec{L}^a = \left[c_{ij}\right] \vec{L}^w$$

$$\vec{L}^p = \left[b_{ij}\right] \vec{L}^a$$

$$\vec{M}_L{}^a = \vec{R}_p{}^a \times \vec{L}^a$$

$$\vec{M}_L{}^p = \left[b_{ij}\right] \vec{M}_L{}^a$$

4.6 Aerodynamic Damping Force and Moment

$$\vec{F}_\omega{}^a = \frac{qd^2 C_{L\alpha}\ \vec{R}_p{}^a \times \vec{\omega}^a}{\left|V_r\right|}$$

$$\vec{F}^p = \left[b_{ij}\right] \vec{F}_\omega{}^a$$

$$M_{\omega 1}{}^a = -\frac{qd^2 C_{\omega 1}\omega_1}{\left|V_r\right|}$$

$$M_{\omega 2}{}^a = -\frac{qd\ C_{\omega 2}\omega_2}{\left|V_r\right|}$$

$$M_{\omega 3}{}^a = -\frac{qd^2 C_{\omega\ 2}\omega^3}{\left|V_r\right|}$$

4.7 Force and Moment Due to Fin Incidence

$$\vec{F}_\delta{}^a = \sum \vec{F}_\delta{}_i{}^a = qd^2 C_{L\alpha\ F} \sum \delta_i \vec{n}_i$$

$$\vec{n}_1 = {}^{a}_{1} = \overline{\vec{n}_3} \qquad \text{[illegible]}$$

$$\vec{n}_2 = {}^{a}_{2} = \vec{n}_0$$

$$\vec{r}_0^{\,p} = \left[b_{ij}\right] \vec{r}_0^{\,a}$$

$$\vec{n}_0^{\,a} = \sum \vec{n}_{0\,i}{}^{a} = \sum \vec{n}_{Fi}{}^{a} \times \vec{r}_{0\,i}{}^{a}$$

$$\vec{n}_0^{\,p} = \left[b_{ij}\right] \vec{n}_0^{\,a}$$

5. Computer Procedures

5.1 The first step in preparation of the dispersion analysis is to compute a standard trajectory utilizing the anticipated gross launch weight and launcher quadrant elevation

5.2 The individual dispersion effects are derived as follows:

5.2.1 One dispersion inducing parameter is varied from the normal by an estimated 3 sigma amount. All other parameters are held constant.

5.2.2 A new trajectory is computed.

5.2.3 The impact displacement of this new trajectory relative to the standard trajectory is determined.

5.2.4 This process is repeated for each factor that results in trajectory perturbation.

5.3 The total vehicle dispersion is then derived by computing the square root of the sum of the squares of all individual factors (Table 5).

5.4 Unit ballistic wind effects as a function of launch quadrant elevation are computed as follows:

5.4.1 A unit wind profile is inserted in the computer and allowed to perturb the range plane of the trajectory from ground level to 100,000 feet altitude, or stage apogee if less than 100,000 feet.

5.4.2 A trajectory is run for several launcher quadrant elevations that will envelope the anticipated firing angle.

5.4.3 The resulting impacts are then compared to the no-wind impact with the same launch conditions.

5.4.4 This complete process is then repeated with the wind acting in a plane normal to the trajectory.

5.5 Wind weighting factors, $f(\bar{z})$, are computed by running a sequence of trajectories with normal launch quadrant elevation and unit wind from ground level to an altitude $\bar{z}c$. The resulting impacts are compared to the standard trajectory to obtain impact displacements (Table 4).

$$f(\bar{z}) = \frac{\text{Displacement Due to Wind up to Altitude } \bar{z}c}{\text{Displacement Due to Wind up to 100,000 Feet}}$$

6. Coriolis Equation

Coriolis displacement is obtained by double integration of the Coriolis acceleration:

$$-2\vec{\omega}_E \times \dot{\vec{R}}$$

Where values of R are taken from the standard trajectory.

7. Equation Symbols

A_E	Motor exit area
a_i	Axes of airframe axis system
a_{ij}	Transformation matrix between l_i and p_i
b_{ij}	Transformation matrix between p_i and a_i
c_{ij}	Transformation matrix between w_i and a_i
C_D	Drag coefficient
C_{Do}	Drag coefficient at zero angle of attack
C_{Di}	Coefficient of induced drag
$C_{L\alpha}$	Lift coefficient slope for entire vehicle
$C_{L\alpha F}$	Lift coefficient slope for one fin
$C_{\omega 1}$	Roll damping coefficient
$C_{\omega 2}$	Pitch damping coefficient
d^2	Aerodynamic reference area; diameter squared
$\vec{D}$	Drag force
$\vec{F}$	Force vector
$\vec{F}\omega$	Force due to rotation (damping force)
$\vec{F}_\delta$	Force due to fin incidence
$\vec{G}$	Gravitational force
g_o	Gravitational force at origin of l_i system
I	Inertia tensor
$I\vec{\omega}$	Angular momentum
$\vec{J}$	Jet Damping force
l_i	Axes of launcher coordinate system
$\vec{L}$	Lift force vector
M	Rocket mass

$\vec{M}$	Moment vector
$\vec{M}_D$	Moment due to drag
$\vec{M}_J$	Moment due to jet damping
$\vec{M}_L$	Moment due to lift
$\vec{M}_T$	Moment due to thrust
$\vec{M}_\delta$	Moment due to fin incidence
$\vec{M}_\omega$	Moment due to aerodynamic damping of rotation
$\vec{n}_i$	Unit vector normal to i^{th} fin: $i = 1, 2, 3, 4$
p_i	Axes of principal axis coordinate system
P_A	Ambient atmospheric pressure
P_S	Sea level atmospheric pressure
q	Dynamic pressure
$\vec{R}$	Position vector
R_o	Radius of earth to origin of l_i system
$\left[R_l (\ ) \right]$	Rotation matrix about i^{th} axis, with angle of rotation in parentheses
$\vec{R}_{Fi}$	Position vector of i^{th} fin
$\vec{R}_m^{\,i}$	Position vector of missile in l_i system
$\vec{R}_p$	Position vector of aerodynamic center of pressure
$\vec{R}_t$	Position vector of point of action of thrust force
$\vec{t}$	Unit vector in direction of thrust force
$\vec{T}$	Thrust force
$\vec{T}_S$	Sea level thrust
$\vec{U}$	Relative wind vector
$\vec{W}$	Wind vector
V_r	Relative wind magnitude; $\left\|\vec{U}\right\|$
w_i	Axes of wind axis system
α	Angle of attack
φ	Orientation of angle of attack
δ_i	Incidence angle of i^{th} fin

θ	Pitch angle
σ	Standard deviation
ϕ	Roll angle
χ	Yaw angle
$\vec{\omega}$	Angular rate vector of rocket
$\vec{\omega}_E$	Angular rate vector of the earth

Bendix – Friez

APPENDIX II

PAULA I FLIGHT FROM AIRCRAFT JETTISON TO TERMINATION

TIME FROM JETTISON (Sec)	RANGE FROM DROP POINT (Feet)	ALTITUDE (Feet)	VELOCITY (Ft/Sec)	MACH NUMBER	DYNAMIC PRESSURE (Lb/Ft^2)
0.	0	35000	931	0.96	321
0.1	93	34995	928	0.95	319
0.2	185	34989	924	0.95	317
0.3	277	34984	921	0.95	314
0.4	369	34978	917	0.94	312
0.5	460	34971	914	0.94	310
0.6	551	34965	910	0.93	307
0.7	642	34958	893	0.92	296
0.8	729	34951	867	0.89	279
0.9	814.	34944	842	0.86	263
1.0	897	34936	819	0.84	249
1.5	1279	34898	720	0.74	193
2.0	1616	34857	642	0.66	154
2.5	1918	34813	581	0.60	126
3.0	2191	34765	531	0.54	105
3.5	2440	34714	489	0.50	90
4.0	2670	34659	455	0.47	78
4.5	2882	34600	426	0.44	68
5.0	3079	34538	401	0.41	61
5.5	3262	34473	380	0.39	55
6.0	3434	34403	362	0.37	50
6.5	3595	34330	347	0.36	46
7.0	3747	34254	334	0.34	42
7.5	3890	34175	323	0.33	40
8.0	4026	34091	313	0.32	38
8.5	4154	34005	305	0.31	36
9.0	4275	33915	299	0.31	34
9.5	4390	33823	293	0.30	33
10.0	4499	33726	289	0.29	32
10.5	4603	33628	285	0.29	32
11.0	4702	33526	282	0.29	31
11.5	4796	33421	280	0.29	31
12.0	4885	33314	278	0.28	31
12.5	4969	33204	277	0.28	30
13.0	5050	33092	276	0.28	30
13.5	5126	32977	275	0.28	30
14.0	5199	32861	275	0.28	30
14.5	5268	32742	275	0.28	30
		MAIN PARACHUTE DEPLOYMENT			
14.5	5268	32742	275	0.28	30
14.6	5281	32718	277	0.28	31
14.7	5295	32694	280	0.28	32
14.8	5308	32669	282	0.29	32
14.9	5322	32644	280	0.29	32
15.0	5335	32620	260	0.26	27
15.1	5346	32598	227	0.23	21
15.2	5355	32580	191	0.19	15
15.3	5363	32564	162	0.16	11
15.4	5370	32551	141	0.14	8
15.5	5376	32539	125	0.13	6

TIME FROM JETTISON (Sec)	RANGE FROM DROP POINT (Feet)	ALTITUDE (Feet)	VELOCITY (Ft/Sec)	MACH NUMBER	DYNAMIC PRESSURE (Lb/Ft^2)
16.0	5396	32492	85	0.09	3
16.5	5409	32456	70	0.07	2
17.0	5418	32425	63	0.06	2
17.5	5425	32395	59	0.06	1
18.0	5429	32366	57	0.06	1
18.5	5433	32338	56	0.06	1
19.0	5435	32310	56	0.06	1
19.5	5437	32283	56	0.06	1
20.0	5439	32255	55	0.06	1
20.5	5440	32227	55	0.06	1
21.0	5441	32200	55	0.06	1
21.5	5441	32172	55	0.06	1
22.0	5442	32145	55	0.06	1
22.5	5442	32117	55	0.06	1
23.0	5442	32089	55	0.06	1
23.5	5443	32062	55	0.06	1
24.0	5443	32034	55	0.06	1
24.5	5443	32007	55	0.06	1
25.0	5443	31979	55	0.06	1
25.5	5443	31952	55	0.06	1
26.0	5443	31924	55	0.06	1
26.5	5443	31897	55	0.06	1
27.0	5443	31869	55	0.06	1
27.5	5443	31842	55	0.06	1
28.0	5443	31814	55	0.06	1
28.5	5443	31787	55	0.06	1
29.0	5443.	31760	55	0.06	1
29.5	5443	31732	55	0.06	1
30.0	5443	31705	55	0.06	1
30.5	5443	31677	55	0.06	1
31.0	5443	31650	55	0.06	1
		SOUNDING ROCKET LAUNCH			
31.0		31650	-55	0.06	1
31.1		31650	9	0.01	0
31.5		31827	797	0.81	263
32.0		32469	1792	1.82	1305
32.5		33614	2644	2.70	2729
33.0		35012	2910	2.99	3132
33.5		36495	2995	3.09	3116
33.7		37093	2984	3.08	3003
34.0		37983	2953	3.05	2803
34.5		39448	2905	3.00	2523
35.0		40888	2858	2.95	2301
35.5		42306	2814	2.91	2095
36.0		43702	2772	2.86	1903
41.0		56663	2433	2.51	778
51.0		78526	1967	2.03	180
61.0		96315	1600	1.61	49
71.0		110617	1264	1.24	16

TIME FROM JETTISON (Sec)	RANGE FROM DROP POINT (Feet)	ALTITUDE (Feet)	VELOCITY (Ft/Sec)	MACH NUMBER	DYN PRE (Lb
81.0		121643	941	0.90	5
91.0		129426	621	0.59	2
101.0		134052	303	0.28	0
111.0		135500	0	0.28	0
		SOUNDING ROCKET APOGEE			
111.0		135500	0		
117.0		134934	186		
131.0		129877	494		
149.0		120000	500		
170.0		110000	398		
198.3		100000	314		
234.3		90000	245		
280.6		80000	191		
339.6		70000	150		
414.6		60000	118		
510.2		50000	93		
630.5		40000	73		
782.5		30000	60		

APPENDIX III

CALCULATIONS OF AERODYNAMIC COEFFICIENTS

The determination of rocket vehicle and parachute aerodynamic coefficients is best made by either wind tunnel or flight testing. For preliminary design purposes, however, many shapes are well enough defined as to aerodynamic parameters to allow close estimates of system performance to be formed.

The sounding rocket illustrated in Figure 1 consists of six basic aerodynamic shapes:

1. The nose, an L/D=3 tangent ogive.
2. An L/D=4 cylinder.
3. A 2 1/2° conical step.
4. An L/D=1.59 cylinder.
5. A cruciform tail assembly consisting of 45% swept wings having a 7.1% double wedge section.
6. The base area, which is aerodynamically equivalent to a flat based cylinder.

The aerodynamic coefficients of interest during preliminary design include:

1. The vehicle coasting drag coefficient.
2. The base drag coefficient.
3. The induced drag coefficient.
4. The vehicle normal force coefficient.
5. The vehicle moment coefficient.

These dimensionless coefficients enable the preliminary designer, using modern computing aids, to form a very accurate estimate of vehicle performance and aerodynamic environment.

Subsonic drag coefficients are determined in general by reference to voluminous wind tunnel data collected over the years by many agencies. Supersonic coefficients above a Mach Number of 2 may be calculated using many available theories. Such methods utilize the equations of gas dynamics to determine atmospheric properties before and after normal and incident shock waves caused by vehicle interference with the supersonic airstream.

An example might be the calculation of normal force coefficients for the supersonic symmetrical double wedge fin shown below:

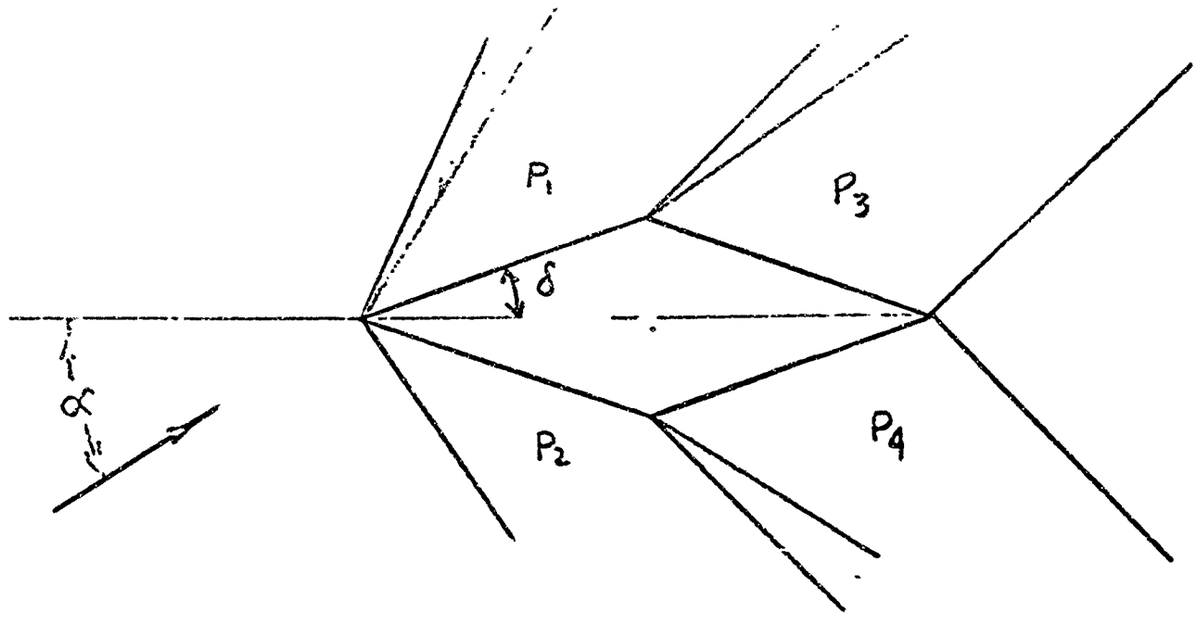

The theory, derived by Busemann, assumes that the angles α and δ are small and that no span wise flow exists (the flow is "two dimensional"). The pressure fields P_1, P_2, P_3, P_4 are determined by small distrubance theory to be functions of a power series based on the flow deflection angle. For the field P_1, the deflection angle is $\alpha - \delta$, for P_2, the deflection angle is $\delta + \delta$ for P_3, it is -2δ, and for P_4 -2δ.

The normal force may be found by integrating pressure over the elements of area, dA, in a chordwise direction.

$$F_n = \int (P_1 + P_3 - P_2 - P_4)\, dA$$

Busemann showed the results of this integration to yield:

$$\frac{F_n}{qS} = \frac{4\alpha}{\sqrt{M^2-1}}, \text{ where}$$

F_n = normal force
q = dynamic pressure, $1/2\,\rho V^2$
S = wing area
M = Mach Number

Similar methods are available for other aerodynamic components. Figure 6 and the table below summarize the principal aerodynamic coefficients for the M-58 Sounding Rocket.

Mach Number	Vehicle $C_{n\alpha}$	Vehicle $C_{m\alpha}$
0	33.85	- 22.47
.6	23.85	- 22.47
1.0	13.59	- 11.67

Mach Number	Vehicle $C_{n\alpha}$	Vehicle $C_{m\alpha}$
1.2	8.96	- 7.18
1.4	8.24	- 6.52
1.6	7.76	- 6.09
1.8	7.38	- 5.74
2.0	7.00	- 5.39
2.2	6.71	- 5.14
2.4	6.44	- 4.90
2.6	6.19	- 4.68
2.8	5.95	- 4.46
3.0	5.72	- 4.26

where: $C_{n\alpha} = \frac{dC_n}{d\alpha} = \frac{dF_n}{1/2\rho V^2 S_{Ref} d\alpha}$ per radian

$C_{m\alpha} = \frac{dC_m}{d\alpha} = \frac{dM}{1/2\rho V^2 S_{Ref} L d\alpha}$ per radian

and: F_n = Total vehicle normal force.

α = Angle of attack

$1/2\rho V^2$ = Dynamic pressure.

$S_{Ref} = \frac{\pi}{4} D_{max}^2 = 34.00 \text{ in}^2$

M = Moment about vehicle nose.

L = Body length = 58.34 in.

The aerodynamics of the parachute systems discussed in this report are based on values obtained from the United States Air Force Parachute Handbook, and are those values recommended for preliminary design.

References:

1. Bonney, E.A. - Engineering Supersonic Aerodynamics
2. Brown, W. D. - Parachutes
3. Chin, S. S. - Missile Configuration Design

4. Dwinnell, J. H. - Principles Of Aerodynamics
5. Hoerner, S. F. - Fluid Dynamic Drag
6. Koelle, H. H. - Handbook Of Astronautical Engineering
7. Liepmann, H. W. and Puckett, A. E. - Aerodynamics Of A Compressible Fluid
8. Merrill, G. (Editor) - Missile Engineering Handbook
9. Morrison, R. B. (Editor) - Design Data For Aeronautics And Astronautics
10. Nielson, Jack N. - Missile Aerodynamics
11. Wright Air Development Center - United States Air Force Parachute Handbook

CODE	ORGANIZATION	NO. OF COPIES
AF 2	A. U. Library Maxwell AFB, Ala.	1
AF 12	AWS(AWSSS/TIPD) Scott AFB, Ill.	1
AF 20	Hq. AFCRL, OAR (CRTTM) L. G. Hanscom Field Bedford, Mass. 01731	1
AF 22	AFCRL, OAR (CRMXR, Mr. John Marple) L. G. Hanscom Field Bedford, Mass. 01731 (U)	1
AF 23	AFCRL, OAR (CRMXRA) Stop 39 L. G. Hanscom Field Bedford, Mass. 01731	Please ship under separate cove as they must be sent to our Documents Unit. (20 cpys)
AF 28	ESD (ESRDG) L. G. Hanscom Field Bedford, Mass. 01731	1
AF 33	ACIC (ACDEL-7) Second and Arsenal St. Louis 18, Mo. (U)	1
AF 40	Aeronautical Systems Division ATTN: ASNXRR W-P AFB, Ohio	1
AF 43	Institute of Technology Library MCLI-LIB., Bldg. 125, Area B W-P AFB, Ohio	1
AF 48	Hq. U. S. Air Force AFBSA, USAF Scientific Advisory Board Washington 25, D. C.	1
AF 49	AFOSR, SRIL Washington 25, D. C.	1
AF 51	Hq. USAF (AFRST) Washington 25, D. C.	1
AF 58	ARL - AROL Library AFL 2292, Bldg. 450 W-P AFB, Ohio	1
AF 64	Hq. AFCRL, OAR Mr. M. B. Gilbert, CRTE L. G. Hanscom Field Bedford, Mass. 01731	1